

General Disclaimer

One or more of the Following Statements may affect this Document

- This document has been reproduced from the best copy furnished by the organizational source. It is being released in the interest of making available as much information as possible.
- This document may contain data, which exceeds the sheet parameters. It was furnished in this condition by the organizational source and is the best copy available.
- This document may contain tone-on-tone or color graphs, charts and/or pictures, which have been reproduced in black and white.
- This document is paginated as submitted by the original source.
- Portions of this document are not fully legible due to the historical nature of some of the material. However, it is the best reproduction available from the original submission.



1. Report No. NASA CR 134879		2. Government Accession No.		3. Recipient's Catalog No.	
4. Title and Subtitle Continued Development of Abradable Gas Path Seals				5. Report Date November, 1975	
				6. Performing Organization Code	
7. Author(s) L. T. Shiembob				8. Performing Organization Report No.	
9. Performing Organization Name and Address Pratt & Whitney Aircraft East Hartford, Connecticut 06108				10. Work Unit No.	
				11. Contract or Grant No. NAS 3-18515	
12. Sponsoring Agency Name and Address U.S. Army Air Mobility Research and Development Lab. Lewis Directorate Cleveland, Ohio 44135				13. Type of Report and Period Covered Contract Report	
				14. Sponsoring Agency Code	
15. Supplementary Notes Project Manager, Robert C. Bill, NASA Lewis Research Center, Cleveland, Ohio					
16. Abstract The objectives of this program were the continued development of the NiCrAlY Feltmetal and the honeycomb systems for knife edge seal applications in the 1144 to 1366°K (1600 to 2000°F) temperature range, and to initiate abradable seal material evaluation for blade tip seal applications in the 1366 to 1589°K (2000 to 2400°F) temperature range. Larger fiber size, higher density feltmetal showed greatly improved erosion resistance with a slight reduction in abradability compared to the baseline feltmetal. Pack aluminide coating of the honeycomb extended the oxidation resistance and slightly improved the abradability of this material. Evaluation through selected abradability, erosion and oxidation testing, and pertinent metallography led to selection of a plasma sprayed yttria stabilized zirconia (ZrO ₂)/CoCrAlY layered system as the system with the most potential to meet the 1589°K (2400°F) requirement for blade tip seals. This system demonstrated structural integrity, erosion resistance, and some degree of abradability. It was recommended that material thermal and mechanical property identification be carried out for purposes of thermal stress analysis and that thermal shock resistance be included in future evaluation.					
17. Key Words (Suggested by Author(s)) Abradable Seals Quartz Fiber Turbine Seals High Temperature Seals Gas Path Seals Abradability Zirconia Erosion Fibermetal Oxidation Honeycomb				18. Distribution Statement	
19. Security Classif. (of this report) Unclassified		20. Security Classif. (of this page) Unclassified		21. No. of Pages 98	
				22. Price*	

* For sale by the National Technical Information Service, Springfield, Virginia 22151

FOREWORD

This report describes the work accomplished under NASA Contract NAS3-18565 and Modification 1 by the Pratt & Whitney Aircraft Division of United Technologies Corporation for the Lewis Research Center of the National Aeronautics and Space Administration. The technical effort was initiated on 25 September 1974 and rig testing was completed on 31 July 1975.

Dr. Robert C. Bill of the National Aeronautics and Space Administration was the Project Manager and Mr. Leonard W. Schopen of the NASA Research Center was the Contracting Officer.

Mr. Lawrence T. Shiembob was the Program Manager for Pratt & Whitney Aircraft from the inception of this contract.

Appreciation is extended for the overall program assistance to P&WA personnel Gerald A. Majocha, Experimental Engineer, and Glenn B. Goodelle and James C. Ray, Engineering Technicians.

Table of Contents

Sections	Subject	Page No.
ABSTRACT		iii
FOREWORD		iv
LIST OF ILLUSTRATIONS		vi
LIST OF TABLES		ix
I.	INTRODUCTION	
	A. Background	1
	B. Program Objective	2
	C. General Approach	2
	D. Seal Systems Evaluated	2
	E. Restrictions	3
II.	SUMMARY AND CONCLUSIONS	4
III.	TECHNICAL PROGRAM	
	A. Knife Edge Seal Systems	6
	1. Seal System Description	6
	2. Test Program	6
	3. Program Details	8
	4. Results and Conclusions	16
	B. Blade Tip Seal Systems	18
	1. Seal System Description	18
	2. Test Program	19
	3. Program Details	20
	4. Results and Conclusions	24
	C. Sprayed Ceramic 1589K (2400°F) Systems	25
	1. Seal System Description	25
	2. Test Program	26
	3. Program Details	27
	4. Results and Conclusions	31
APPENDICES	A. Test Equipment and Procedures	76
	B. Rub Test Data Summary	89
	C. Technical Report Distribution	97

LIST OF ILLUSTRATIONS

Figure	Title	Page No.
1	Volume Ratio vs. Test Temperature	33
2	Volume Ratio vs. Interaction Rate	34
3	Pack Aluminide Honeycomb Seal/Knife Edge	35
4	Volume Ratio vs. Interaction Rate	36
5	Standard Knife Edge Surface Profile	37
6	Smooth Knife Edge Surface Profile	38
7	Volume Ratio vs. Surface Speed	39
8	Interaction Torque vs. Temperature	40
9	Interaction Torque vs. Interaction Rate	41
10	Interaction Torque vs. Interaction Rate	42
11	NiCrAlY 33% Dense Fibermetal Seal/Knife Edge	43
12	Pack Aluminide Honeycomb Seal/Knife Edge	44
13	Interaction Torque vs. Axial Sweep	45
14	NiCrAlY 33% Dense Fibermetal Seal/Knife Edge	46
15	NiCrAlY Fibermetal Microsection - Test #11	47
16	NiCrAlY Fibermetal Microsection - Test #12	48
17	Pack Aluminide Honeycomb Microsection	49
18	Erosion Rate vs. Temperature - Knife Edge Seals	50
19	Pack Aluminide Honeycomb Erosion Specimens	51
20	NiCrAlY Fibermetal Erosion Specimens	52
21	Volume Loss Erosion Rate vs. Temperature	53
22	Pack Aluminide Coated Honeycomb - Top View	54
23	Uncoated Hastelloy-X Honeycomb - Top View	55
24	Pre-Sectioning Blade Tip Seals	56
25	Quartz Woven Fiber Rub Specimen	57

Figure	Title	Page No.
26	Quartz Woven Fiber Microsection	58
27	CeO ₂ /NiCoCrAlY Rub Specimen	59
28	CeO ₂ /NiCoCrAlY Microsection	60
29	CaO Stabilized ZrO ₂ /CoCrAlY Rub Specimen	61
30	CaO Stabilized ZrO ₂ /CoCrAlY Microsection	62
31	Volume Loss Erosion Rate vs. Temperature	63
32	Erosion Weight Loss vs. Time Comparison	64
33	Quartz Woven Fiber Erosion Specimens	65
34	CeO ₂ /NiCoCrAlY Erosion Specimens	66
35	CaO Stabilized ZrO ₂ /CoCrAlY Erosion Specimens	67
36	Y ₂ O ₃ Stabilized ZrO ₂ /CoCrAlY Rub Specimens (Graded Layers)	68
37	Y ₂ O ₃ Stabilized ZrO ₂ /CoCrAlY Rub Specimens (Continuously Graded)	69
38	Typical Radial Cross Section Through Sprayed Graded Y ₂ O ₃ -ZrO ₂ /CoCrAlY Seal Systems	70
39	Section Through Rubbed Area of Continuously Graded Y ₂ O ₃ -ZrO ₂ /CoCrAlY Seal	71
40	Rubbed and Unrubbed Surfaces of Sprayed Continuously Graded Y ₂ O ₃ -ZrO ₂ /CoCrAlY Seal Tested At 2400F	72
41	Y ₂ O ₃ Stabilized ZrO ₂ /CoCrAlY Erosion Specimens	73
42	Erosion Weight Loss vs. Time Comparison	74

Appendices

A	Dynamic Abradability Rig	79
B	Knife Edge/Seal Heating Scheme	80
C	Blade Tip/Seal Heating Scheme	81
D	Typical Knife Edge Seal Configuration	82
E	Typical Blade Tip Seal Configuration	83
F	Knife Edge Configuration	84
G	Bladed Disk Configuration	85

Figure	Title	Page No.
H	Hot Particulate Erosion Rig	86
I	Typical Erosion Specimen	87
J	Close-up Erosion Rig	88

LIST OF TABLES

Table	Title	Page No.
I	Seal Systems Evaluated	2
II	Abradability Test Matrix - Knife Edge Seals	7
III	Erosion Test Matrix - Knife Edge Seals	7
IV	Cumulative Erosion Weight Loss - Knife Edge Seals	13
V	Calculated Particulate Erosion Rate - Knife Edge Seals	14
VI	CaO Stabilized ZrO ₂ /CoCrAlY - Coating Specification	19
VII	Abradability Test Matrix - Blade Tip Seals	19
VIII	Erosion Test Matrix - Blade Tip Seals	20
IX	Cumulative Erosion Weight Loss - Blade Tip Seals	23
X	Layered Y ₂ O ₃ Stabilized ZrO ₂ /CoCrAlY - Coating Details	25
XI	Continuously Graded Y ₂ O ₃ Stabilized ZrO ₂ /CoCrAlY - Coating Details	26
XII	Abradability Test Matrix - Ceramic 1589K (2400°F) Seals	26
XIII	Abradability Results - Ceramic 1589K (2400°F) Seals	29
XIV	Cumulative Erosion Weight Loss - Ceramic Seals	30
XV	Erosion Results - Ceramic 1589K(2400°F) Seals	31
XVI	Rub Test Data Summary (SI Units)	89-92
XVIA	Rub Test Data Summary (English Engineering Units)	93-96

I. INTRODUCTION

A. Background

The increasing urgency for fuel conservation has added impetus to the effort to improve gas turbine efficiency. Gas path sealing is a proven and accepted method of improving engine performance and, thereby, reducing fuel consumption. Generally, the engine turbine section presents the most potential for the greatest engine efficiency gains through the use of gas path seals.

Turbine abradable gas path seals perform two primary functions: 1) permit operation at minimum clearances by reducing the potential of rotor damage during rotor/seal interaction, and 2) protect critical turbine parts from excessive temperatures by providing a thermal barrier between the hot turbine gas and the conventional metallic turbine seal.

Reduced clearances limit the loss of high energy, high pressure gas from the main gas path without extracting useful work from it, thereby, resulting in an increase in turbine efficiency. As an illustration, it is estimated that reducing the first stage turbine blade tip clearance in a typical commercial aircraft (four engines) by $2.54 \times 10^{-4} \text{ m}$ (0.010 inch) will result in a fuel savings of approximately $4.68 \times 10^2 \text{ m}^3$ (124,900 gallons) per year.

The trend in gas turbine engine development is directed toward higher turbine inlet temperatures (TIT) to obtain improved performance with minimum engine size and weight. Projections indicate that growth versions of current commercial aircraft engines will approach 1811K (2800 °F) TIT, while future engine generations for the 1980's will approach 2033K (3200 °F). High pressure compressor bleed air is now used to cool the turbine gas path seals and maintain them within acceptable material operating temperature limits. This results in an engine performance penalty due to loss of high pressure air from the cycle. Increasing the allowable operating temperature of the seal materials will reduce the cooling air requirements and result in improved engine efficiency. Increasing the seal temperature capability from the current state-of-the-art value of approximately 1366K (2000 °F) to 1589K (2400 °F) will generally satisfy current and near term engine turbine requirements without the use of cooling air. For future engines operating at 1811K (2800 °F) TIT, a fuel savings of $7.40 \times 10^2 \text{ m}^3$ (193,000 gallons) per year per aircraft would result. This savings is in addition to that attributable to clearance reduction mentioned earlier.

Tight operating clearances result in rubs between the turbine rotor components and the static gas path seals due to differential heating and cooling rates, case distortions such as ovalization due to circumferential heat flux variations and imposed loads, and rotor shift or bending. The seal must be capable of tolerating these rubs without catastrophic failure such as blade destruction. Therefore, the static gas path seal component should be abradable to preferentially wear during rotor/seal interaction and, thereby, restrict the clearance increase to the local rubbed arc area.

Turbine gas path seals must also be capable of withstanding exposure to the scrubbing action of the high temperature gas and entrained particulate matter, such as, ingested dirt and dust, wear debris and unburned carbon, without excessive degradation due to oxidation or erosion for the life cycle of the seal. The durability of the seal to withstand the turbine environment not only refers to its replacement rate, but also extends the life of other related critical turbine hardware and reduces considerably overhaul maintenance costs.

B. Program Objective

This effort is the continuation of a program conducted for NASA to evaluate abradable gas path seals for gas turbine engines. The initial effort (1) conducted in 1974 evaluated the abradability and erosion characteristics of five seal systems for use in 1144-1366K (1600-2000°F) applications. The objective of the contract effort reported herein was 1) continued development of the most promising systems identified by the previous program, and 2) initiation of evaluation of selected seal systems with 1366-1589K (2000-2400°F) capability.

C. General Approach

Based on review of results from the initial phase of the previous contract, the most promising seal systems for knife edge seal applications at temperatures in the 1144-1366K (1600-2000°F) range were selected for modification with the goal of increasing their temperature capability and improving their abradability and erosion resistance. Three seal systems with potential for unshrouded blade tip seal applications in the 1366-1589K (2000-2400°F) range were also selected based upon considerations of temperature capability, fabrication technology and previous P&WA experience with similar systems during P&WA funded and other contractual development programs.(2,3)

The abradability and erosion characteristics were evaluated in a series of rig tests. Data on the relative wear and rub generated temperatures in the rotor and static seal components were determined in dynamic abradability rig tests in which simulated rotor tip configurations were rubbed against static seal specimens at typical engine operating conditions of temperature, speed and interaction rate. Durability of the seal material was evaluated by particulate and hot gas erosion tests. The greater the erosion susceptibility the more seal material that will be removed per unit time and the larger the rotor/seal clearance will become.

Following completion of rig testing and evaluation of the five systems, a system with potential to meet the maximum temperature requirement 1589K (2400°F) within blade tip seal systems was selected with NASA approval. Four (4) variations were sprayed and similar rig testing was conducted.

D. Seal Systems Evaluated

A listing of the nine (9) seal systems evaluated in this program is presented below in Table I. A description of the material systems, specific seal application and temperature category has also been included in the table.

TABLE I

Seal Systems Evaluated

<u>Material</u>	<u>Application</u>	<u>Temperature Range</u>	
		K	(°F)
° NiCrAlY 33% Dense Fibermetal	Knife Edge Seal	1144-1366	(1600-2000)
° Pack Aluminide Hastelloy-X Honeycomb	Knife Edge Seal	1144-1366	(1600-2000)
° Quartz Woven Fiber	Blade Tip Seal	1366-1589	(2000-2400)

TABLE I (Cont'd.)

<u>Material</u>	<u>Application</u>	<u>Temperature Range</u>	
		K	(°F)
° Sprayed $\text{CeO}_2/\text{NiCoCrAlY}$	Blade Tip Seal	1366-1589	(2000-2400)
° Sprayed CaO Stabilized $\text{ZrO}_2/\text{CoCrAlY}$	Blade Tip Seal	1366-1589	(2000-2400)
° Sprayed Y_2O_3 Stabilized $\text{ZrO}_2/\text{CoCrAlY}$ (Graded Layers)	Blade Tip Seal	1589	(2400)
° Sprayed Y_2O_3 Stabilized $\text{ZrO}_2/\text{CoCrAlY}$ With CeO_2 Additive (Graded Layers)	Blade Tip Seal	1589	(2400)
° Sprayed Y_2O_3 Stabilized $\text{ZrO}_2/\text{CoCrAlY}$ (Continuously Graded)	Blade Tip Seal	1589	(2400)
° Sprayed Y_2O_3 Stabilized ZrO_2 with CeO_2 Additive/ CoCrAlY (Continuously Graded)	Blade Tip Seal	1589	(2400)

E. Restrictions

Abradability and erosion resistance are two of the important characteristics of an abradable seal system and form a sound basis for a preliminary comparative evaluation of materials with potential for high temperature seal applications. However, thermal shock capability is of equal importance and should be evaluated in future effort. Additional various other characteristics such as thermal conductivity of the material and the associated effect on thermal response may be of equal importance with regards to a particular application. Therefore, the results of this program should not be used as the sole basis for determining the acceptability of any material for a particular application.

II. SUMMARY AND CONCLUSIONS

Based upon the abrasability and erosion test results obtained from contract NAS3-18023, sintered NiCrAlY fibermetal and 1.5875×10^{-3} m (1/16 inch) cell size, 1.016×10^{-4} m (0.004 inch) wall Hastelloy-X honeycomb were selected and modified for continued evaluation for 1144-1366K (1600-2000°F) knife edge seal application. The modifications are described below.

<u>System</u>	<u>Modification</u>	<u>Objective</u>
Fibermetal	1) Increased fiber size from $8-10 \times 10^{-6}$ m to 25×10^{-6} m	Improve temperature capability
	2) Increase density 19% to 33%	Improve erosion resistance
Honeycomb	1) Pack aluminide coating	Improve oxidation resistance and abrasability through elimination of braze wicking

Erosion resistance of the fibermetal system was improved by approximately 5-10x, but consequently abrasability was also reduced. The pack aluminide treatment significantly reduced the braze wicking of the honeycomb system and resulted in improved abrasability. Both materials demonstrated unsatisfactory oxidation resistance in static oxidation tests at 1366K (2000°F). Estimated long term temperature capability of these systems is estimated to be somewhat less than 1255K (1800°F) with the honeycomb having slightly higher capability than the fibermetal. Significant improvements were obtained within both of these systems. However, further development would be necessary to adapt these systems to the requirements of any specific application.

A quartz woven fiber structure, plasma sprayed NiCoCrAlY with CeO₂ additive and plasma sprayed graded CaO stabilized ZrO₂/CoCrAlY seal systems were evaluated for 1366-1589K (2000-2400°F) blade tip seal applications. The quartz woven fiber structure exhibited excellent abrasability at room temperature, but completely disintegrated at 1589K (2400°F) and eroded extremely rapidly. The sprayed NiCoCrAlY plus CeO₂ and continuously graded CaO stabilized ZrO₂/CoCrAlY demonstrated poor abrasability. Thermal distress in the form of localized melting and debonding was exhibited for the CeO₂/NiCoCrAlY system. Particulate erosion resistance of the CeO₂/NiCoCrAlY system was slightly better than that for the graded CaO stabilized ZrO₂/CoCrAlY system. Only the graded ZrO₂/CoCrAlY system demonstrated potential for 1589K (2400°F) capability and yet that system also exhibited seal spalling and delamination at 1589K (2400°F). The other systems are temperature limited at approximately 1477K (2200°F) for the CeO₂/NiCoCrAlY and less than 1366K (2000°F) for the quartz woven fiber system.

The plasma sprayed ZrO₂/CoCrAlY system, with a Y₂O₃ stabilizer for higher temperature capability, was selected for further evaluation. The coating thickness and structure gradation was selected based on similar systems being developed by P&WA for 1922K (3000°F) applications. Two (2) spray processes, layered and continuously graded, and the addition of CeO₂ to each process as a solid high temperature lubricant were evaluated.

All four (4) systems showed marked temperature capability improvement in that they survived exposure to 1589K (2400°F) temperatures during abrasability and erosion tests with no evidence of thermal distress. Particulate erosion resistance was basically the same as CaO stabilized sprayed graded ZrO₂/CoCrAlY system. Some slight grooving

of the seal surface occurred on some of these systems, thereby, demonstrating that the system might provide a desired degree of abrasability with additional modification. The CeO_2 additive did not have any discernible effect on the abrasability of these seal systems.

In conclusion, feasibility of methods to improve the fibermetal and honeycomb seal systems has been demonstrated and will offer potential means for satisfying seal requirements up to 1255K (1800°F).

The sprayed Y_2O_3 stabilized $\text{ZrO}_2/\text{CoCrAlY}$ systems demonstrated promise for 1589K (2400°F) application, but further development is still required. The thermal shock tolerance of this system must be defined. Thermal stress analysis methods have been developed by P&WA to aid in optimizing coating design, but knowledge of certain physical and mechanical properties of the seal coating materials is necessary. Development of material properties, evaluation and optimization of the thermal shock characteristics, as well as further definition and/or improvement of abrasability and erosion resistance characteristics of the Y_2O_3 stabilized $\text{ZrO}_2/\text{CoCrAlY}$ system are recommended.

III. TECHNICAL PROGRAM

A. Knife Edge Seal Systems 1144-1366K (1600-2000°F)

1. Seal System Description

Seal system selections for the 1144-1366K (1600-2000°F) temperature range knife edge seals were made from the systems evaluated under contract NAS3-18023. The two most promising systems, fibermetal and honeycomb, were selected on the basis of performance, relative adaptability of the system for engine application, and potential to complete specimen fabrication and rig testing within the time and cost constraints of the program. Modifications were made to the two (2) selected systems to increase their temperature capability and improve their performance. The following systems were selected and modified as discussed below:

Sintered NiCrAlY 33% Dense Fibermetal:

The 19% dense NiCrAlY fibermetal system demonstrated the best abrasability, but poorest erosion resistance of all systems evaluated under contract NAS3-18023. To improve the erosion resistance and increase temperature capability of this system, a modification from a 19% dense structure of $8-10 \times 10^{-6}\text{m}$ ($3.1-3.9 \times 10^{-4}$ inch) fiber diameter size to a 33% dense structure of $25 \times 10^{-6}\text{m}$ (1.0×10^{-3} inch) diameter fibers was recommended. Aspect ratio of the fibers was maintained approximately the same. The increased fiber size was expected to improve oxidation resistance and, thus, result in increased temperature capability. To maintain the same permeability (leakage), the density was also increased. A further benefit expected with the increased density was better erosion resistance.

Pack Aluminide Coated Hastelloy-X Honeycomb:

The $1.58 \times 10^{-3}\text{m}$ (1/16 inch) cell size, $1.02 \times 10^{-4}\text{m}$ (.004 inch) thick wall, hexagonal cell honeycomb of Hastelloy-X material also tested under contract NAS3-18023, demonstrated less than 1366K (2000°F) temperature capability. A pack aluminide (Al_2O_3) coating $1.27 \times 10^{-5}\text{m}$ (.0005 inch) thick was applied to the honeycomb to improve oxidation resistance and increase the temperature capability. The coating also was expected to reduce braze material wicking over the walls and down the sides of the honeycomb, which contributed to knife edge heat distress in the previous testing. The reduction of metal rub area was expected to reduce knife edge wear and heat generation during rub interaction.

2. Test Program

Eighteen (18) abrasability, eight (8) erosion and two (2) static oxidation tests were conducted on the knife edge/seal systems. The objective of the abrasability tests was evaluation of the relative rub tolerance and wear characteristics of the selected seal systems as a function of temperature, rubbing velocity and interaction rate. The test parameters were chosen to simulate conditions typically experienced in engine applications and are summarized in Table II. The slower rubbing velocity conditions relate to interactions occurring during engine startup or shutdown cycles. The axial sweep tests simulate rotor shift conditions corresponding to thrust changes which occur in most engines. The effect of the knife edge rub contact length due to knife edge surface finish was also evaluated by repeating a high wear test with a specially machined knife edge. All tests were made with a Waspalloy knife edge disk configuration. The disk configuration,

test rig and procedures are described fully in Appendix A. Multiple tests were made on each seal specimen and knife edge disk. The knife edges were refinished as necessary between subsequent tests.

TABLE II

Abradability Test Matrix

Knife Edge Seal Systems 1144-1366K (1600-2000°F)
Programmed Penetration Depth - 7.62×10^{-4} m (0.030 inch)

<u>Temperature</u>		<u>Peripheral Speed</u>		<u>Penetration Speed</u>	
K	(°F)	m/s	(ft/sec)	m/s x 10 ⁻⁵	(inch/sec x 10 ⁻³)
Ambient		305	(1000)	2.54	(1.0)
1144	(1600)	305	(1000)	2.54	(1.0)
1366	(2000)	305	(1000)	2.54	(1.0)*
1366	(2000)	305	(1000)	0.254	(0.1)
1366	(2000)	305	(1000)	25.4	(10.0)
1366	(2000)	183	(600)	2.54	(1.0)
Ambient		305	(1000)	0.254	(0.1)
Ambient		305	(1000)	25.4	(1.0)**
Ambient		305	(1000)	25.4	(10.0)***

* Repeated with "smooth" knife edge for fibermetal only.

** Includes 5.08×10^{-3} m (0.200 inch) axial sweep at 2.54×10^{-4} m/s (0.010 inch/sec) for both systems.

*** Fibermetal system only.

Hot gas erosion tests with and without entrained aluminum oxide particles were conducted using the test rig and procedures described in Appendix A, to evaluate the relative durability of the selected seal systems. Test conditions for each seal system are presented in Table III.

TABLE III

Erosion Test Matrix

1144-1366K (1600-2000°F) Knife Edge Seal Systems

Impingement Angle - 7°

<u>Specimen Temperature</u>		<u>Test Duration</u>		<u>Abrasive Particles</u>
K	(°F)	s	(min)	Included
1144	(1600)	1200	(20)	Yes
1255	(1800)	1200	(20)	Yes
1366	(2000)	1200	(20)	Yes
1366	(2000)	1200	(20)	No

One 1.80×10^5 s (50 hr.) static oxidation test at 1366K (2000°F) was conducted on each seal system to evaluate relative temperature capability.

3. Program Details

Abradability

Eighteen (18) abrasability tests were conducted on the knife edge 1144-1366K (1600-2000°F) systems at various temperatures, surface speeds, and interaction rates. Test conditions, rotor and seal wear, maximum torque, normal load and other information are presented in Table XVI of Appendix B. The table is arranged according to material systems tested. The first part of the table includes testing completed on the knife edge seal systems, the second part, blade tip seal systems. Actual sequential order of testing is included at the far left of the table for possible reference to the raw data available in P&WA files.

Figure 1 depicts volume ratio (knife edge or blade volume removed or adhered/seal volume removed) vs. test temperature for both the fibermetal and honeycomb systems. As illustrated, the NiCrAlY 33% dense fibermetal system produced knife edge pickup at ambient temperature but knife edge wear at 1033K (1500°F) test temperature. This wear mode could be the result of the fiber-metal structure weakening at temperature and the resulting interaction causing compression or densification at the point of penetration. (Previous test experience had indicated that surface densification produces high wear rates.) As shown in Figure 2, increasing the interaction rate tended to produce knife edge pickup at the 1366K (2000°F) condition.

The pack aluminide coated Hastelloy-X honeycomb testing produced no knife edge wear and low torque for all tests. However, some localized heat discoloration and pickup was evident on the outer diameter of all the tested knife edges. In general, the heat distress and pickup was confined to one area of the knife edge, 5-10° in length. One test, #10, conducted at the faster interaction rate of 2.54×10^{-4} m/s (.010 inch/sec) resulted in four distinct distress areas totalling 20 degrees of the knife edge. A photograph of the post test appearance of this knife edge is shown in Figure 3.

As depicted in Figure 4, a high wear test point (3.27×10^{-4} m (.0129 inch) radial wear) resulted from testing of the fibermetal system at ambient temperature, 305 m/s (1000 ft/sec) surface speed, and 2.54×10^{-4} m/s (.010 inch/sec) interaction rate, test #25. A comparison with test #17, which had the same test conditions except temperature which was 1366K (2000°F), illustrates the effect of temperature on the rub mechanism - test #17 resulted in pickup. Since all tests conducted at 1366K (2000°F), Figure 2, showed a general trend toward less wear and/or more pickup as interaction rate was increased, the expectation was that the same trend would hold for the ambient tests and that test, #25, would have produced pickup and not wear. Investigation into the cause of the unexpected high wear of test #25 revealed a relatively rough pre-test O.D. knife edge profile compared to a machined surface. It may be that the knife edge profile rather than the controlled test condition was the cause of the high wear.

A review of all available knife edge test results indicated the possibility of a dependence of rub mechanism, whether pickup or wear, on knife edge surface finish and waviness. A repeat test (#26) of test #12, reference Table XVI, on a fibermetal system using a knife edge machined as "smooth" as possible ($\pm 2.54 \times 10^{-6}$ m (.0001 inch) OD tolerance) at conditions of 305 m/s (1000 ft/sec), 2.54×10^{-5} m/s (.001 inch/sec), and 1366K (2000°F) was conducted.

The pre and post test OD surface profile for the two comparative knife edge disks, one "standard" and one "smooth", rubbed against fibermetal specimens are depicted in Figures 5 and 6 respectively. It should be noted that the initial interaction area for the machined disk is 5-10x longer in length than the standard refurbished knife edge. As illustrated in Figures 1 and 2, increasing the "smoothness" produced knife edge pickup rather than wear. This repeat test indicated the possibility that the larger knife edge area participating in the interaction, the lesser wear (or more pickup) will result. This phenomena could have masked the effect of test parameters to some extent.

Figure 7 presents the effect of surface speed on the volume ratio factor. Pickup resulted from testing at 183 m/s (600 ft/sec) surface speed whereas wear resulted from testing at 305 m/s (1000 ft/sec) for the NiCrAlY fibermetal system. The "smooth" knife edge repeat test revealed pickup at the 305 m/s (1000 ft/sec) test condition, the reasoning for this was discussed previously. The honeycomb tests produced knife edge pickup at both surface speed test conditions.

Figure 8 illustrates rub interaction torque as a function of temperature at 305 m/s (1000 ft/sec) and 2.54×10^{-5} m/s (.001 inch/sec) interaction rate conditions. Torques generated by interaction with the NiCrAlY 33% dense fibermetal and pack aluminide honeycomb were relatively low and independent of temperature.

Figures 9 and 10 show rub interaction torque as a function of interaction rate for both ambient and 1366K (2000°F) temperature respectively. Higher torques were recorded for increasing interaction rate at ambient temperature conditions (Figure 9). However, the high torque test, #25, resulted from unknown reasons as discussed previously. Therefore, this trend could be misleading. The coated honeycomb produced low torque at all test conditions.

One axial sweep test was conducted on each of the two knife edge systems, NiCrAlY fibermetal and coated Hastelloy-X honeycomb, tests #27 and #28 respectively. In these tests the specimen was injected into the rotor to a depth of 7.62×10^{-4} m (0.030 inch) and then moved axially 5.08×10^{-3} m (0.200 inch). The fibermetal test produced heavy knife edge ~~heat~~ distress and 1.78×10^{-5} m (.0007 inch) average radial knife edge wear, the second highest wear test result on the low temperature systems. Pickup was also noted on the post test knife edge profile. The pickup occurred on an isolated area of knife edge during the axial sweep portion of the test. The pickup deposited completely on the sweep direction side of the knife edge. It was also noted that the surface of the specimen groove floor was highly glazed. The seal specimen and corresponding knife edge for this test are shown in Figure 11. The honeycomb test resulted in a clean removal of seal material with minimal cell fold over at the groove floor. The knife edge exhibited only two isolated areas of pickup (no wear). The seal specimen and corresponding knife edge for this test are shown in Figure 12.

Figure 13 illustrates the maximum torque recorded during the axial sweep test of both the honeycomb and fibermetal. Test results indicate that under axial sweep conditions, the fibermetal produces more knife edge wear than the honeycomb system.

In order to better define the fibermetal system rub mechanism and identify differences in rub surface morphology between a wear and pickup test result, two fibermetal specimens were sectioned.

The initial fibermetal specimen sectioned, test #11 (no wear), was tested at ambient temperature, 305 m/s (1000 ft/sec), and 2.54×10^{-5} m/s (.001 inch/sec) interaction rate. The pre-sectioned test specimen is depicted in Figure 14. Binocular examination of the rub groove revealed complete loss of fiber definition in the walls of the rub groove as a result of severe plastic deformation of the fibers. The fibers in the floor of the groove were free of gross plastic deformation but somewhat flattened.

There was no apparent densification of the fibermetal structure beneath the rubbed area in the microsection examined (Figure 15). Supplemental spectroanalysis identified some non-metallic inclusions within the microstructure which may have occurred because of an undetected oxygen leak during the cool down of the brazing process. These inclusions were not considered important to the overall test program in establishing abrasability and erosion characteristics. Scanning electron microscopy of the smeared areas of the groove floor showed thin layers of plastically deformed fiber material and the occurrence of microcracks. Although discrete particles of knife edge material were not observed, an element, cobalt, peculiar to the knife edge was identified by dispersed x-ray analysis on the rubbed surface.

The second fibermetal specimen sectioned, test #12, was tested at 1366K (2000°F) temperature with other conditions remaining unchanged. The walls and floor of this specimen showed severe plastic deformation leaving very little or no fiber definition. The microsection (Figure 16) showed densification of fibers immediately beneath the rub groove, which also included an agglomerate of broken non-metallic inclusion and partially oxidized knife edge material. The knife edge material was also observed in the surface structure of the rub groove walls. Discrete particles of the knife edge material were not observed in the rub path, although the constituent elements of the material were detected by dispersed x-ray analysis. Scanning electron microscopy of the rub groove showed severely deformed smeared metal layers.

In the high temperature test, the structure may have densified beneath the penetrating knife edge because the NiCrAlY fibers, having undergone a thermally-induced ductility increase, were deformed under the load and were compressed. In addition, the environmental and frictional temperatures created by rubbing a densified structure could have reduced the knife edge strength, which drops off rapidly above 978°K (1300°F), causing subsequent wear. The significance of knife edge surface finish in establishing these seal surface structural changes could not be identified within the scope of the program.

One pack aluminide honeycomb specimen was sectioned, test #7. Macroscopic examination revealed little or no smearing in the rub path, although a small number of honeycomb nodes were folded perpendicular to the rub direction.

Microscopic examination of the rub path cross-section (Figure 17A) did not show knife edge material deposits on the rubbed nodes which appeared to have sheared transgrannularly. The aluminide coating appeared to be sheared along with the honeycomb by the knife edge rub. Some intergrannular diffusion of the aluminide coating is also evident.

The honeycomb cell walls at the bottom of the groove, studied with the scanning electron microscope, were plastically deformed in the rub direction and smearing and cracking were observed parallel to the rub direction (Figure 17B).

Erosion Results

Particulate erosion testing was conducted with 80 grit, Al_2O_3 particles injected into the gas stream with a particulate mass flow rate of approximately 7.50×10^{-3} kg/s (6.0 lbs/hr). Test time of 1200 seconds was used for comparative evaluation purposes and weight measurements were taken at 300 second intervals to provide information relative to the erosion/time characteristics of each seal system. Testing was conducted with a gas velocity of .35 Mach number and impingement angle of 7° . A JP5 burner was used to heat the air to required temperatures.

Since the tests were of relatively short duration the effect of long term oxidation on the structural integrity of each of the materials was not evaluated.

The NiCrAlY 33% dense fibermetal system exhibited greater erosion resistance than the pack aluminide coated honeycomb. The fibermetal erosion path was significantly greater at 1255K (1800°F) and 1366K (2000°F) than at 1144K (1600°F). The 1366K (2000°F) specimen was eroded to the base material. The strength of the NiCrAlY fibermetal structure weakens considerably after 1144K (1600°F) and could have contributed to the greater erosion rate at the higher temperatures. Testing with hot gas only at 1366K (2000°F) resulted in a weight gain apparently due to oxidation of the fibermetal.

The coated honeycomb walls perpendicular to the particulate flow experienced material removal down to the braze fillets. Two possible reasons for this result include the 1) lack of braze support on the sides of the walls of the honeycomb cells caused by the pack aluminide successfully reducing braze wicking and 2) possible weakening of the Hastelloy-X walls by the aluminide penetration. The hot gas erosion test resulted in no degradation of the honeycomb material.

The actual weight loss or gain for each specimen for both knife edge systems is recorded in Table IV. The resultant slope of these points was converted to volume loss/unit time to obtain the steady-state erosion rates shown in Table V. Figure 18 is a graphic representation of the resultant erosion rates of the candidate materials as a function of test temperature. Figures 19 and 20 display the respective honeycomb and fibermetal tested erosion specimens.

The four (4) NiCrAlY fibermetal erosion specimens were tested for 2400 seconds, somewhat longer than programmed. Weight measurements were taken at 300 second intervals during the extended time and the added data points were used to more accurately calculate steady state erosion rates.

Oxidation

Comparative oxidation testing at 1366K (2000°F) for 1.8×10^5 s (50 hours) was performed in a static air furnace using equally sized tabs of both the honeycomb and fibermetal seal systems which had been brazed onto Waspaloy substrates. Where possible, hardness measurements of the fibermetal structure was performed with a Rockwell Superficial Hardness Tester using a 1.91×10^{-2} m (0.75 inch) diameter ball and 15 kg load. Weight measurements of pre and post oxidation specimens and metallographic examination were also used to evaluate the oxidation results.

Table IV

Cumulative Weight Loss (kg) Due to Hot Particulate Erosion

<u>Designation</u>	<u>Temperature</u>		<u>Elapsed Time (s)</u>						
	<u>K</u>	<u>(°F)</u>	<u>300</u>	<u>600</u>	<u>900</u>	<u>1200</u>	<u>1500</u>	<u>1800</u>	<u>2100</u>
			<u>(Weight Loss kg x 10⁻³)</u>						
Pack Aluminide	1144	(1600)	.065	.145	.227	.325			
Hast-X Honeycomb	1255	(1800)	.101	.224	.359	.484			
	1366	(2000)	.173	.388	.613	Base Material			
*	1366	(2000)	.000	.000	.000	.002			
33% Dense NiCrAlY	1144	(1600)	.068	.133	.213	.288	.363	.429	.503
Fibermetal	1255	(1800)	.135	.340	.480	.657	.840	1.007	1.200
	1366	(2000)	.233	.510	.833	1.283	1.698	Base Material	
*	1366	(2000)	+.035	+.035	+.060	+.070	+.070	+.080	+.080

* No particulate (hot gas)

+ Initial weight gains observed during the 1366K(2000°F) are the result of oxidation of the fibermetal substructure.

Table V

Calculated Particulate Erosion Rate For Knife Edge Seal Systems

<u>Designation</u>	<u>Temperature K (°F)</u>		
	1144 (1600)	1255 (1800)	1366 (2000)
	<u>Volume Loss/Time</u>		
	$\frac{\text{m}^3}{\text{s} \times 10^{-10}}$ (cc/min $\times 10^{-3}$)		
Pack Aluminide Coated Hast-X Honeycomb	2.19 (13.2)	3.35 (20.2)	5.21 (31.4)
33% Dense NiCrAlY Fibermetal	.96 (5.8)	2.32 (14.0)	4.48 (27.0)

The NiCrAlY fibermetal experienced oxidation of 2/3 of the tested specimen. Furthermore, the top third of the specimen was completely oxidized. Post oxidation values of hardness could not be obtained due to brittle failure of the 1366K (2000°F) aged specimen when the load was applied. In comparison, the pack aluminide honeycomb exhibited some oxidation of the braze and pitting of the aluminide coating but no visible oxidation of the honeycomb walls. Experience in other programs has indicated that uncoated Hastelloy-X at the same temperature would have been oxidized. The comparatively greater oxidation experienced by the fibermetal structure is due to 1) the very large surface area of the structure and 2) insufficient Al content. The approximate 7.5% by weight Al content of the NiCrAlY is too low to provide an adequate aluminum reservoir for the formation of a sufficiently thick Al_2O_3 scale to be protective for this large surface area to volume ratio fiber metal structure.

Comparison of Modification to Baseline System

Comparison of the test results of this program with results from Contract NAS3-18023 indicated definite improvements to the respective modified materials. The 33% dense 25×10^{-6} m diameter NiCrAlY fibermetal system exhibited approximately 5x greater erosion resistance than the 19% dense $8-10 \times 10^{-6}$ m diameter fibermetal system tested previously as shown in Figure 21. Note that the 33% dense fibermetal system exhibited almost as good erosion resistance at 1144K (1600°F) as the baseline uncoated honeycomb system. The increase in fiber size and structure density did, however, result in some reduction in abrasability. The 33% dense fibermetal system did cause some knife edge wear while the 19% dense system previously tested exhibited no knife edge wear for any of the tests conducted.

These results indicate that it is possible to increase the temperature capability of the fibermetal system to approximately 1144K (1600°F) by these modifications with some slight reduction in abrasability.

The pack aluminide coated Hastelloy-X honeycomb did reduce braze wicking compared with the uncoated Hastelloy-X honeycomb tested previously as shown by Figures 22 and 23. A slight improvement in abrasability, exhibited by reduced knife edge heat distress and pickup, is attributed to the reduction of braze material at the rub surface of the coated honeycomb system.

Based upon material weight loss results, the aluminide coated Hastelloy-X honeycomb exhibited poorer erosion resistance than the uncoated honeycomb previously tested as shown in Figure 21. The coated honeycomb walls perpendicular to the particulate flow experienced material removal down to the braze fillets. In comparison, the uncoated honeycomb tested at the same conditions resulted in more deformation than material removal. That is, the honeycomb walls perpendicular to the particulate flow folded over instead of being removed. Two possible reasons for this result may be developed around 1) the lack of braze support on the sides of the walls of the honeycomb cells caused by the aluminide coating successfully reducing the braze wicking and 2) possible weakening or embrittlement of the Hastelloy-X wall due to aluminide diffusion.

From the practical standpoint of the effect of erosion on seal clearance, both the coated and uncoated honeycomb systems were equivalent. The depth of material removal is approximately the same for both systems, resulting in equivalent amounts of leakage.

Comparison of the static oxidation resistance of the coated honeycomb system with results of similar data for uncoated honeycomb conducted under another P&WA funded program indicates increased temperature capability of the aluminide coated system, as expected.

In summary, the pack aluminide coating demonstrated the following benefits:

1) increased temperature capability in terms of oxidation resistance, 2) improved abrasability in terms of reduced knife edge heat distress, and 3) comparable erosion resistance on the basis of measured material removal depth.

4. Results and Conclusions

The effectiveness of the modifications to the knife edge seal materials can be determined by their relative performance under similar test conditions.

The NiCrAlY 33% dense fibermetal, with increased fiber size definitely showed less abrasability than the coated honeycomb or the less dense, small fiber fibermetal tested in the previous contract. The increased density system provided a seal surface more susceptible to knife edge transfer and showed increased knife edge wear. On the other hand, abrasability results for the pack aluminide system showed no knife wear with only localized (5-10° length) heat discoloration areas along the knife edge circumference. The reduced braze wicking for this honeycomb variation promoted abrasability improvement over the baseline untreated honeycomb.

The NiCrAlY fibermetal with increased density and larger fibers exhibited greatly improved particulate erosion resistance, especially at the 1144K (1600°F) temperature compared to the fibermetal evaluated in the previous contract. The coated honeycomb exhibited a higher erosion weight loss rate but approximately equal material removal depth compared with the uncoated honeycomb system tested under the previous contract due to the uncoated honeycomb walls perpendicular to the particulate flow bending over instead of actually being eroded away.

Oxidation testing at 1366K (2000°F) for 1.8×10^5 s (50 hours) revealed severe oxidation of the NiCrAlY 33% dense fibermetal. In fact, the top third of the specimen was completely oxidized. In comparison, the pack aluminide honeycomb exhibited some oxidation of the braze and only pitting of the aluminide coating with little damage to the Hastelloy-X cells.

An evaluation of the system modifications and test results indicate them to be viable means for increasing the temperature capability of the fibermetal and honeycomb seal systems. The long term temperature capability of the two systems, increased density fibermetal and coated honeycomb, is estimated at somewhat less than 1255K (1800°F) maximum. The honeycomb has the higher temperature capability of the two systems as illustrated through the abbreviated oxidation test results. The increased fiber size fibermetal resulted in significantly reduced erosion, but abrasability was somewhat decreased. The honeycomb modification resulted in increased abrasability, but comparable erosion resistance characteristics from the practical basis of depth of material removed.

Significant improvements have been achieved by these modifications for both systems, however, the specific application must be considered before these seal systems can be implemented for engine use. Additional evaluation and analysis will be required to consider either of these seal systems for a specific application.

B. Blade Tip Seal Systems 1366-1589K (2000-2400°F)

1. Seal System Description

Materials from the three (3) following categories were reviewed for use in abradable turbine blade tip seal applications requiring 1366-1589K (2000-2400°F) temperature capability:

- a. M (Metal) - CrAlY based cermets with the inclusion of a rare earth oxide lubricating phase.
- b. Woven ceramic fiber structures, possibly with a high temperature solid lubricant addition.
- c. Low density ceramic or glass-ceramic sintered structures, possibly with the addition of a solid high temperature lubricant.

The following systems were selected for rig test evaluation based on consideration of 1) the potential of the system to perform satisfactorily in the required temperature range, 2) adaptability of the system for engine hardware application, and 3) material availability.

Quartz Woven Fiber Structure:

This concept utilizes a quartz mat woven together and around metallic attachment devices of an "I" configuration by quartz fibers. The flexible porous structure is infiltrated with silica particles in a manner to provide a graded system dense at the seal surface, to resist the hot gas and particulate erosion environment, and less dense and more compliant at the metal support interface to compensate for the metal/ceramic thermal expansion mismatch. The base of the "I" supports provided a metal surface for brazing to the metal backing, in this case a Mar-M-509 cobalt alloy.

Sprayed NiCoCrAlY with CeO₂ Additive:

The combination of NiCoCrAlY and rare earth oxide system was selected to provide a system with up to 1533K (2300°F) temperature capability. A 10% composition by weight of cerium oxide was co-sprayed with the NiCoCrAlY on a Mar-M-509 cobalt alloy backing. The cerium oxide was included with the expectation that transfer of blade material to the seal would be inhibited above 1366°K (2000°F).

Sprayed, Graded Layers CaO Stabilized ZrO₂/CoCrAlY:

This system is a graded layer, plasma sprayed coating of CoCrAlY and 5% calcia (CaO) stabilized zirconia (ZrO₂). The CoCrAlY constituent provides a method of bonding the ZrO₂ to the Mar-M-509 backing and for grading the structure to accommodate the stresses induced by the metal/ceramic thermal mismatch. The composition of the structure immediately adjacent to the metal backing is 100% metallic. The remaining structure is a composition of graded layers of CaO-ZrO₂/CoCrAlY gradually increasing to 100% CaO-ZrO₂ surface layer. The thickness of the respective layers within the total coating are

summarized in Table VI. The CaO constituent reacts with the ZrO₂ and acts as a stabilizer to prevent the monoclinic-to-tetragonal and reverse phase transformation which occurs in the 1255-1366K (1800-2000°F) temperature range with an accompanying volume change of approximately 10% in unstabilized ZrO₂. This system is expected to provide a temperature capability of approximately 1700K (2600°F) and would provide a thermal barrier for the seal metal substrate.

TABLE VI

CaO Stabilized ZrO₂/CoCrAlY - Coating Thickness Specification

<u>Layers</u>	<u>Thickness</u>	
	<u>mx10⁻⁴</u>	<u>(inch)</u>
Metallic Bond Coat	2.29	(.009)
Six (6) Graded Layers CaO-ZrO ₂ /CoCrAlY	1.78	(.007)
	2.03	(.008)
	2.03	(.008)
	1.52	(.006)
	1.52	(.006)
CaO-ZrO ₂ Ceramic Top Coat	1.52	(.006)
	2.54	(.010)
	15.23	(.060)

2. Test Program

Ten (10) abrasability and twelve (12) erosion tests were conducted as outlined in Table VII. The abrasability tests were conducted using B-1900 alloy blade tip, seal specimen configurations, and the test rig described in Appendix A.

TABLE VII

Abrasability Test Matrix

Blade Tip Seal Systems 1366-1589K (2000-2400°F)
Programmed Penetration Depth - 7.62×10^{-4} m (.030 inch)

<u>Temperature</u>		<u>Blade Tip Speed</u>		<u>Penetration Speed</u>	
<u>K</u>	<u>(°F)</u>	<u>m/s</u>	<u>(ft/sec)</u>	<u>m/s x 10⁻⁵</u>	<u>(inch/sec x 10⁻³)</u>
	Ambient	305	(1000)	2.54	(1.0) *
1366	(2000)	305	(1000)	2.54	(1.0)
1589	(2400)	305	(1000)	2.54	(1.0)
1589	(2400)	305	(1000)	25.4	(10.0)**
1589	(2400)	183	(600)	2.54	(1.0) ***

*Except CaO Stabilized ZrO₂/CoCrAlY System

**Quartz Woven Fiber System Only

***CaO Stabilized ZrO₂/CoCrAlY System Only

Hot gas erosion tests with and without aluminum oxide particles were conducted to evaluate the relative durability of the three (3) selected seal systems using the test rig and procedures described in Appendix A. Test conditions to which each system was exposed are presented in Table VIII.

Testing was initially attempted at 7° impingement angle, but melting of the metal backing support occurred. The impingement angle was increased to 15° to solve this problem and the balance of the testing was done at that angle.

TABLE VIII

Erosion Test Matrix

Blade Tip Seal Systems 1366-1589K (2000-2400°F)

Specimen Temperature		Test Duration		Abrasive Particles
K	(°F)	s	(min)	Included
1366	(2000)	1200	(20)	Yes
1477	(2200)	1200	(20)	Yes
1589	(2400)	1200	(20)	Yes
1589	(2400)	1200	(20)	No

3. Program Details

Abradability

Ten (10) abrasability tests were conducted on the blade tip 1366-1589K (2000-2400°F) systems at various temperatures, surface speeds, and interaction rates. A tabulation of test information is presented in Table XVI of Appendix B.

One (1) rub specimen of each blade tip system was sectioned to inspect the seal structure and to identify wear mechanisms. Scanning electron microscopy and X-ray dispersion analysis were conducted to examine rub surface morphology and any transfer material. Binocular examination was completed to assess specimen appearance and gross rub characteristics. The presectioned specimens for each system are exhibited in Figure 24.

Four (4) bladed rub tests were completed on the quartz woven fiber system. The ambient and 1366K (2000°F) tests produced complete seal grooving with no measurable blade tip wear. However, two (2) tests at 1589K (2400°F) resulted in complete seal disintegration at the rubbing interface and some crystallization directly in line with the torch impingement, adjacent to the rubbing surface. This specimen is shown in Figure 25. The quartz woven fiber system had excellent abrasability but could not survive the 1589K (2400°F) temperature environment.

A silica particle impregnated quartz woven fiber specimen, shown in Figure 24C test #20, was sectioned. No blade material transfer or rub-induced smearing of the seal material was observed. Metallographic examination revealed no indications of densification beneath the rub path and no

difference between the structure beneath the rub path and beneath the unrubbed surface (Figure 26A). Scanning electron microscopy revealed broken fibers and fibers separated from spheroidal matrix particles on the surface of the rubbed portion (Figure 26B). Rub-induced fracture of the spheroidal particles was also observed.

Observations of brittle fracture within the SiO_2 system implies that the low strength, low strain to failure fibers and fiber-to-matrix bonds were broken by the high strength blade material for the specimen sectioned. However, at the 1589K (2400°F) temperature where crystallization of the quartz had initiated, the seal structure was so weakened that under the applied blade interaction load the seal experienced total brittle fracture down to the metal support backing.

Three (3) rub tests were completed on the sprayed NiCoCrAlY with CeO_2 ceramic additive. These tests produced extensive blade wear and no measurable grooving of the seal segment during normal test conditions. However, a light localized groove ($1.78 \times 10^{-4}\text{m}$ (.007 inch) maximum) occurred when the seal specimen shifted during the 1366K (2000°F) test. A review of the situation failed to reveal any significant change in the rub condition which resulted in the specimen groove which could be duplicated. The two (2) high temperature tests resulted in localized seal melting and debonding as shown in Figure 27. Incipient melting of this material occurs near 1532K (2300°F). These specimens lacked abrasability and fell short of the targeted 1589K (2400°F) requirement.

The NiCoCrAlY specimen shown in Figure 27, test #6, was sectioned and exhibited intermittent and some continuous metal transfer deposits attached to the large asperities of the seal material. The large area indented at the right edge of the specimen was a result of localized over heating and a holding fixture failure which resulted in some slight edge grooving. There was no noticeable loss of seal material due to wear or spallation in areas which were rubbed normally.

The seal material structure appeared unaffected beneath the transferred alloy (Figure 28A) except for an oxidized layer between the blade material deposit and the seal material. A thinner oxide layer was observed on the seal surface outside the rub path. The smeared blade material transfer areas (Figure 28B) were characterized by cracks orientated normal to the rub direction, however, no indication of crack propagation into the seal material was observed.

The 10% by weight CeO_2 additive did not provide a sufficiently effective surface shear film to prevent the transfer of blade tip material to the cermet seal, as indicated by the presence of transferred material to the seal surface. However, the dense NiCoCrAlY structure provided sufficiently high surface strength to promote extensive blade transfer and wear.

Three (3) rub tests were completed on the graded layer CaO stabilized ZrO_2 /CoCrAlY spray system. All tests resulted in heavy blade tip wear with no measurable seal grooving. The two (2) specimens tested at 1589K (2400°F) exhibited some spallation and severe delamination at various interfacial locations throughout the specimen thickness. One of these specimens is shown in Figure 29. The delamination occurred when unacceptably high stresses were generated within the ceramic coating. These stresses are a function of the difference between the coefficient of thermal expansion, strength, thickness and cool down rates of the ceramic coating and metal support.

The CaO stabilized ZrO₂/CoCrAlY rub specimen which was sectioned is shown in Figure 24A (test #3). Its surface was characterized by both continuous and intermittent deposits of smeared blade material, similar to the NiCoCrAlY system results. The CaO stabilized ZrO₂ layer exhibited microcracks generally perpendicular to the rub direction both under and adjacent to the rub path. The blade material deposited on the CaO-ZrO₂ surface was completely oxidized as shown in Figure 30A. Rub induced spallation entirely within the Ca-ZrO₂ top layer were also observed. Scanning electron microscopy showed that these portions of the surface exhibited a combination of ceramic particle fracture and particulate rub debris. Figure 30D shows a typical spalled area in the rub path. Note the transferred blade debris on the raised surface of the central plateau and the fractured surface surrounding it. Regions of ceramic material spalled during the test apparently as the result of crack formation and propagation first normal to the rub surface and subsequently parallel to and beneath the rub surface.

Erosion

Erosion testing was initially conducted at the 7° impingement angle but melting of the metal support backing occurred during the 1477K (2200°F) and 1589K (2400°F) tests of the CeO₂/NiCoCrAlY system. To provide valid data a larger impingement angle was necessary to prevent metal support melting which would confuse weight loss measurements. A 15° angle was selected and the last test for that system at 1589K (2400°F) and subsequent testing on the quartz fiber and ZrO₂/CoCrAlY systems were conducted at that impingement angle.

The quartz woven fiber specimen lasted only about ten (10) seconds during the particulate erosion tests. After this time period, all three (3) specimens tested were eroded to the backing support. The rapidity with which this material eroded did not provide sufficient data points to calculate an erosion curve for this system. It should be noted, however, that the particulate erosion rate was exceedingly high in comparison to the other two high temperature systems.

Volume loss/time comparison of the other two systems is depicted in Figure 31. The CeO₂/NiCoCrAlY system provided slightly better erosion resistance than the graded ZrO₂/NiCoCrAlY system. The ZrO₂ top layer, however, was dissipated very quickly and, as a result, the steady state erosion rate test points shown in Figure 31 are derived from conditions after significant removal of the ZrO₂ material from the impingement location had occurred.

The actual weight loss for each erosion specimen for the three (3) blade tip systems is recorded in Table IX. Figure 32 is a graphic comparison of weight loss vs. time for the metallic NiCoCrAlY system and the CaO stabilized ZrO₂/CoCrAlY ceramic system. Highlighted in this figure is the larger initial rate of weight loss experienced by the ceramic material during the first 300 seconds (5 minutes). Figure 33, 34 and 35 display the respective quartz fiber, CeO₂/NiCoCrAlY and CaO stabilized ZrO₂/CoCrAlY tested erosion specimens.

Table IX

Cumulative Erosion Weight Loss (kg) for Blade Tip Seal Systems

Designation	Test Temperature K (°F)	Elapsed Time (s)			
		300	600	900	1200
		Weight Loss (kg x 10 ⁻³)			
Quartz Woven Fiber System	1366 (2000)	Base Material Exposed			
	1477 (2200)	Base Material Exposed			
	1589 (2400)	Base Material Exposed			
	1589 (2400)*	.263	.298	2.853	Base Material Exposed
Sprayed CaO ₂ / NiCoCrAlY	1366 (2000)	.237	.517	.794	1.052
	1477 (2200)**	.166	.376	.536	.796
	1589 (2400)	.565	1.215	1.493	1.805
	1589 (2400)*	Backing Melted, Deposited on Seal Surface			
Sprayed CaO Stabilized ZrO ₂ /CoCrAlY	1366 (2000)	1.340	2.250	2.850	3.360
	1477 (2200)	1.225	1.975	2.545	3.040
	1589 (2400)	1.060	1.725	2.185	2.585
	1589 (2400)*	+.070	+.085	+.103	+.055

* Hot gas erosion evaluation - no particulate

** Metal backing melted and some material deposited on seal surface during this test

+ Denotes weight gain resulting from intermediate layer oxidation

4. Results and Conclusions

All abrasability tests on the $\text{CeO}_2/\text{NiCoCrAlY}$ and CaO stabilized $\text{ZrO}_2/\text{CoCrAlY}$ spray systems resulted in extensive blade wear and no seal grooving. The high temperature tests for $\text{CeO}_2/\text{NiCoCrAlY}$ system resulted in localized seal melting and debonding. The ZrO_2 specimens tested at 1589K (2400°F) exhibited some spallation and severe delamination at various interfacial locations throughout the specimen. On the other hand, the quartz woven fiber system produced complete seal grooving with no measurable blade tip wear. However, the two tests at 1589K (2400°F) exhibited seal disintegration at the rubbing interface and some crystallization directly in line with the torch impingement, adjacent to the rubbing surface.

The quartz woven fiber specimen lasted only about 10 seconds during the particulate erosion tests. The rapidity with which this material eroded did not provide sufficient data points to calculate an erosion rate curve for this system, but the erosion rate was exceedingly high in comparison to the other two systems. The $\text{CeO}_2/\text{NiCoCrAlY}$ system provided slightly better particulate erosion resistance than the graded CaO stabilized $\text{ZrO}_2/\text{CoCrAlY}$ system. The ZrO_2 top layer, however, was removed very quickly. As a result, the steady state erosion rate test points are derived from conditions after significant removal of the ZrO_2 top coat from the impingement location had occurred. Therefore, the actual erosion rate of the CaO stabilized ZrO_2 top coat is expected to be somewhat greater than the volume removal reported here.

The temperature capability of the three (3) systems evaluated is somewhat less than 1589K (2400°F). The quartz fiber and metallic $\text{CeO}_2/\text{NiCoCrAlY}$ systems are basically limited due to material thermal properties, i.e. incipient melting and loss of structural strength. The graded CaO stabilized $\text{ZrO}_2/\text{CoCrAlY}$ system is inherently capable of withstanding temperatures in excess of 1589K (2400°F) but requires redesign to limit thermally induced stresses within the material capabilities. The maximum temperature capability of the quartz fiber system is close to 1366K (2000°F). Other problems such as attachment difficulties further reduce the attractiveness of this system. The $\text{CeO}_2/\text{NiCoCrAlY}$ system is estimated to have a maximum long term temperature capability of approximately 1477K (2200°F).

The thermal effects of 1589K (2400°F) during abrasability testing indicated that these systems lacked capability to perform satisfactorily at the 1589K (2400°F) temperature condition. Because of interest in a system which could satisfy the maximum temperature requirement, and because metal systems could not be expected to perform adequately at 1589K (2400°F), a ceramic system was recommended for further evaluation.

A plasma sprayed ZrO_2 system, with a yttria (Y_2O_3) stabilizer for greater thermal stability than CaO and with a structure refined to reduce thermal stresses, was recommended for further evaluation in the final phase of the program.

C. Graded Layer Y₂O₃ Stabilized ZrO₂/CoCrAlY Blade Tip Seal System 1589K (2400°F)

1. Seal System Description

Experience with porous sprayed graded Y₂O₃ stabilized ZrO₂/CoCrAlY seal system being developed by P&WA for 1922K (3000°F) applications indicated potential for good abrasability with an untreated B-1900 metal blade tip and reasonable hot gas erosion resistance. This system utilizes a 75% dense surface layer of yttria (Y₂O₃) stabilized zirconium oxide (ZrO₂) over a graded ZrO₂/CoCrAlY intermediate layer. On the basis of this experience, four (4) variations of the basic system with modifications to reflect the reduced temperature, 1589K (2400°F), requirement were selected for rig test evaluation. A review of thermal and stress analyses conducted on higher temperature configurations considering both the lower maximum seal surface temperature and the smaller thermal gradient through the seal thickness led to a determination of the top and intermediate layers. The fabrication of the structure in terms of a continuously sprayed or layered configuration was selected as a variable to evaluate. Also, addition of CeO₂ to the ZrO₂ for potential benefit as a high temperature lubricant and to inhibit blade tip material transfer was the second variable to be investigated. Details of the four (4) selected system variations are summarized in the following listing.

Layered Sprayed Y₂O₃ Stabilized ZrO₂/CoCrAlY

This system consisted of five (5) discrete layers. The all-ceramic surface layer of 1.39-1.65 x 10⁻³m (.055-.065 inch) was sprayed to produce a proposed 70-80% dense structure to promote abrasability. The graded metal/ceramic intermediate layers comprised a total thickness of 1.90-2.67 x 10⁻³m (.075-.085 inch). A thin NiCrAl bond coat was sprayed directly on the Mar-M-509. Coating details are delineated in Table X.

TABLE X

Layered Sprayed Y₂O₃ Stabilized ZrO₂/CoCrAlY - Coating Details

<u>m x 10⁻²</u>	<u>Thickness</u> <u>(inch)</u>	<u>% ZrO₂</u> <u>Powder (Sprayed Struct)</u>	<u>% Metallic</u> <u>Powder (Sprayed Struct)</u>
7.62-12.7	(.003-.005)	---	100
63.5--88.9	(.025-.035)	40 w/o (20 v/o)	60 w/o (80 v/o)
63.5--88.9	(.025-.035)	70 w/o (50 v/o)	30 w/o (50 v/o)
63.5--88.9	(.025-.035)	85 w/o (70 v/o)	15 w/o (30 v/o)
139.7-165.1	(.055-.065)	100	---

This system is essentially identical to a system developed for 1922K (3000°F) applications which indicated good abrasability and erosion resistance potential as discussed above except that the configuration has been modified to accommodate the lower temperature requirements.

Layered Sprayed Y₂O₃ Stabilized ZrO₂/CoCrAlY Plus CeO₂

This system is identical to the above system except that 10% by weight of CeO₂ was added to the ZrO₂ surface layer to evaluate CeO₂ potential to inhibit blade material transfer. The surface layer was again sprayed to produce a proposed 70-80% dense structure.

Continuously Graded Sprayed Y₂O₃ Stabilized ZrO₂/CoCrAlY

This system utilized a continuous spraying technique while continually changing the ZrO₂/CoCrAlY ratio during spraying. The surface layer was again sprayed to produce a proposed 70-80% dense structure. A thin CoCrAlY bond coat was applied to the cast Mar-M-509 substrate and treated by a proprietary process before starting the continuous spraying process. Details of this coating are summarized in Table XI.

TABLE XI

Continuously Graded Sprayed Y₂O₃ Stabilized ZrO₂/CoCrAlY - Coating Details

<u>Material</u>	<u>Thickness</u>		
	<u>m x 10⁻³</u>	<u>(inch)</u>	
CoCrAlY	12.7	(.005)	Complete System Continuously Sprayed and Graded
ZrO ₂ /CoCrAlY	215.9-241.3	(.085-.095)	
ZrO ₂	139.7-165.1	(.055-.065)	

This system is essentially identical to the 1922K (3000°F) system developed for P&WA except that the coating thickness has been reduced for 1589K (2400°F) application.

Continuously Graded Sprayed Y₂O₃ Stabilized ZrO₂/CoCrAlY Plus CeO₂

This system is identical to the previous system except 10% by weight of CeO₂ was added to the ZrO₂ constituent throughout the coating. Again, the surface layer was sprayed to produce a proposed 70-80% dense structure.

2. Test Program

Eight (8) abrasability and four (4) erosion tests were conducted on the four (4) ceramic system variations; two (2) abrasability and one (1) erosion test on each system. Abrasability tests were conducted using B-1900 alloy blade material. Seal specimen configurations and the test rig utilized for testing are described in Appendix A. Abrasability test conditions are outlined in Table XII.

TABLE XII

Abrasability Test Matrix

1589K (2400°F) Ceramic Seal Systems

Programmed Interaction Depth - 7.62×10^{-4} m (.030 inch)

Temperature <u>K</u>	<u>(°F)</u>	<u>Blade Tip Speed</u>		<u>Penetration Speed</u>	
		<u>m/s</u>	<u>(ft/sec)</u>	<u>m/s x 10⁻⁵</u>	<u>(inch/sec x 10⁻³)</u>
1589	(Ambient)	305	(1000)	2.54	(1.0)
	(2400)	305	(1000)	2.54	(1.0)

A hot gas erosion test with aluminum oxide particulate was conducted on each ceramic system. Specimen temperature was held constant at 1589K (2400°F) for the duration of the 1200 second (20 min) test.

3. Program Details

Abradability

A total of eight (8) abrasability tests were conducted on the four (4) modified ceramic 1589K (2400°F) spray systems. A tabulation of the detailed test information is listed in Table XVI of Appendix B.

Surface hardness measurements were recorded as an initial attempt to correlate physical property and performance of the seal system. No direct correlation could be made with the available data. Both the graded layer and continuously graded systems experienced similar rub results. The CeO₂ additive variations did not exhibit any indications of prohibiting blade material transfer to the ceramic seal.

A listing of the pertinent comparative abrasability results is depicted in Table XIII. Seal grooving up to 2.02×10^{-4} m (.008 inch) in one location was measured on four (4) of the eight (8) tests conducted. It should be noted that seal material removal also resulted from surface fatigue of the metal transfer/ceramic rubbed area for the remaining specimens, measured up to 1.01×10^{-4} m (.004 inch). Since this material removal does not directly involve the groove mechanism, it was not included in volume ratio determination presented in Table XVI. Post-test photographs of the graded layer and continuously graded Y₂O₃ stabilized ZrO₂ abrasability specimens are shown in Figures 36 and 37 respectively.

The most important characteristic illustrated by these modified ceramic seal configurations were their ability to withstand the 1589K (2400°F) temperature environment and maintain their structural integrity. No seal spalling or delamination was noted for any of the four (4) temperature tests.

The two seals without the CeO₂ additive which were tested at 2400F, shown in Figures 36B and 37B, were sectioned and microscopically examined. A typical radial section through each system is shown in Figure 38 and illustrates the difference in metal distribution through the graded ceramic-metal region and density of the abrasable ceramic layer.

The density of the top layer of the continuously graded system, measured using a point count method, was approximately 95% except for a local area approximately 2.54×10^{-4} m (0.010 inch) deep under the wear groove as shown in Figure 39. This area was approximately 50% dense and discolored. The cause of this local condition is unknown. Several small radial cracks and one large laminar crack approximately 7.62×10^{-4} m (0.030 inch) below the ceramic surface near the grooved area were also noted. Scanning electron microscope and spectroscopic examination indicated no metal transfer in the wear groove and a smeared and fused surface appearance in the groove as shown in Figure 40. An unrubbed surface area is included in Figure 40 for comparison.

The density of the top layer of the graded layer system varied radially over most of the area examined. The density of the top 2.54×10^{-4} m (0.010 inch) was 40% and the density of the remaining ceramic layer below this depth was 64%. No radial or laminar cracking was observed in this specimen. This specimen was sectioned through the rubbed area in the circumferential direction instead of the axial direction as done for the continuously graded system. Therefore, it is not certain that the reduced density noted is not a localized condition similar to the reduced density area in the continuously graded system.

Transferred blade tip material was smeared over the surface and into the irregularities over most of the rubbed surface of both specimens to a depth of $0.254 - 0.508 \times 10^{-4} \text{ m}$ (0.001 - 0.002 inch). This was mostly oxidized although some of the deeper areas in surface irregularities were unoxidized.

Erosion

The erosion tests were conducted with a 15° impingement angle and other test conditions the same as the blade tip system testing described earlier. Slightly better erosion resistance resulted with testing of the continuously graded systems. The best erosion performance occurred for the specimens with the hardest top surface structure. Slight delamination occurred in layers within the top coat for the continuously graded variations, not typical of a continuously sprayed system. On the other hand, the graded layer system exhibited heavy zirconia top coat delamination at the edge of the specimen nearest the flow nozzle. The resultant chipped material contributed significantly to the comparatively higher erosion rate. The erosion post test specimens for each ceramic system variation is shown in Figure 41. Actual weight loss for each specimen for the four (4) systems is recorded in Table XIV. Table XV lists pertinent erosion results including volume loss/time at 1589K (2400°F).

The four (4) ceramic system variations of Y_2O_3 stabilized $\text{ZrO}_2/\text{CoCrAlY}$ collectively showed improved results over the CaO stabilized $\text{ZrO}_2/\text{CoCrAlY}$ ceramic system. Improved abrasability and increased thermal shock resistance was obtained without any sacrifice to the erosion resistance characteristics. The improved abrasability was characterized by measurable seal grooving exhibited by the Y_2O_3 stabilized ZrO_2 systems. (The CaO stabilized ZrO_2 system produced no seal wear at any of the test conditions.) The improvement in ceramic structural integrity was demonstrated by the fact that no delamination or seal spalling resulted from any of the eight (8) tests.

The erosion rate (volume loss/time) for the CaO and Y_2O_3 stabilized systems were basically the same. However, the erosion rate noted for the Y_2O_3 system reveals the capability of the ceramic system more accurately than the CaO stabilized ZrO_2 testing. (As described in Figure 42, a high initial weight loss was experienced by the CaO stabilized system (total loss of ZrO_2 top coat). These steady state erosion rates reflected the intermediate layer structural strength and not the ceramics. As a result, it is expected that the yttria stabilized system should have somewhat greater erosion resistance than the previously tested CaO stabilized $\text{ZrO}_2/\text{CoCrAlY}$ system.

4. Results and Conclusions

The abrasability testing of the ceramic system variations, in general, resulted in slight seal grooving with no seal spalling or delamination occurring in any testing. The Y_2O_3 stabilized ZrO_2 systems sprayed to the configurations documented earlier produced structures that maintained their integrity during a thermal cycle up to 1589K (2400°F). This result coupled with the fact that the seal segments did groove represents a significant improvement over the earlier CaO stabilized ZrO_2 configuration. There was no significant difference in abrasability results between the graded layer and continuously sprayed ceramic systems. The cerium oxide additive did not provide any visible advantage in prohibiting blade material transfer to the seal material.

Table XIII

Abradability Results For 1589K (2400°F) Ceramic Systems

Test#	Material	Type	Surface Hardness R _s 45Y *		Actual Test Temperature		Max Blade Wear		Max Seal Groove	
			Ave	Range	K	(°F)	mx10 ⁻⁴	(inch)	mx10 ⁻⁴	(inch)
29	ZrO ₂ /CoCrAlY Without CeO ₂	Continuously Graded	76	(72-80)	Ambient		6.60	.026	0.0	.000
30	"	"	77	(74-81)	1561	(2350)	6.60	.026	2.03	.008
31	"	Graded Layers	71	(68-77)	Ambient		8.89	.035	.76	.003
32	"	"	70	(60-78)	1589	(2400)	7.62	.030	0.0	.000
33	ZrO ₂ /CoCrAlY With CeO ₂	Graded Layers	70	(65-75)	Ambient		7.87	.031	0.0	.000
34	"	"	65	(54-75)	1617	(2450)	8.63	.034	.51	.002
35	"	Continuously Graded	79	(76-83)	Ambient		8.38	.033	0.0	.000
36	"	"	79	(74-82)	1617	(2450)	8.38	.033	.25	.001

* R_s45Y - Measurements taken with 45 kg load - 1.27 x 10⁻²m (.50 inch) diameter ball

Table XIV

Cumulative Erosion Weight Loss (kg) For 1589K (2400°F) Ceramic Seal Systems

<u>Designation</u>	<u>Test Temperature</u> K (°F)		<u>Elapsed Time (s)</u>			
			300	600	900	1200
			<u>Weight Loss (kg x 10⁻³)</u>			
Y ₂ O ₃ Stabilized ZrO ₂ /CoCrAlY Without CeO ₂ - Graded Layers	1589	(2400)	.674	1.134	1.624	2.154
Y ₂ O ₃ Stabilized ZrO ₂ /CoCrAlY With CeO ₂ - Graded Layers	1589	(2400)	.838	1.472	2.202	2.877
Y ₂ O ₃ Stabilized ZrO ₂ /CoCrAlY Without CeO ₂ - Continuously Graded	1589	(2400)	.376	.850	1.230	1.580
Y ₂ O ₃ Stabilized ZrO ₂ /CoCrAlY With CeO ₂ - Continuously Graded	1589	(2400)	.305	.582	.845	1.080

Table XV
Erosion Results For 1589K (2400°F) Ceramic Systems

<u>Materials</u>	<u>Type</u>	<u>Surface Hardness (R_{545Y})</u>		<u>Erosion Rate</u>		<u>Comments</u>
		Ave	Range	m ³ /sx10 ⁻¹⁰	(cc/min)	
ZrO ₂ /CoCrAlY Without CeO ₂	Graded Layers	69	(66-74)	3.32	(.020)	Surface cracking and some delamination on top layer
ZrO ₂ /CoCrAlY With CeO ₂	Graded Layers	70	(64-74)	4.43	(.027)	Very extensive erosion to intermediate layer near impingement area
ZrO ₂ /CoCrAlY Without CeO ₂	Continuously Graded	71	(62-78)	2.66	(.016)	Localized heavy erosion at closest to nozzle impingement area
ZrO ₂ /CoCrAlY With CeO ₂	Continuously Graded	80	(78-83)	1.66	(.010)	Relative light erosion, some delamination within ceramic top coat

The erosion results, measured in steady state volume loss/time, were basically unchanged from results of the first round ceramic material. Erosion results showed slightly better performance for the continuously graded systems, which were also measured to be the harder surface structures. Slight delamination was occurring in layers within the ceramic top coat for the continuously graded variation, untypical for a continuously sprayed system. The graded layer system exhibited some zirconia top coat delamination at the specimen edge closest to the particulate impingement. This result contributed significantly to the increased erosion rate.

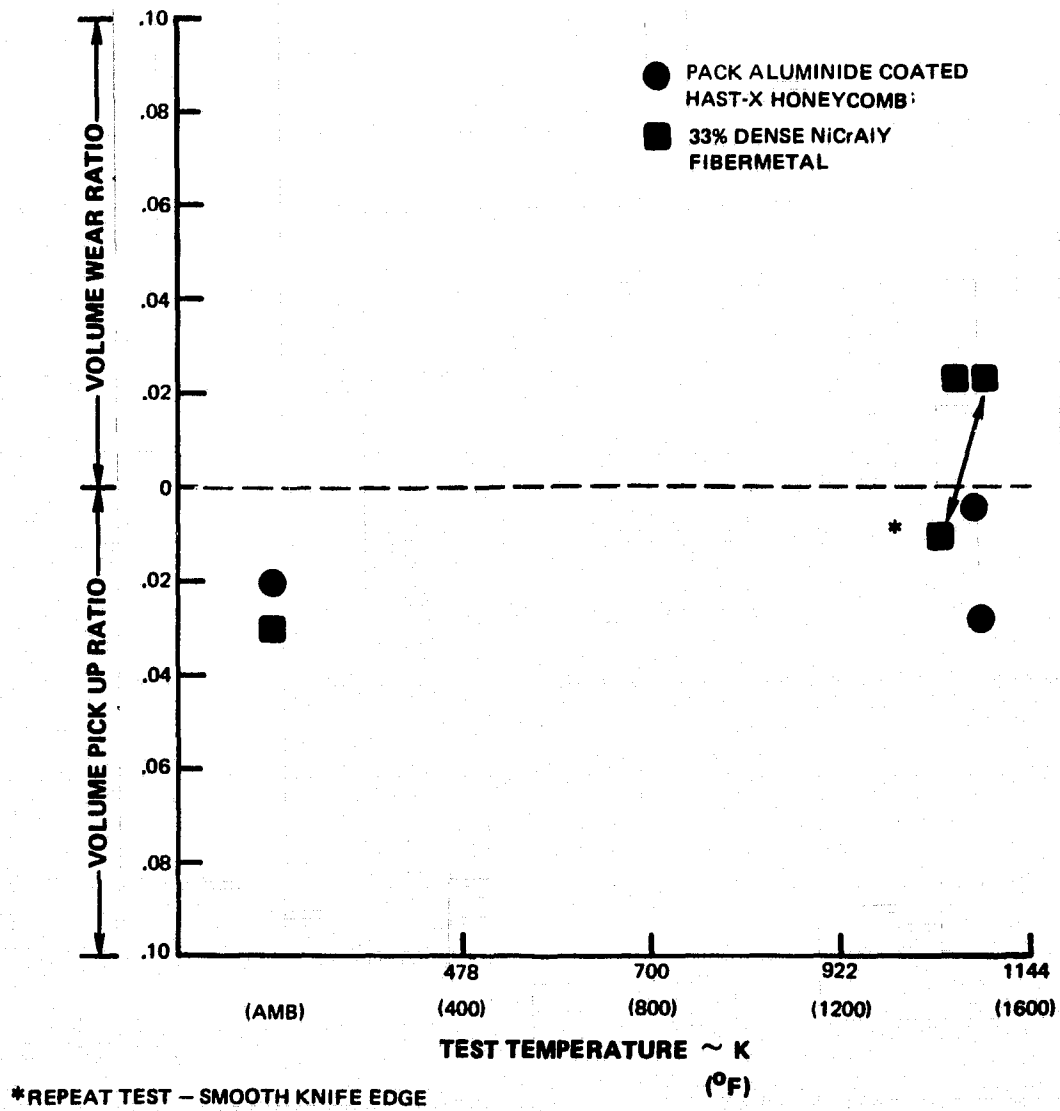


FIGURE 1

VOLUME RATIO VS TEST TEMPERATURE

SURFACE SPEED = 305 M/S (1000 FT/SEC)
 INTERACTION RATE = $2.54 \text{ M/S} \times 10^{-5}$ (1.0×10^{-3} INCH/SEC)

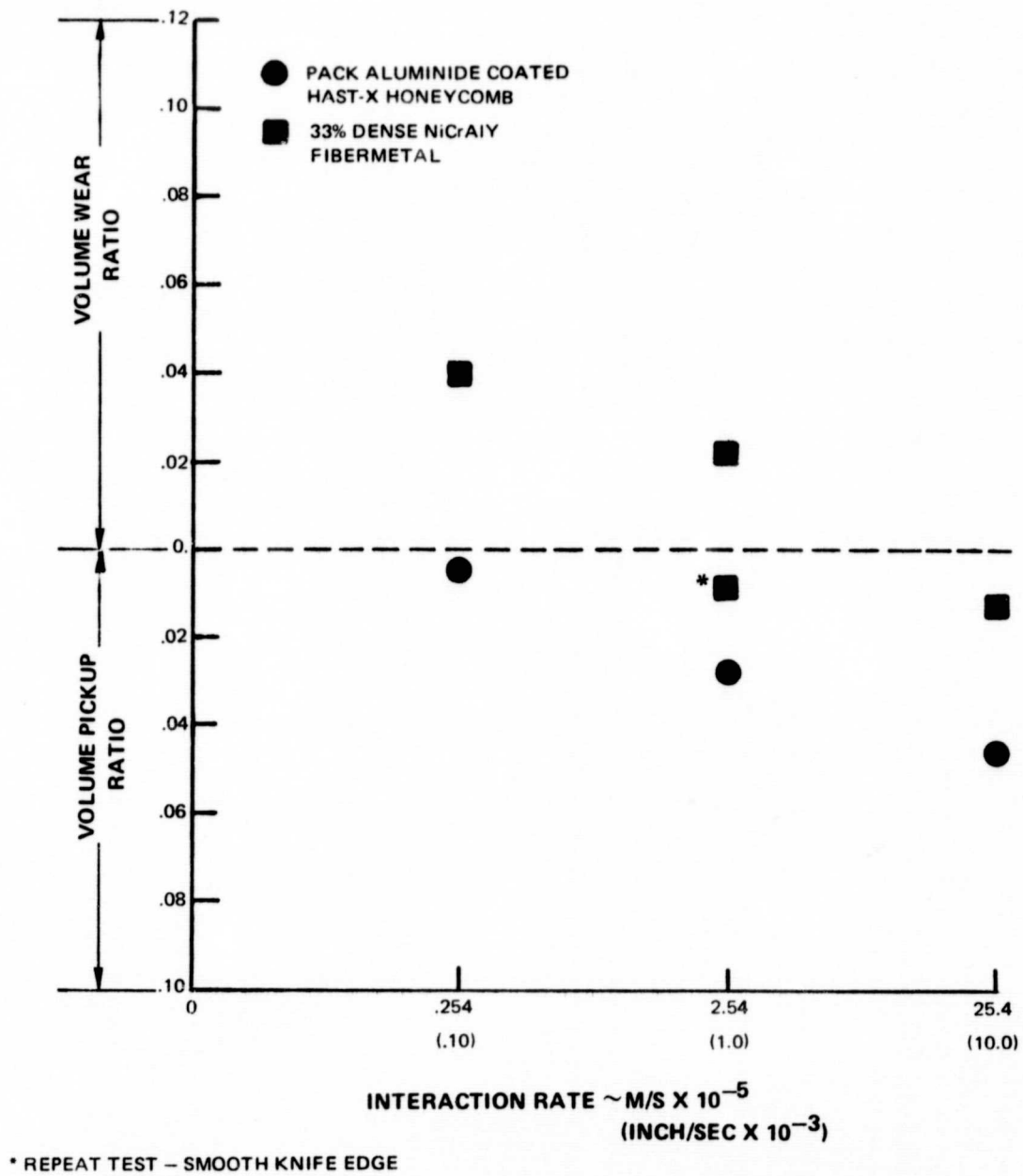


FIGURE 2
VOLUME RATIO VS INTERACTION RATE

SURFACE SPEED = 305 M/S (1000 FT/SEC)
TEMPERATURE = 1366 K (2000°F)

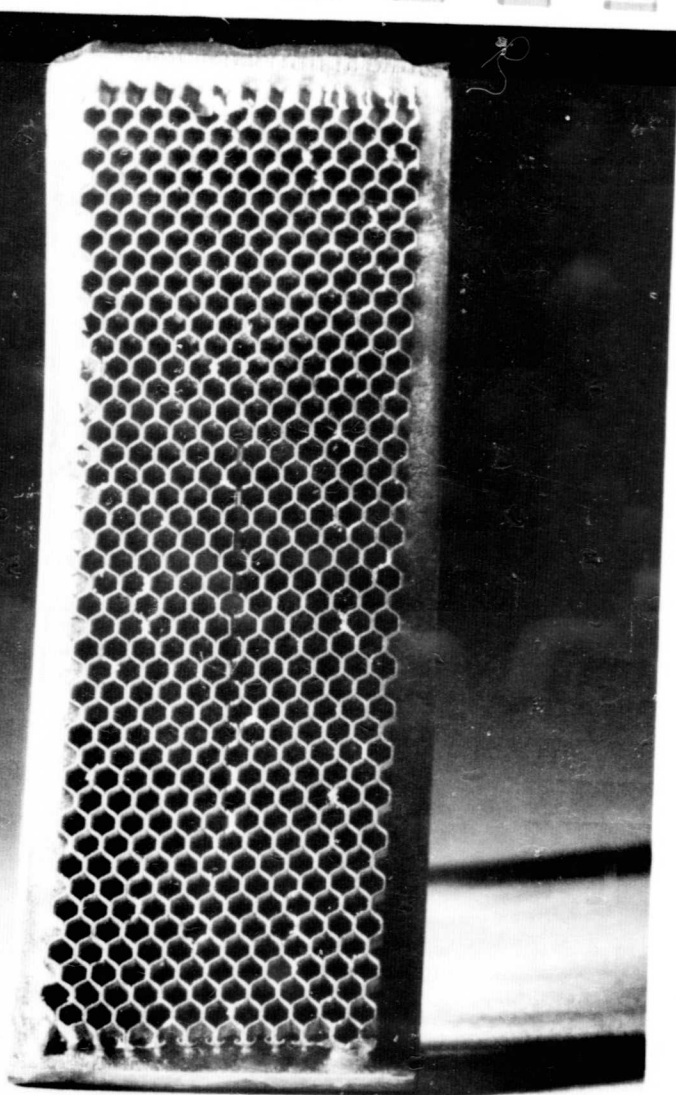


FIGURE 3

TEST #10 PACK-ALUMINIDE COATED HAST-X HONEYCOMB VS. WASPALOY KNIFE EDGE. TEST CONDITIONS: 305 m/s (1000 FT/SEC) SURFACE SPEED, 2.54×10^{-4} m/s (.010 INCH/SEC) INTERACTION RATE AND 1366K (2000°F) TEMPERATURE. NOTE FOUR LOCATIONS OF HEAT DISCOLORATION WITH MAXIMUM PICKUP 3.30×10^{-5} m (.0013 INCH). NO KNIFE EDGE WEAR.

XPN-52375



XPN-52375

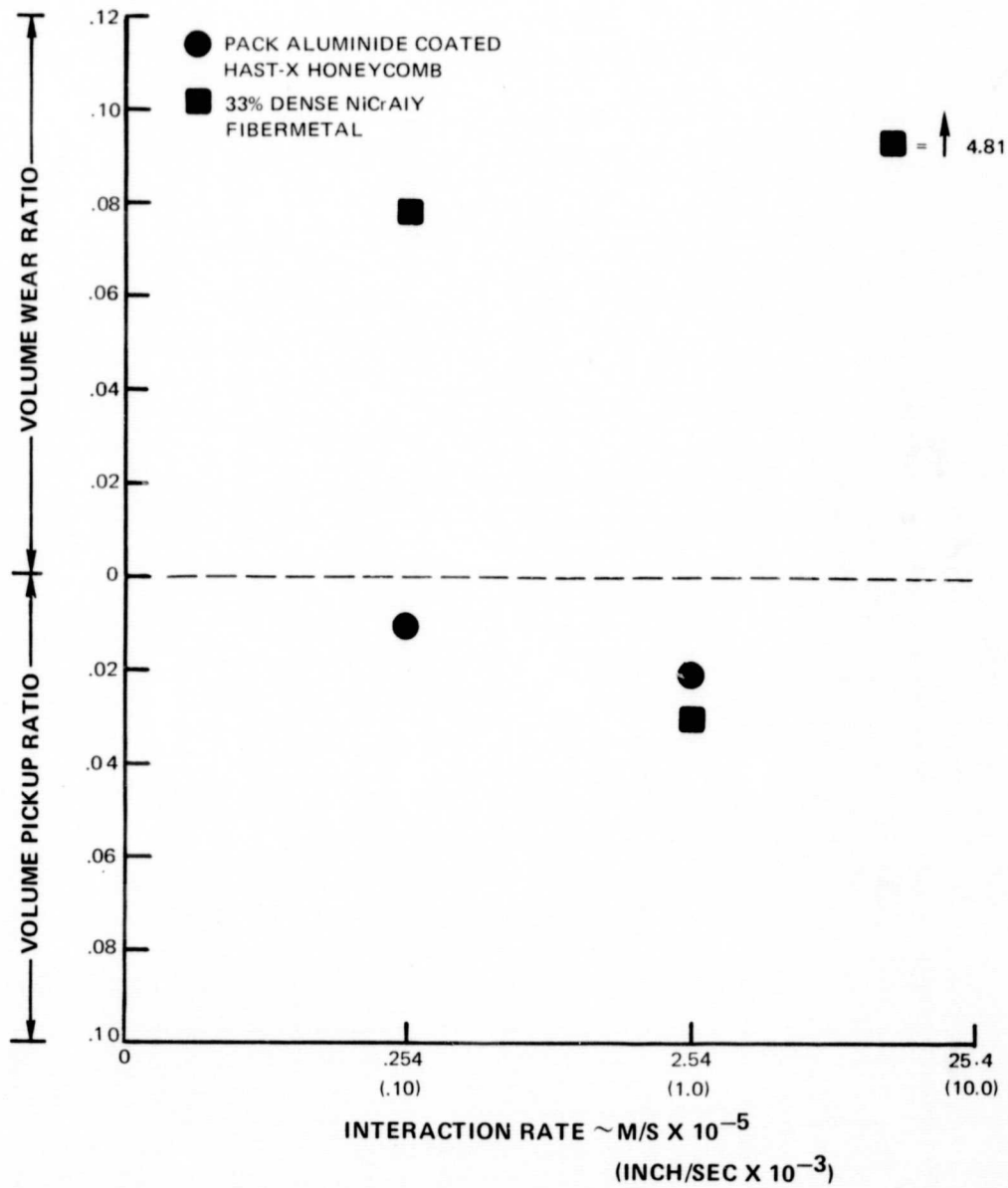


FIGURE 4

VOLUME RATIO VS INTERACTION RATE

SURFACE SPEED = 305 M/S (1000 FT/SEC)
TEMPERATURE = AMBIENT

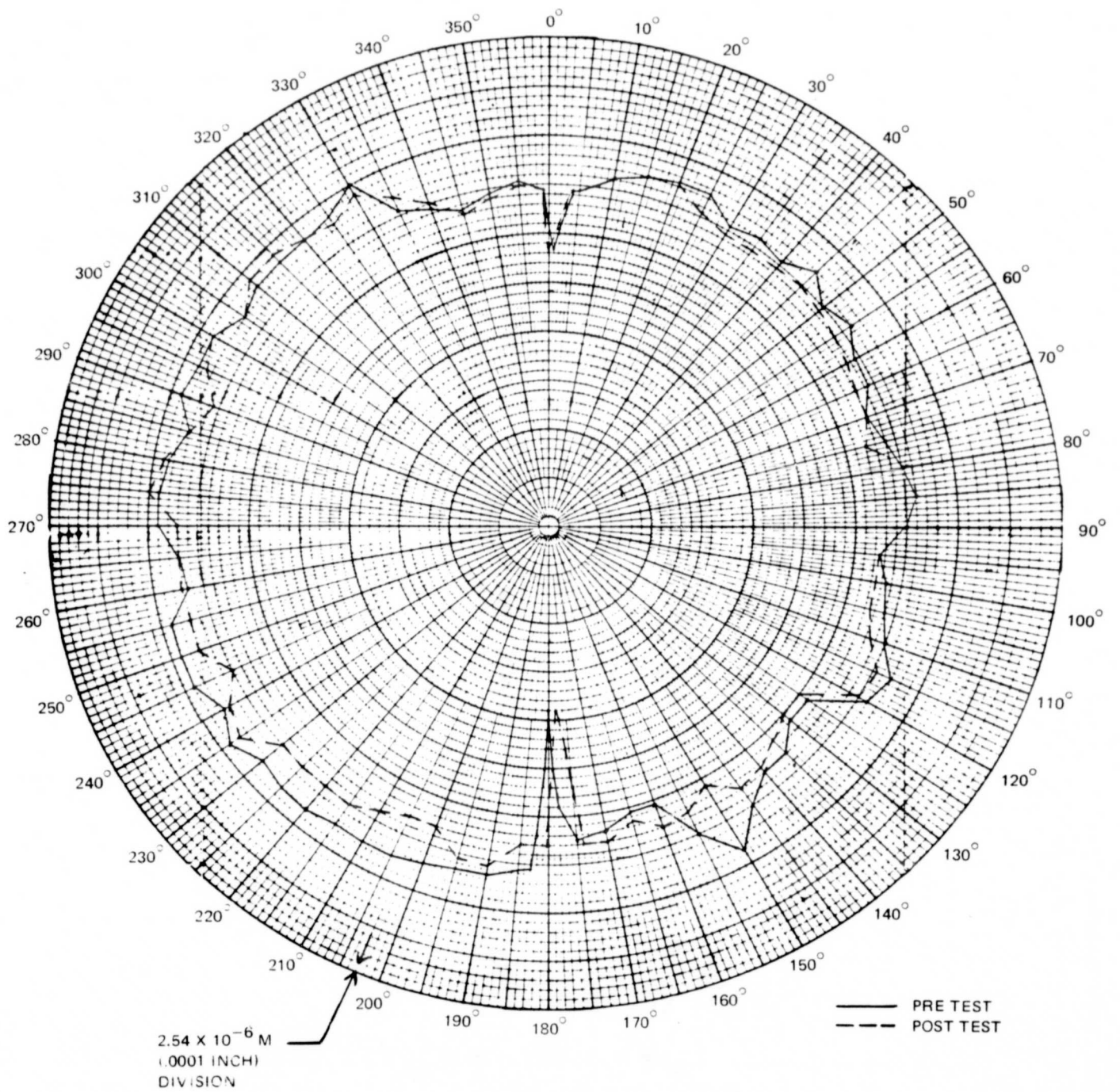


FIGURE 5

STANDARD KNIFE EDGE. SURFACE PROFILE

FIBERMETAL TEST # 12

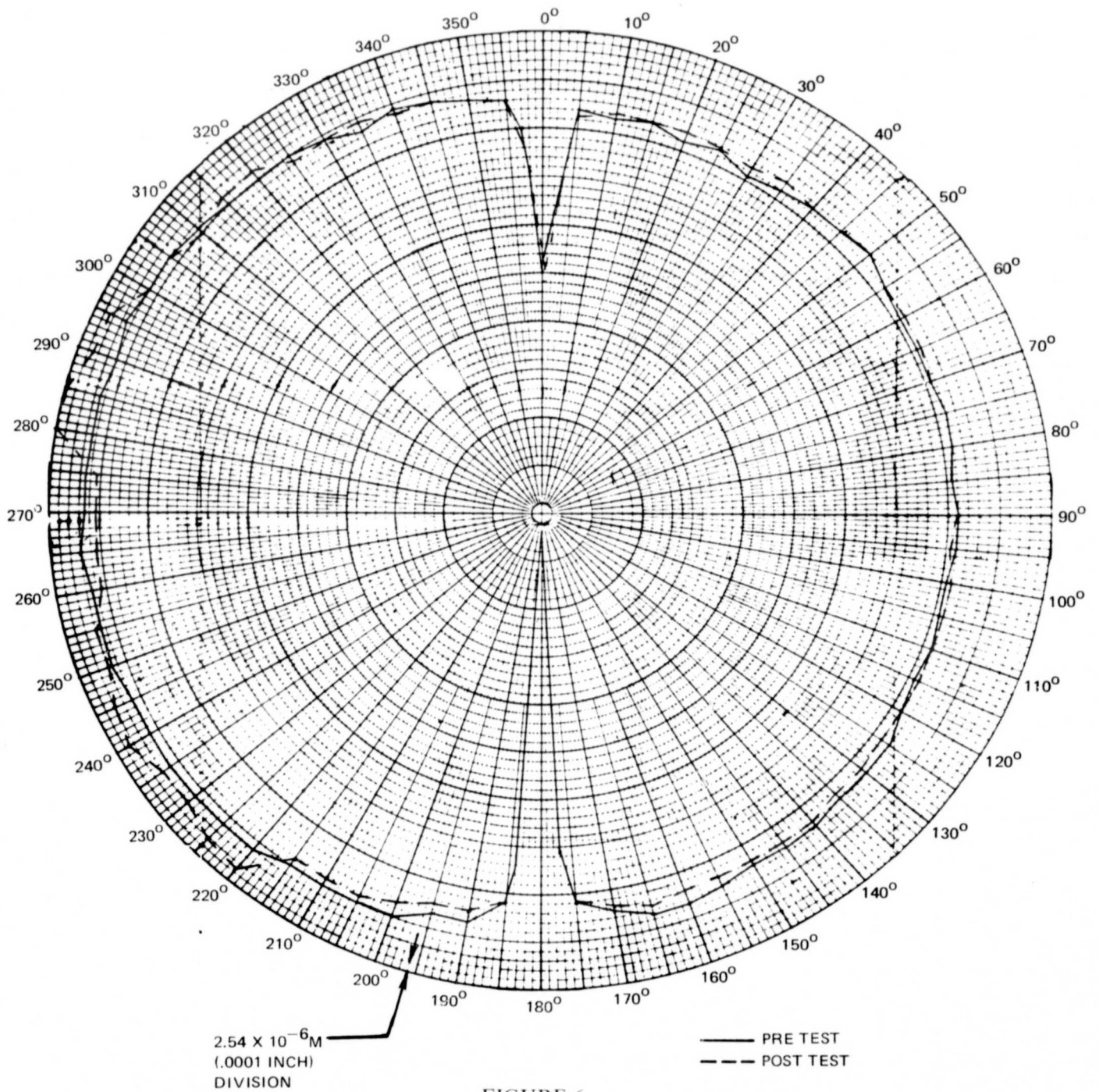


FIGURE 6

SMOOTH KNIFE EDGE, SURFACE PROFILE

FIBERMETAL TEST # 26
(REPEAT TEST)

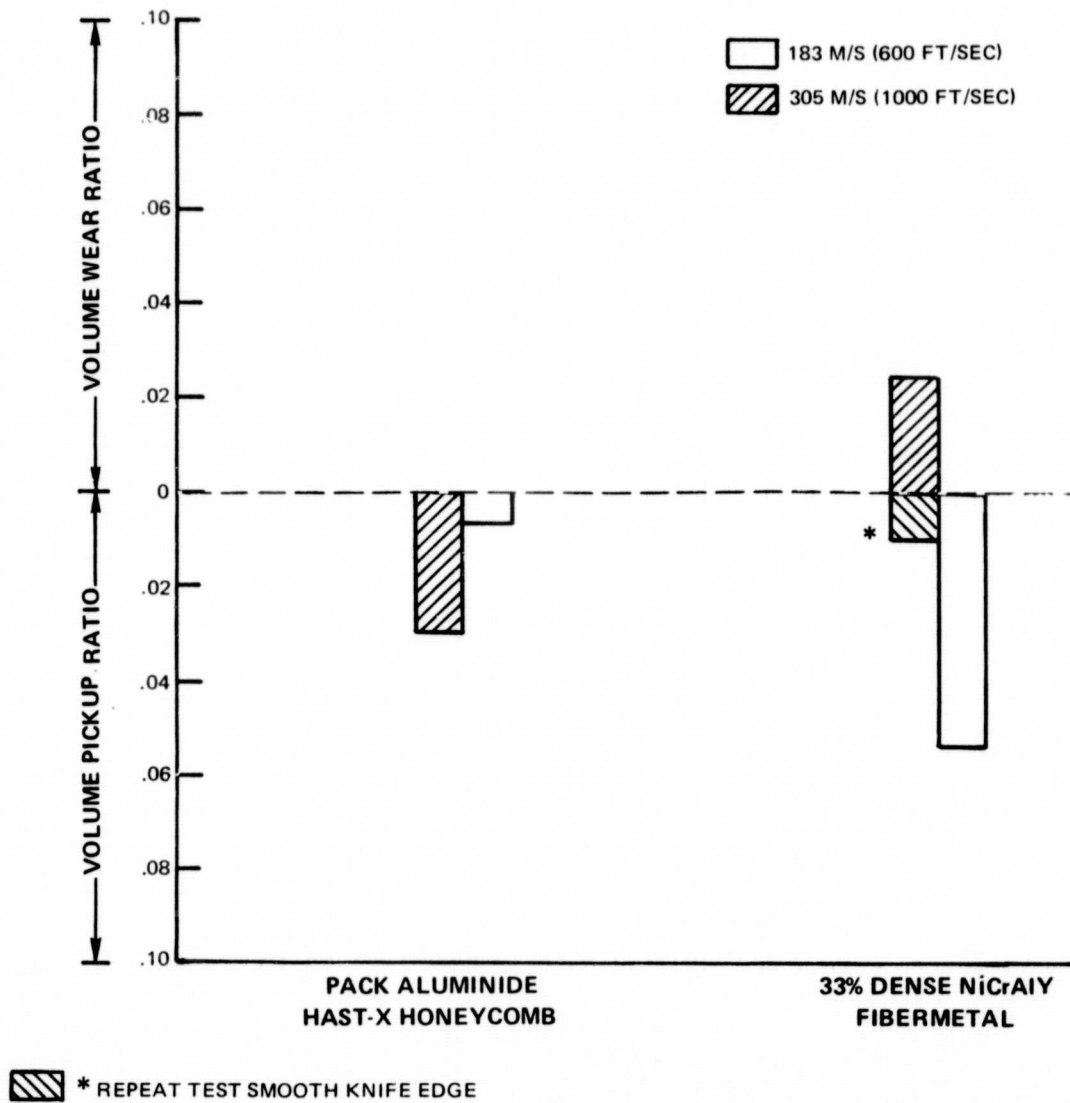


FIGURE 7
VOLUME RATIO VS SURFACE SPEED

INTERACTION RATE = $2.4 \text{ M/S} \times 10^{-5}$ (.001 INCH/SEC)
TEMPERATURE = 1366 K (2000°F)

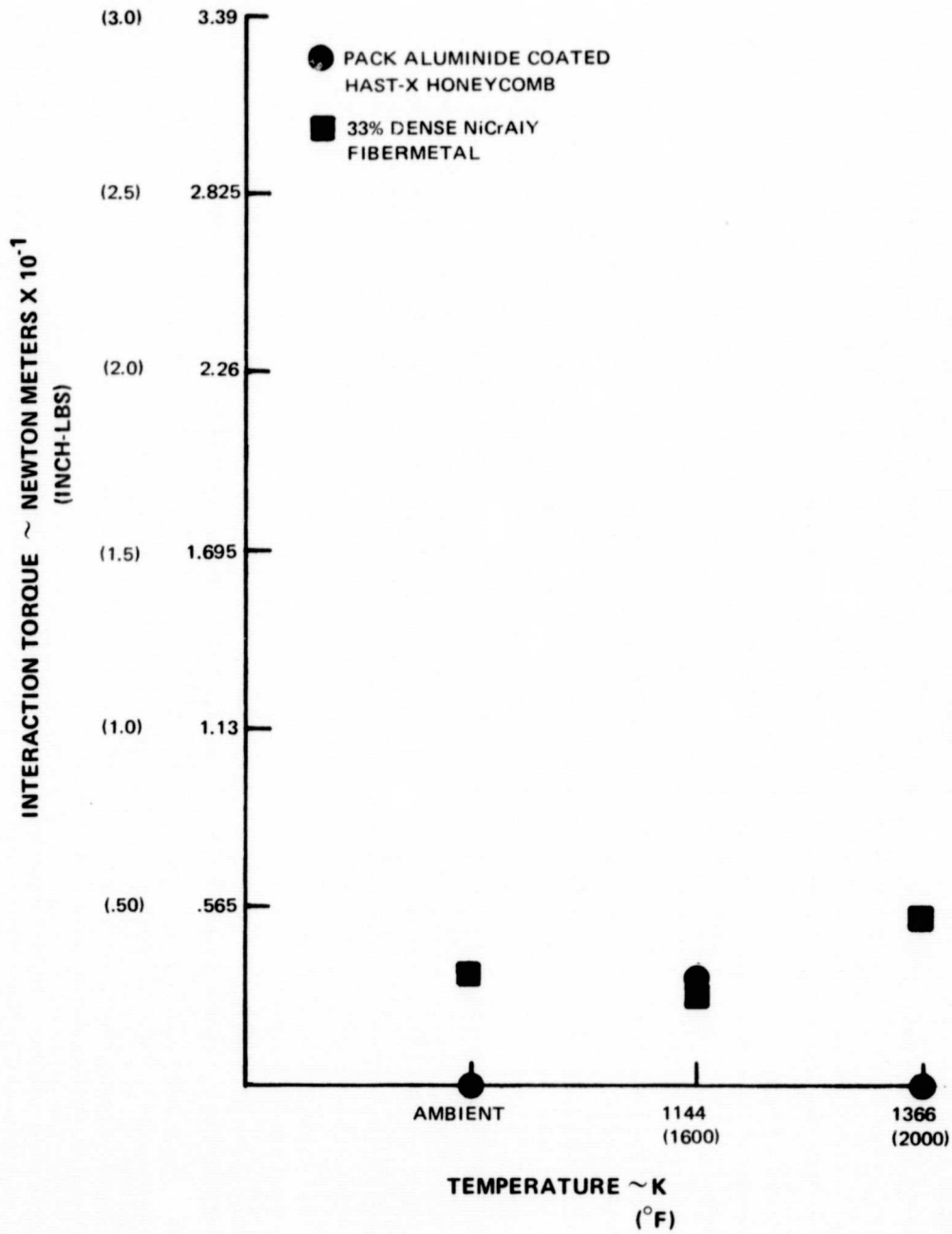


FIGURE 8

INTERACTION TORQUE VS TEMPERATURE

SURFACE SPEED 305 M/S (1000 FT/SEC)
INTERACTION RATE $2.54 \text{ MS} \times 10^{-6}$ (.001 INCH/SEC)

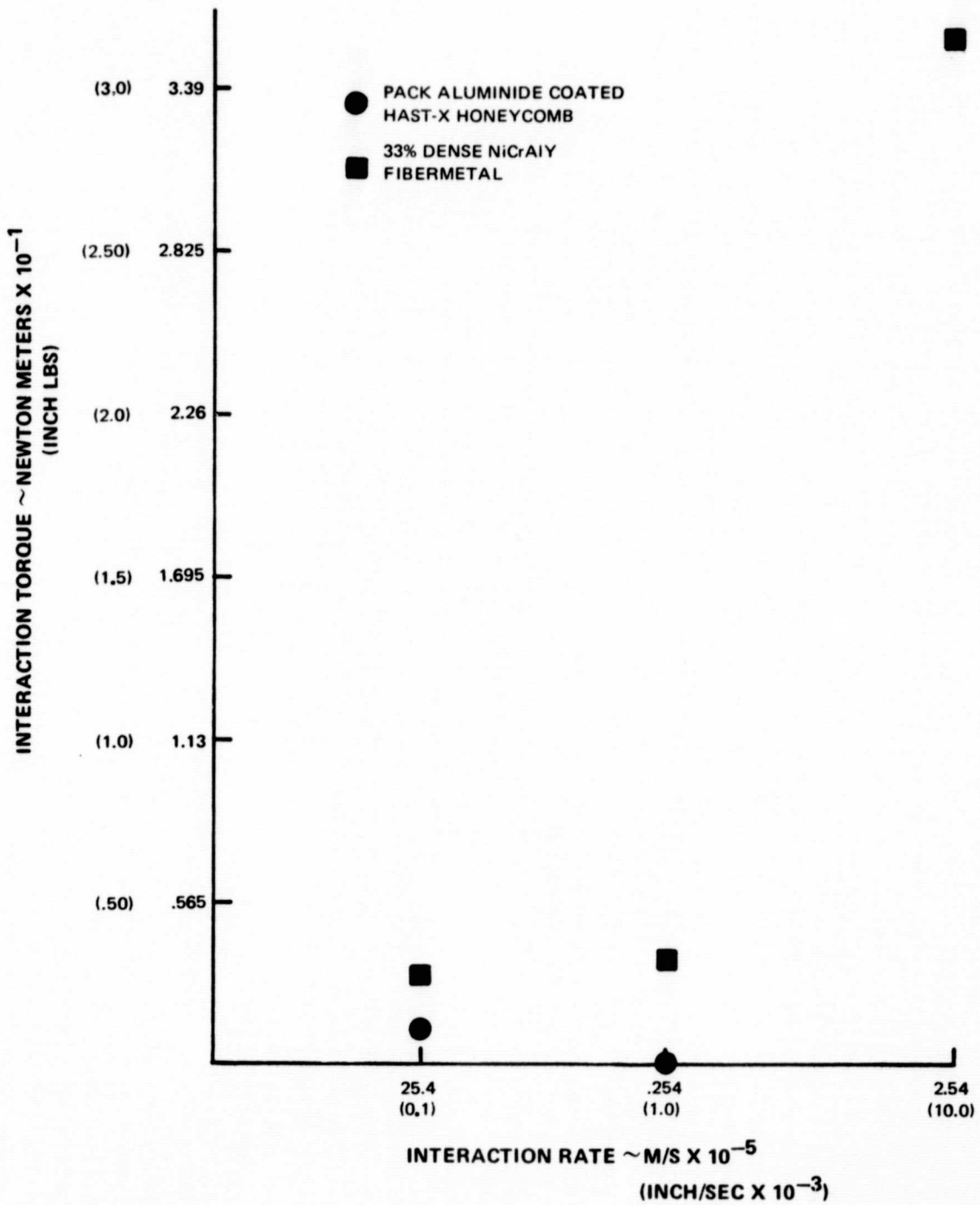


FIGURE 9

INTERACTION TORQUE VS INTERACTION RATE

SURFACE TEMPERATURE = AMBIENT
SURFACE SPEED 305 M/S (1000 FT/SEC)

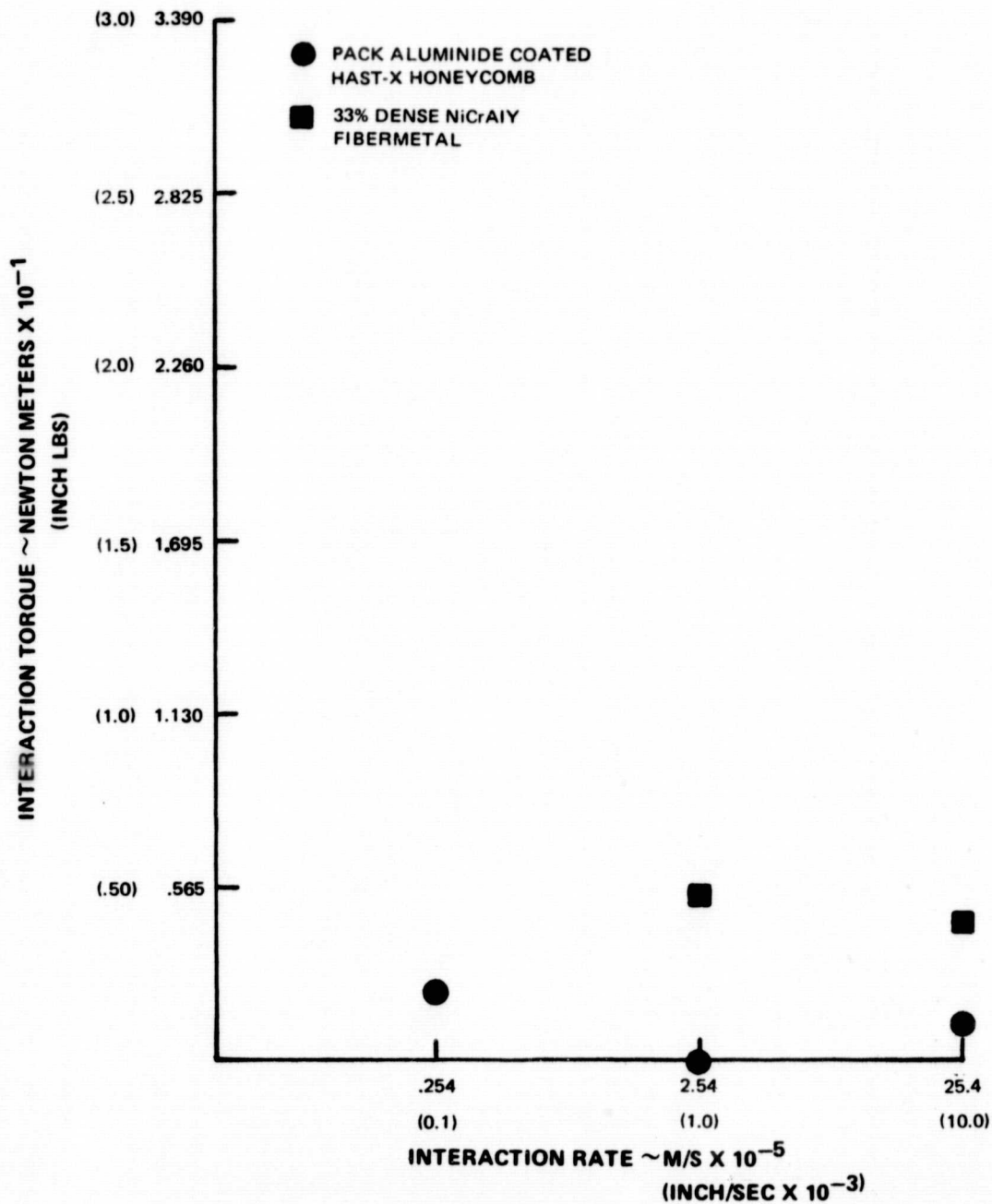
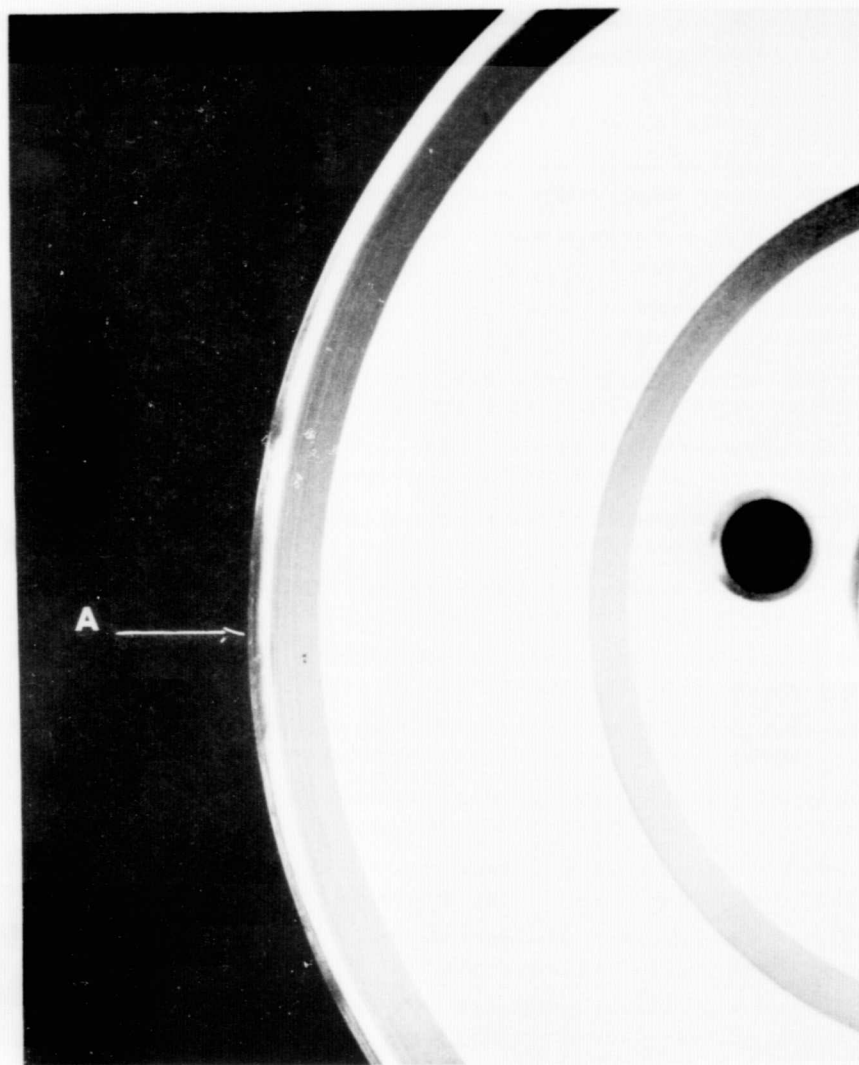
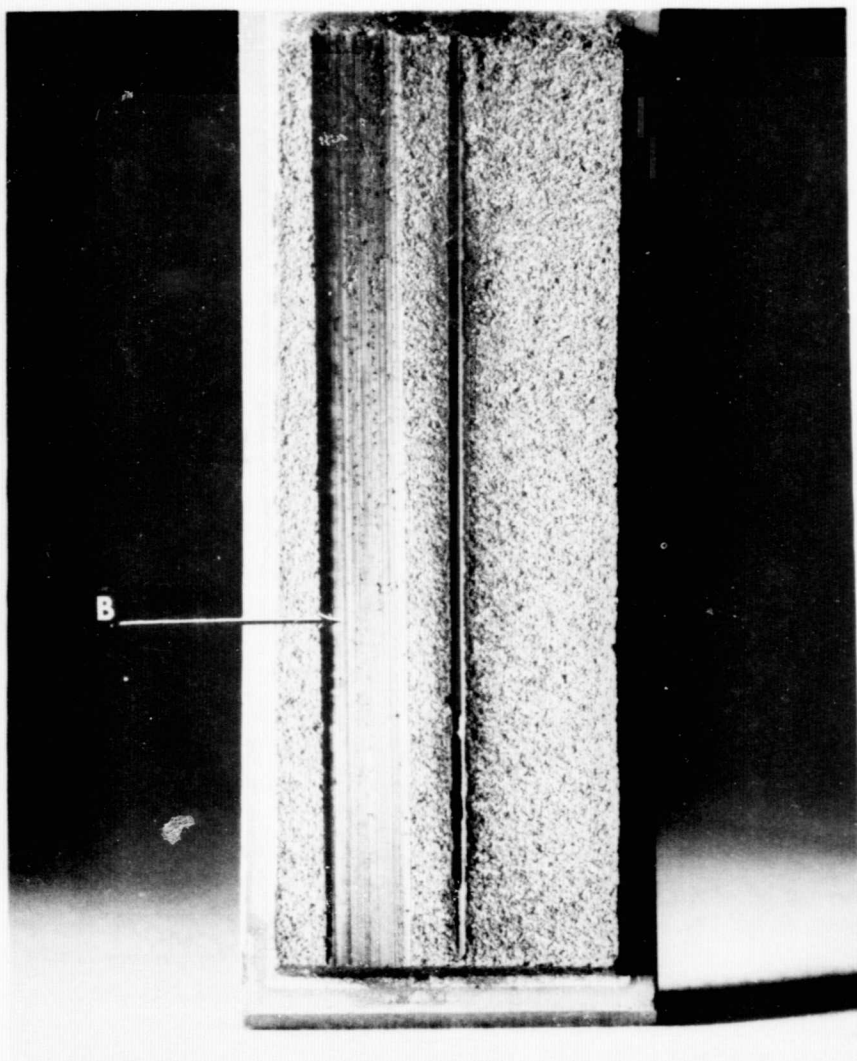


FIGURE 10

INTERACTION TORQUE VS INTERACTION RATE

SURFACE TEMPERATURE = 1366 K (2000°F)

SURFACE SPEED = 305 M/S (1000 FT/SEC)



-43-

FIGURE 11

TEST #28 NiCrAlY 33% DENSE FIBERMETAL (LEFT RUB) VS. WASPALOY KNIFE EDGE. TEST CONDITIONS: 305 m/s (1000 FT/SEC) SURFACE SPEED, 2.54×10^{-5} m/s (.001 INCH/SEC) INTERACTION RATE, AMBIENT TEMPERATURE, SWEEP RATE 2.54×10^{-4} m/s (.010 INCH/SEC) FOR 5.08×10^{-3} m (.200 INCH) WIDTH. A) HEAVY KE HEAT DISTRESS WITH 2.54×10^{-5} m (.0010 INCH) RADIAL WEAR (MAXIMUM), B) HEAVY GLAZING ON SPECIMEN RUB FLOOR.



XPN-53100

XPN-53100

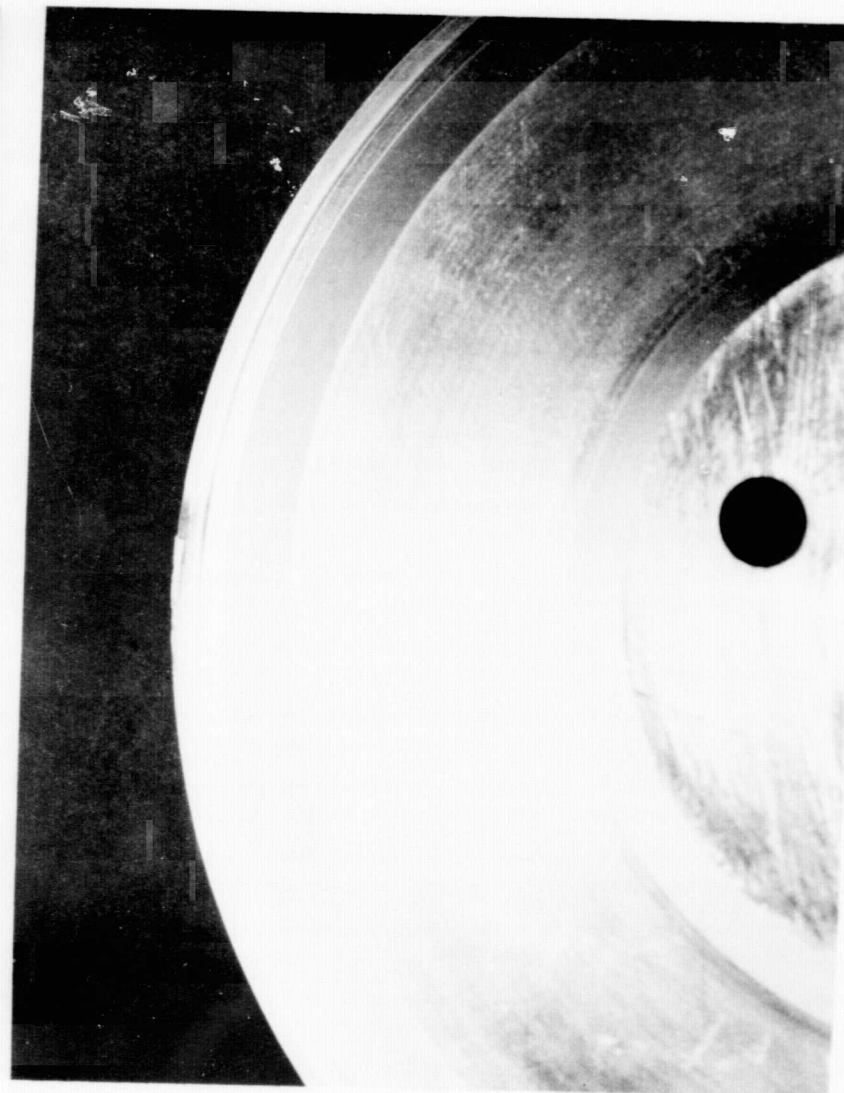
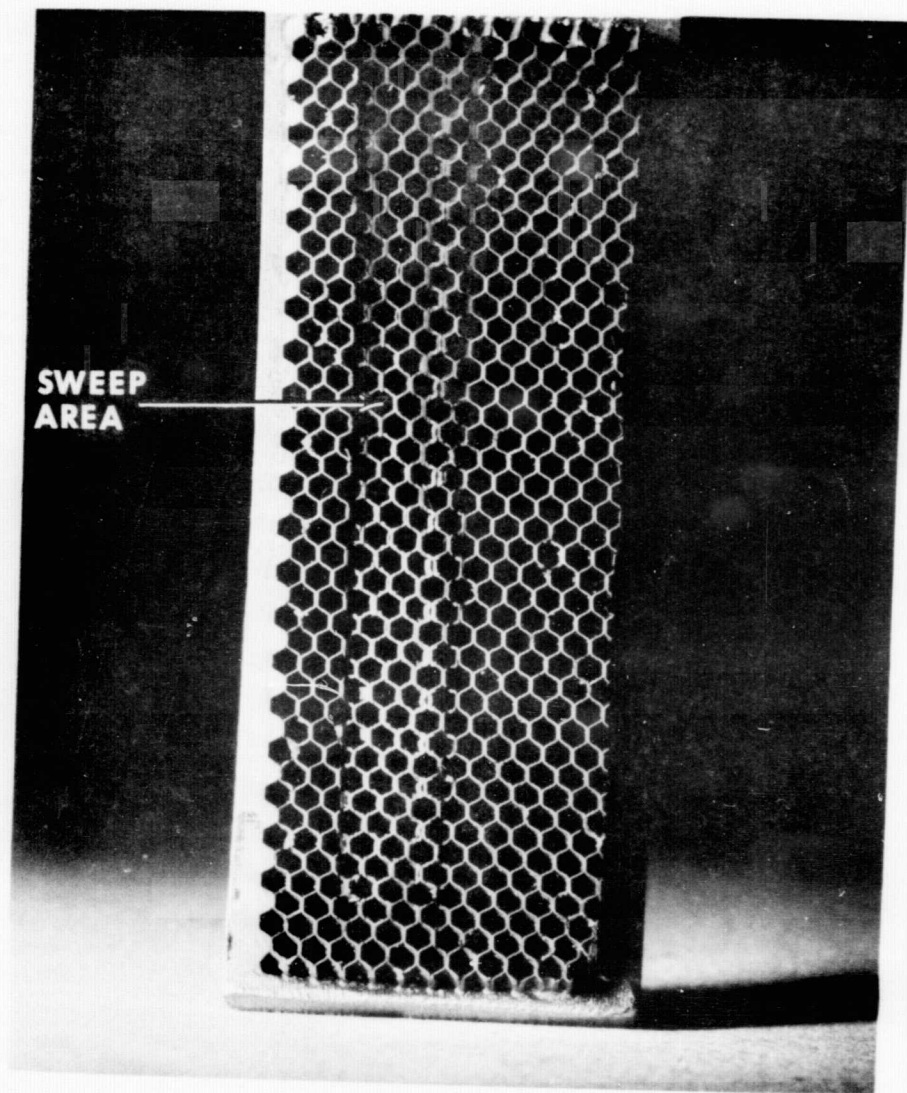


FIGURE 12

TEST #27, PACK-ALUMINIDE COATED HAST-X HONEYCOMB (LEFT RUB) VS. WASPALOY KNIFE EDGE. TEST CONDITIONS: 305 m/s (1000 FT/SEC) SURFACE SPEED, 2.54×10^{-5} m/s (.001 INCH/SEC) INTERACTION RATE, AMBIENT TEMPERATURE, SWEEP RATE 2.54×10^{-4} m/s (.010 INCH/SEC) FOR 5.08×10^{-3} m (.200 INCH) WIDTH. THREE AREAS OF HEAT DISTRESS AND PICKUP - 1.17×10^{-4} m (.0046 INCH) MAXIMUM

XPN-53099



XPN-53099

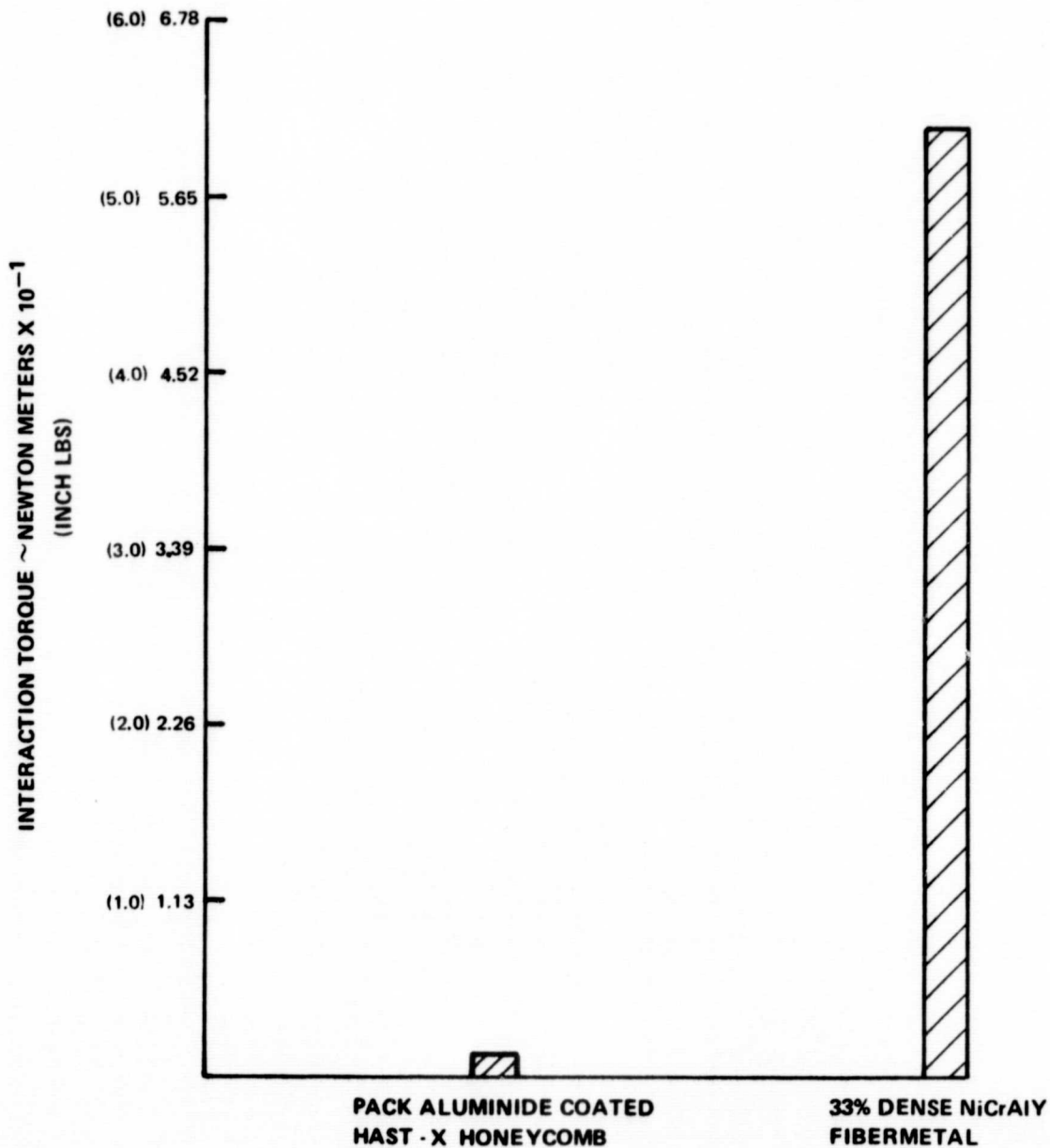
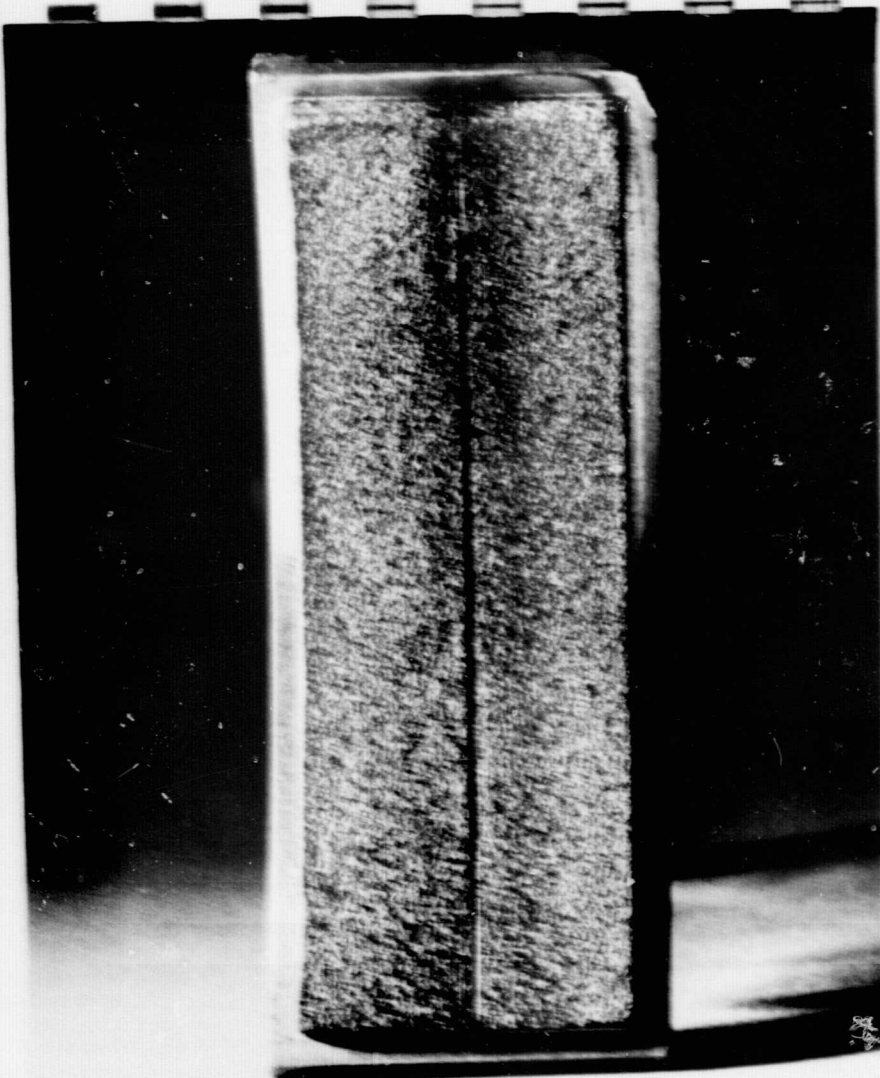


FIGURE 13

INTERACTION TORQUE VS AXIAL SWEEP

SURFACE SPEED = 305 M/S (1000 FT/SEC)
 TEMPERATURE = AMBIENT
 INTERACTION RATE $2.54 \text{ M/S} \times 10^{-5}$ (.001 INCH/SEC)
 AXIAL SWEEP $5.08 \text{ M} \times 10^{-3}$ (.200 INCH)
 SWEEP RATE $25.4 \text{ M/S} \times 10^{-5}$ (.010 INCH/SEC)



SCALLOPED-EDGE
HEAT DISCOLORATION

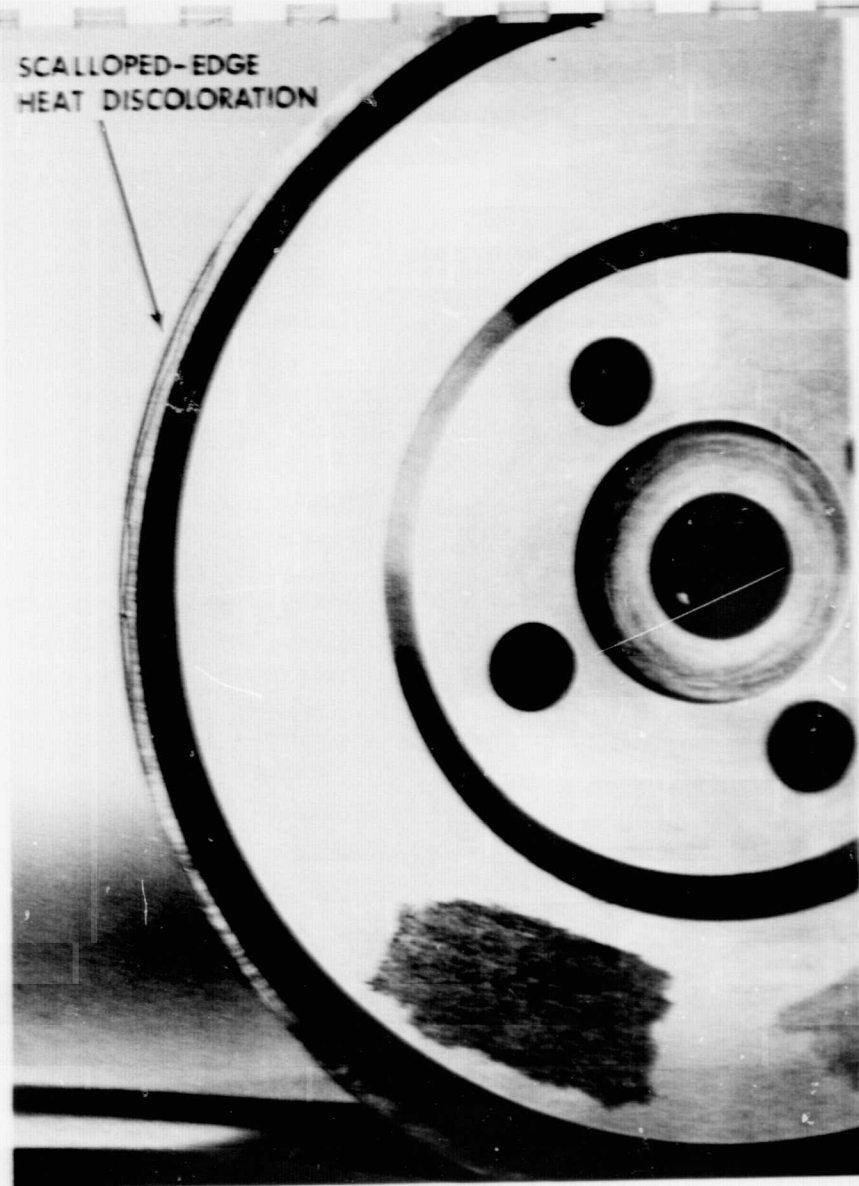
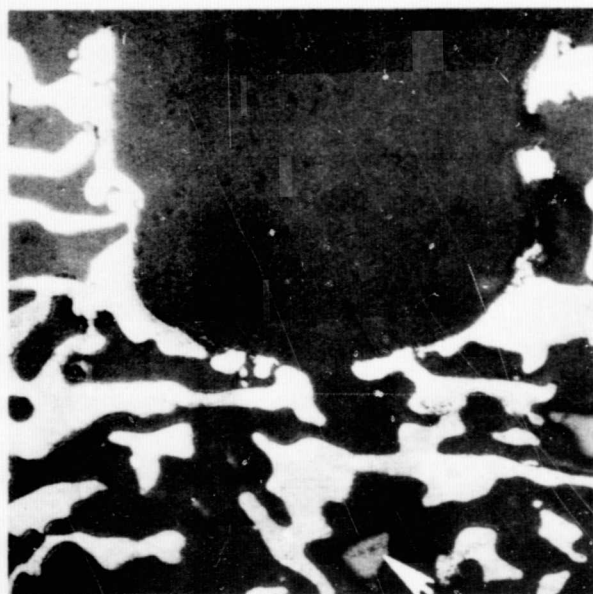


FIGURE 14

TEST #11, NiCrAlY (33% DENSE) FIBERMETAL VS. WASPALOY
KNIFE EDGE. TEST CONDITIONS: 305 m/s (1000 FT/SEC)
SURFACE SPEED, 2.54×10^{-5} m/s (.001 INCH/SEC) INTERACTION
RATE, AMBIENT TEMPERATURE. NOTE - SCALLOPED EDGE
HEAT DISCOLORATION FOR 100° OF DISC, MAXIMUM PICKUP
 3.30×10^{-5} m (.0013 INCH). NO KNIFE EDGE WEAR.



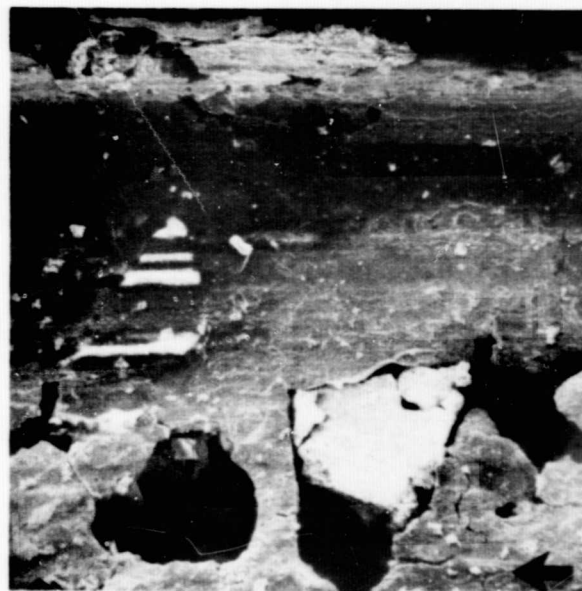
XPN-52374



ETCHED

MAG: 100X

A



MAG: 240X

B

FIGURE 15



33% DENSE NiCrAlY FIBER METAL - TEST NO. 11: MICRO-SECTION SHOWING RUB GROOVE AND NON-METALLIC INCLUSIONS FOUND WITHIN STRUCTURE (A), AND SCANNING ELECTRON PHOTOMICROGRAPH OF RUBBED SURFACE (B). NOTE NON-METALLIC INCLUSION JUST BELOW RUBBED SURFACE (B) ABOVE AND LEFT OF ARROW AND MICROCRACKING OF RUBBED SURFACE. ARROW DENOTES RUB DIRECTION.



A

100X



B

180X

48



FIGURE 16

33% DENSE NiCrAlY FIBER METAL - TEST NO. 12: (A) MICROSECTION OF RUB GROOVE SHOWING DENSIFICATION AND KNIFE-EDGE MATERIAL DEPOSITS. NON-METALLIC INCLUSIONS ARE PRESENT; (B) SCANNING ELECTRON PHOTOMICROGRAPH OF RUBBED SURFACE. ARROW DENOTES RUB DIRECTION.

K-16370



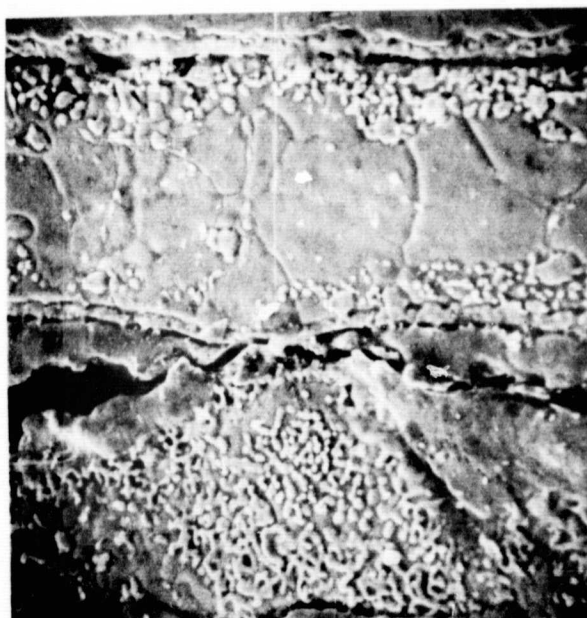
A

200X



B

530X



C

530X

FIGURE 17

PACK ALUMINIDE COATED HASTELLOY X HONEYCOMB - TEST NO. 7: (A) MICROSECTION OF RUBBED NODE; (B) SCANNING ELECTRON PHOTOMICROGRAPH OF RUBBED NODE. (C) UNRUBBED NODE.

K-16371



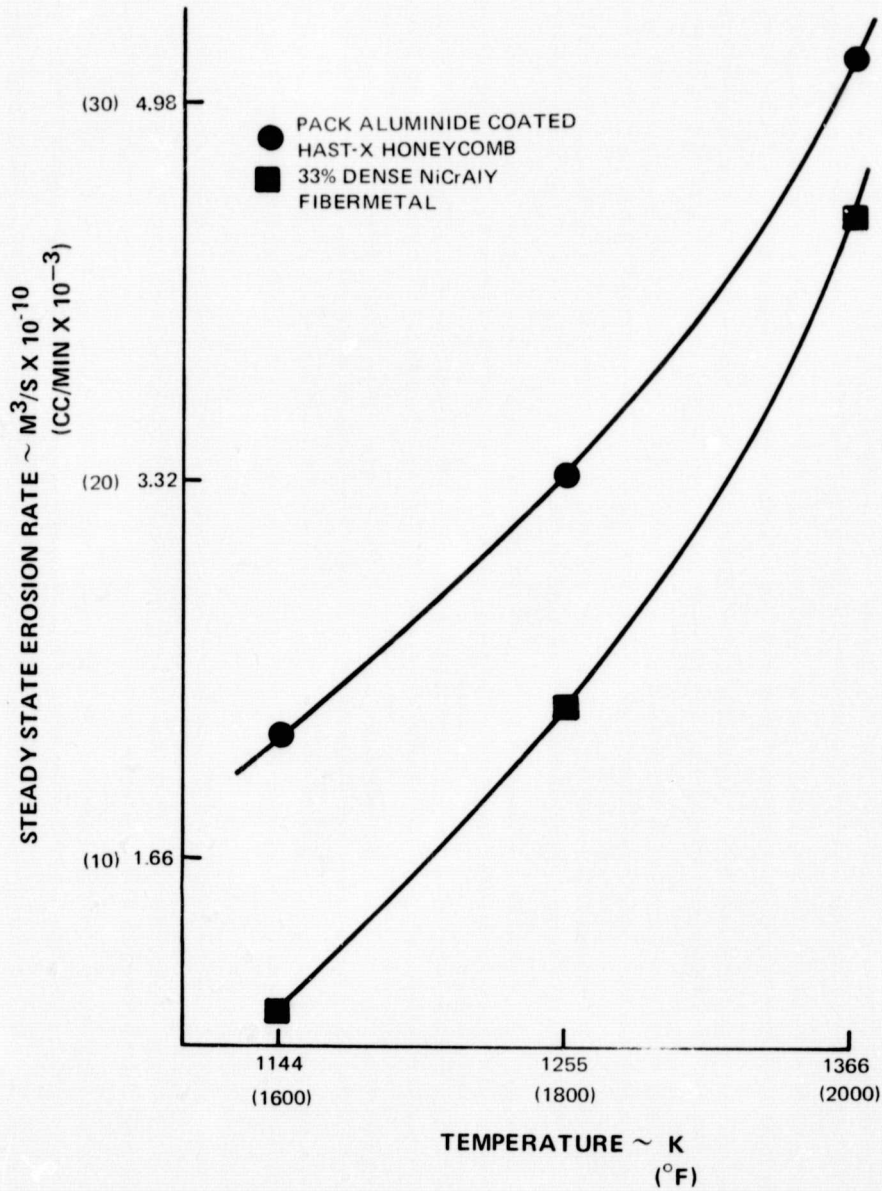
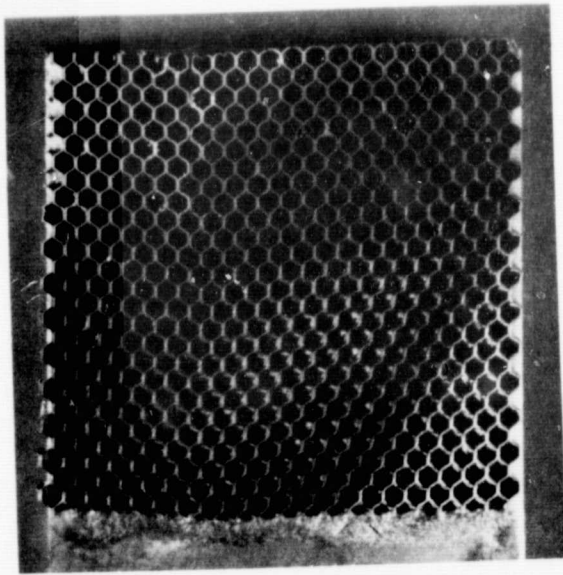
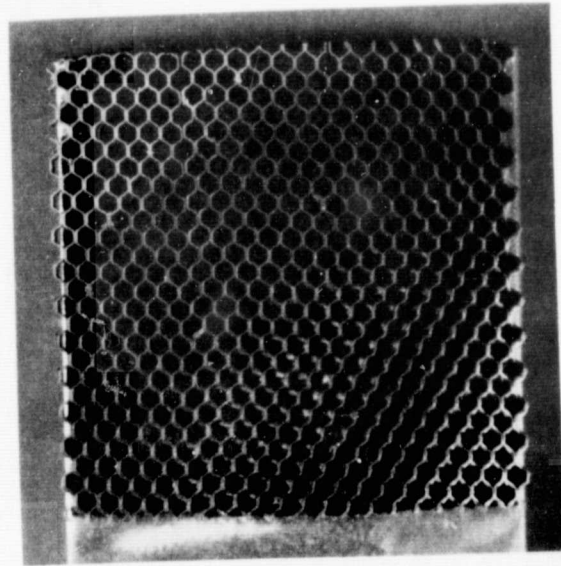


FIGURE 18

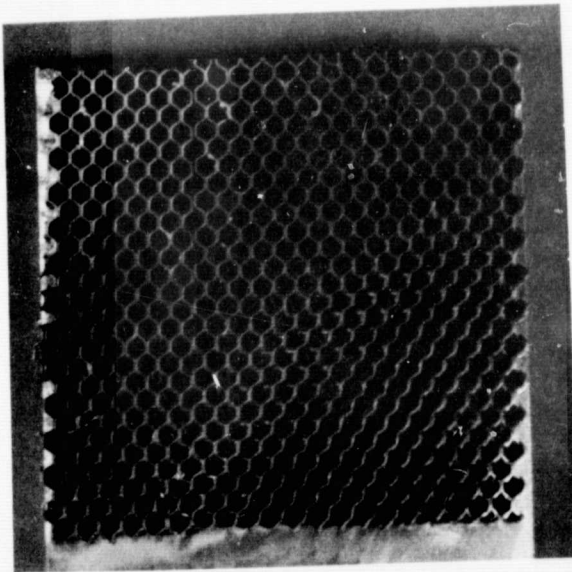
VOLUME LOSS PARTICULATE EROSION RATE VS TEMPERATURE
KNIFE EDGE SYSTEMS



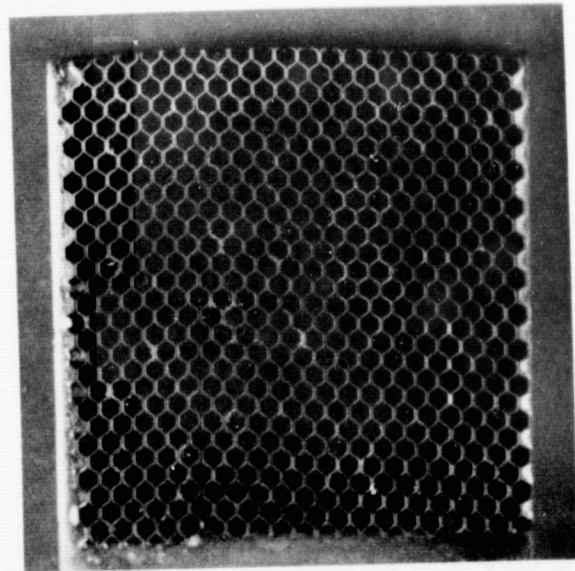
1144K
(1600 °F)



1255K
(1800 °F)



1366K
(2000 °F)



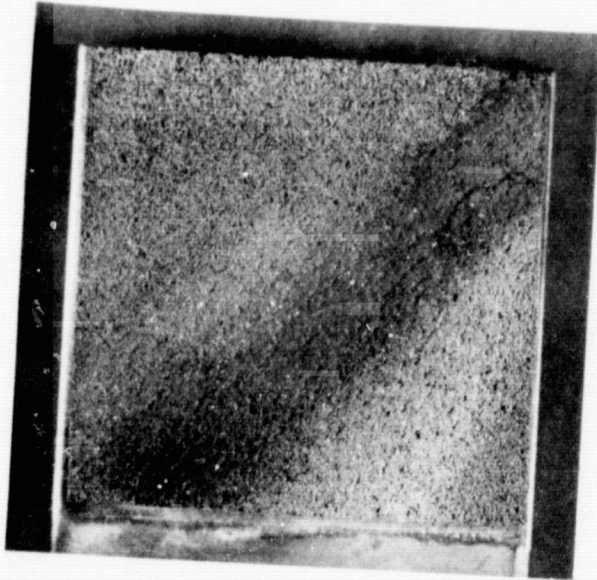
1366K
(2000 °F)
(WITHOUT PARTICULATE)

FIGURE 19

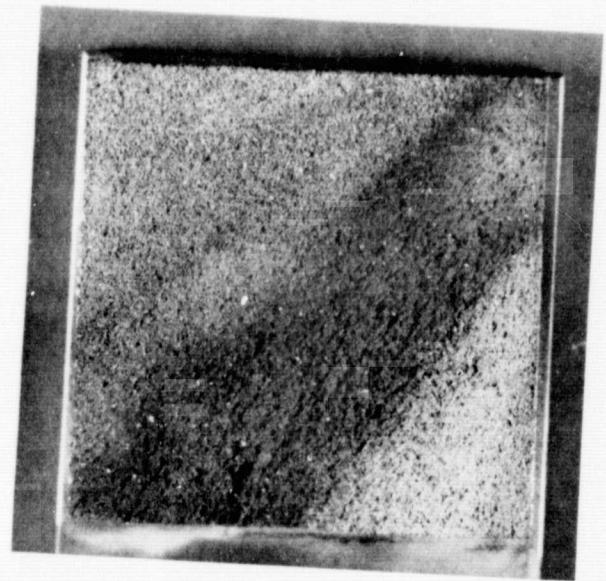
POST-PARTICULATE EROSION IMPINGEMENT SURFACE OF
PACK ALUMINIDE COATED HASTELLOY-X HONEYCOMB
SPECIMENS. TEST PARAMETERS: TEST TEMPERATURES
INDICATED, 7° IMPINGEMENT ANGLE, 1200 SECOND TEST
DURATION, .35 MACH GAS VELOCITY, 80 GRIT - Al₂O₃
ABRASIVE PARTICLES, AND 7.50×10^{-3} 9.79×10^{-3} kg/s
(6.0 LBS/HR) MASS FLOW RATE. ARROW INDICATES PARTICLE
FLOW DIRECTION. MAG 2X

XPN-54835

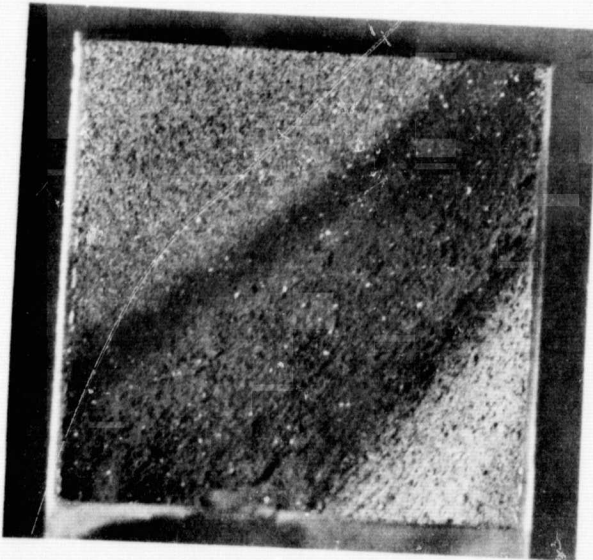




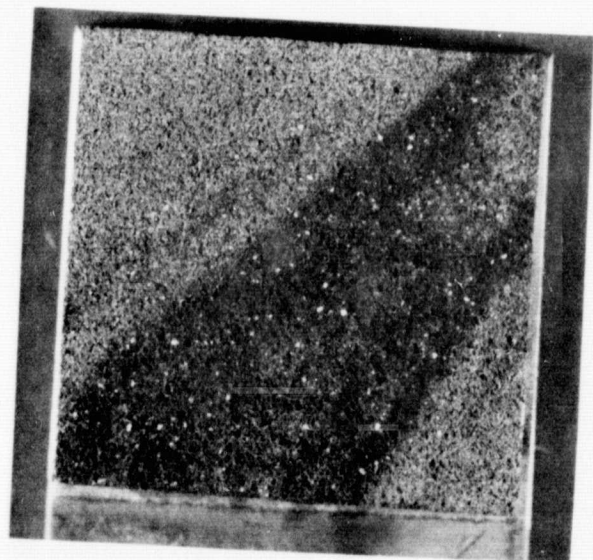
1144K
(1600 °F)



1255K
(1800 °F)



1366K
(2000 °F)



1366K
(2000 °F)
(WITHOUT PARTICULATE)

FIGURE 20

POST-PARTICULATE EROSION IMPINGEMENT SURFACE OF
NiCrAlY 33% DENSE FIBERMETAL SPECIMENS. TEST
PARAMETERS: TEST TEMPERATURES INDICATED, 7°
IMPINGEMENT ANGLE, 1200 SECOND TEST DURATION, .35
MACH GAS VELOCITY, 80 GRIT - Al₂O₃ ABRASIVE PARTICLES
AND 7.50 X 10⁻³ kg/s (6.0 LBS/HR) MASS FLOW RATE. ARROW
INDICATES PARTICLE FLOW DIRECTION. MAG 2X

XPN-54832



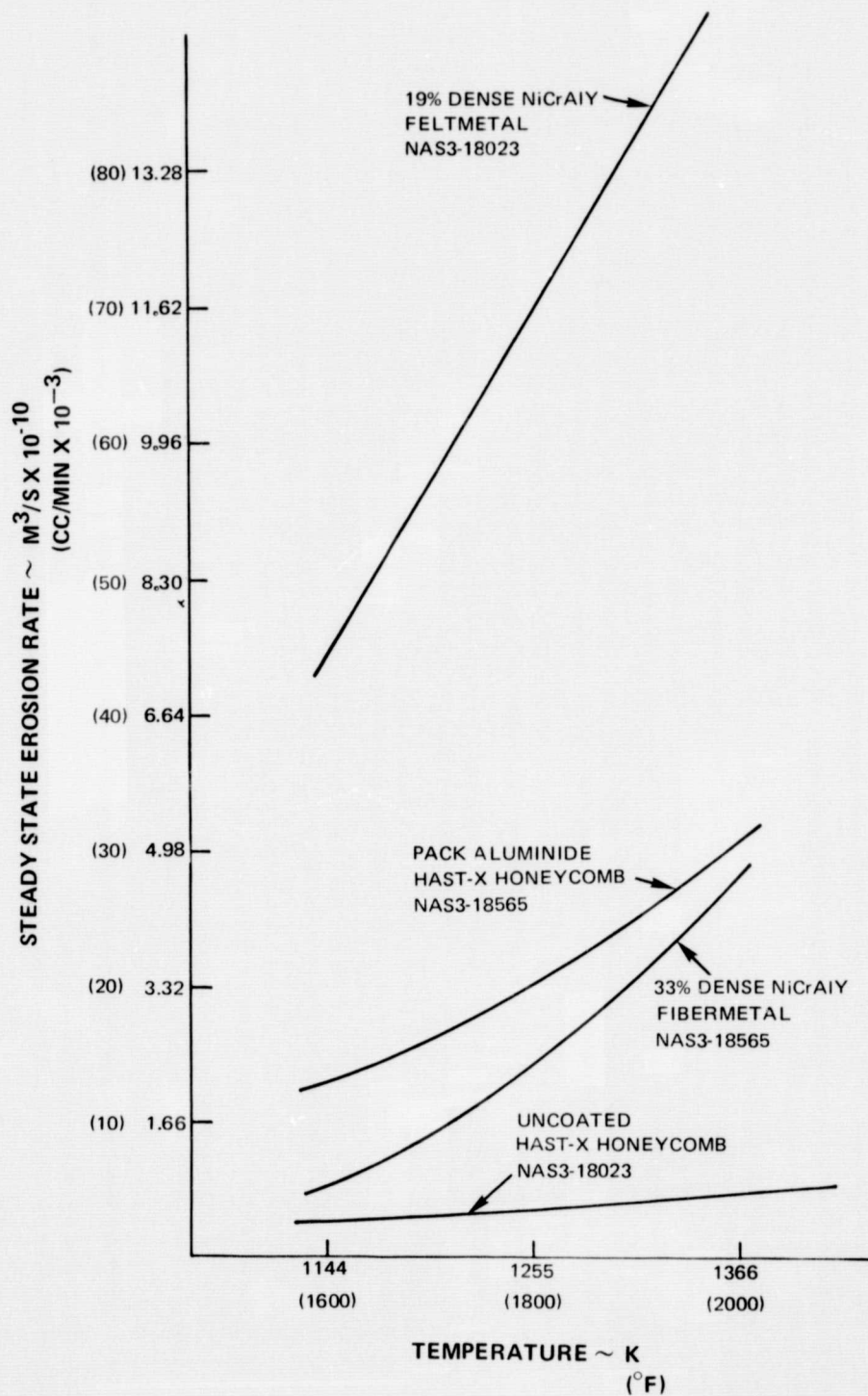


FIGURE 21

VOLUME LOSS PARTICULATE EROSION RATE VS TEMPERATURE

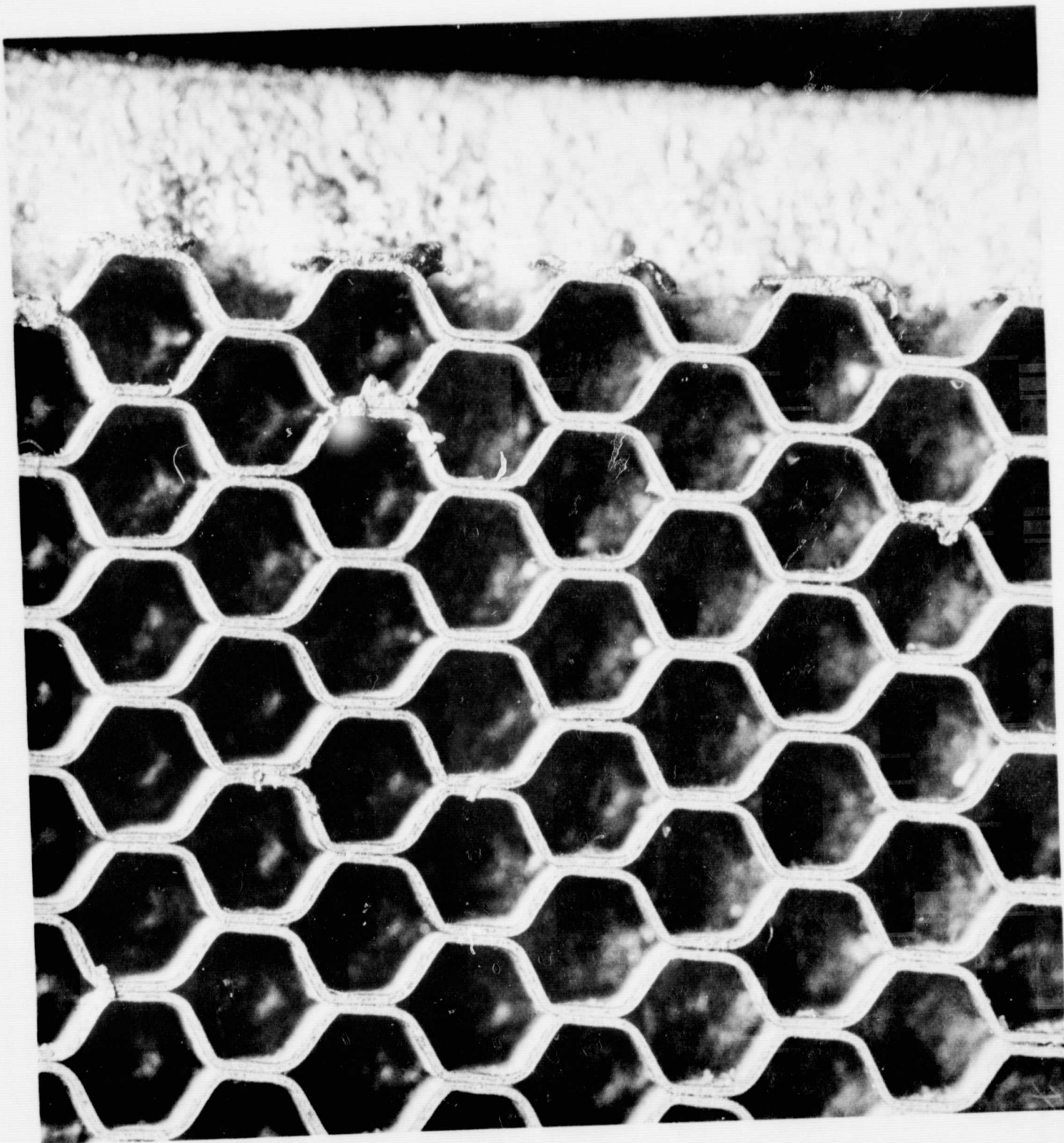


FIGURE 22

PACK-ALUMINIDE COATED HAST-X HONEYCOMB, (TOP VIEW.)
XPN-52299



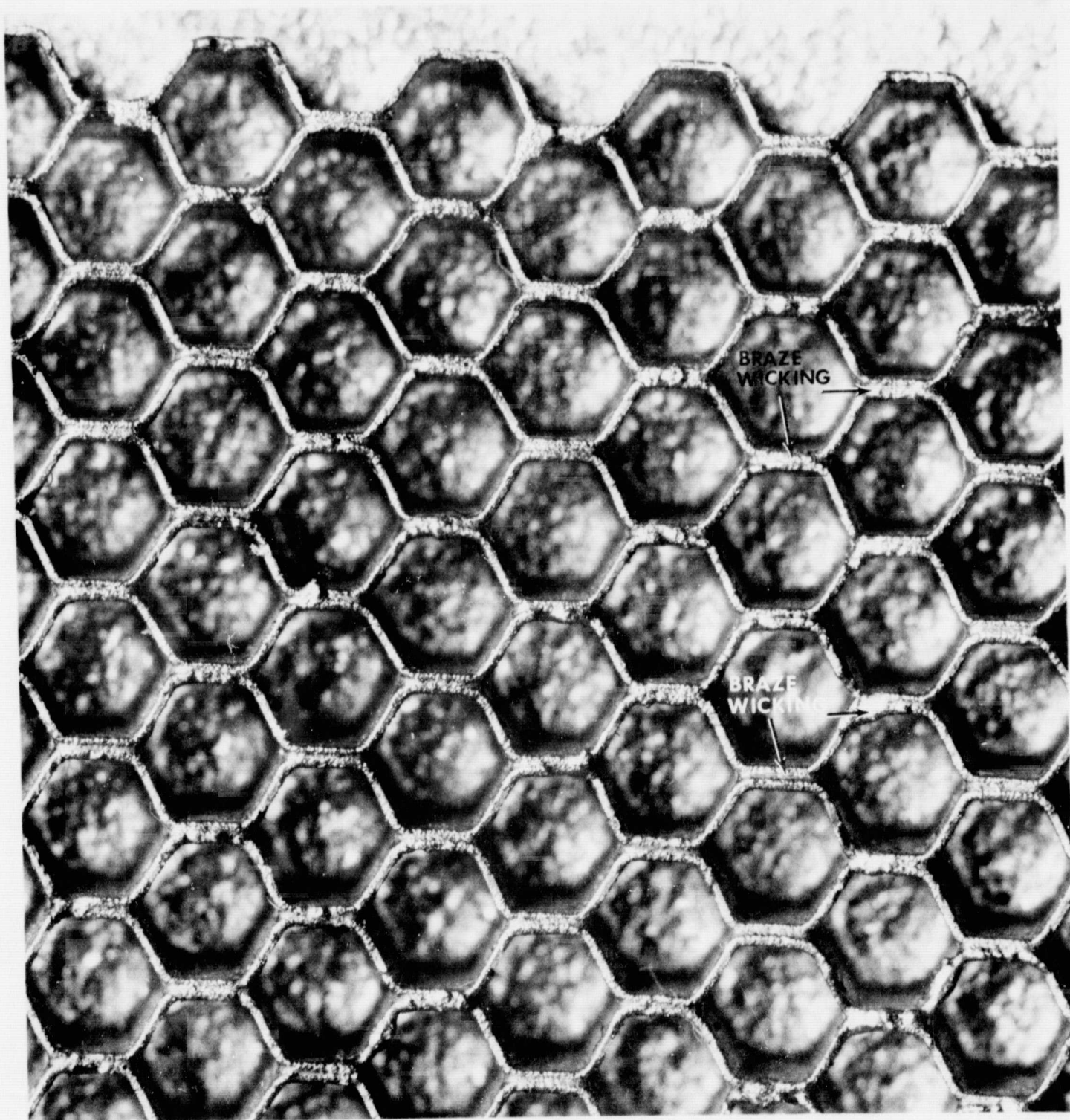


FIGURE 23

UNCOATED HAST-X HONEYCOMB TESTED UNDER
CONTRACT NAS 3-18023 (TOP VIEW).

XPN-52302





FIGURE 24

MAG: 1.75X

PRE-SECTIONING BLADE TIP SEAL SYSTEM SPECIMENS
(A) PLASMA SPRAYED ZrO_2 APPLIED TO A $ZrO_2/CoCrAlY$
INTERMEDIATE LAYER; (B) PLASMA SPRAYED 10% CeO_2 -
 $NiCoCrAlY$ COMPOSITE; (C) WOVEN QUARTZ.

K-16372



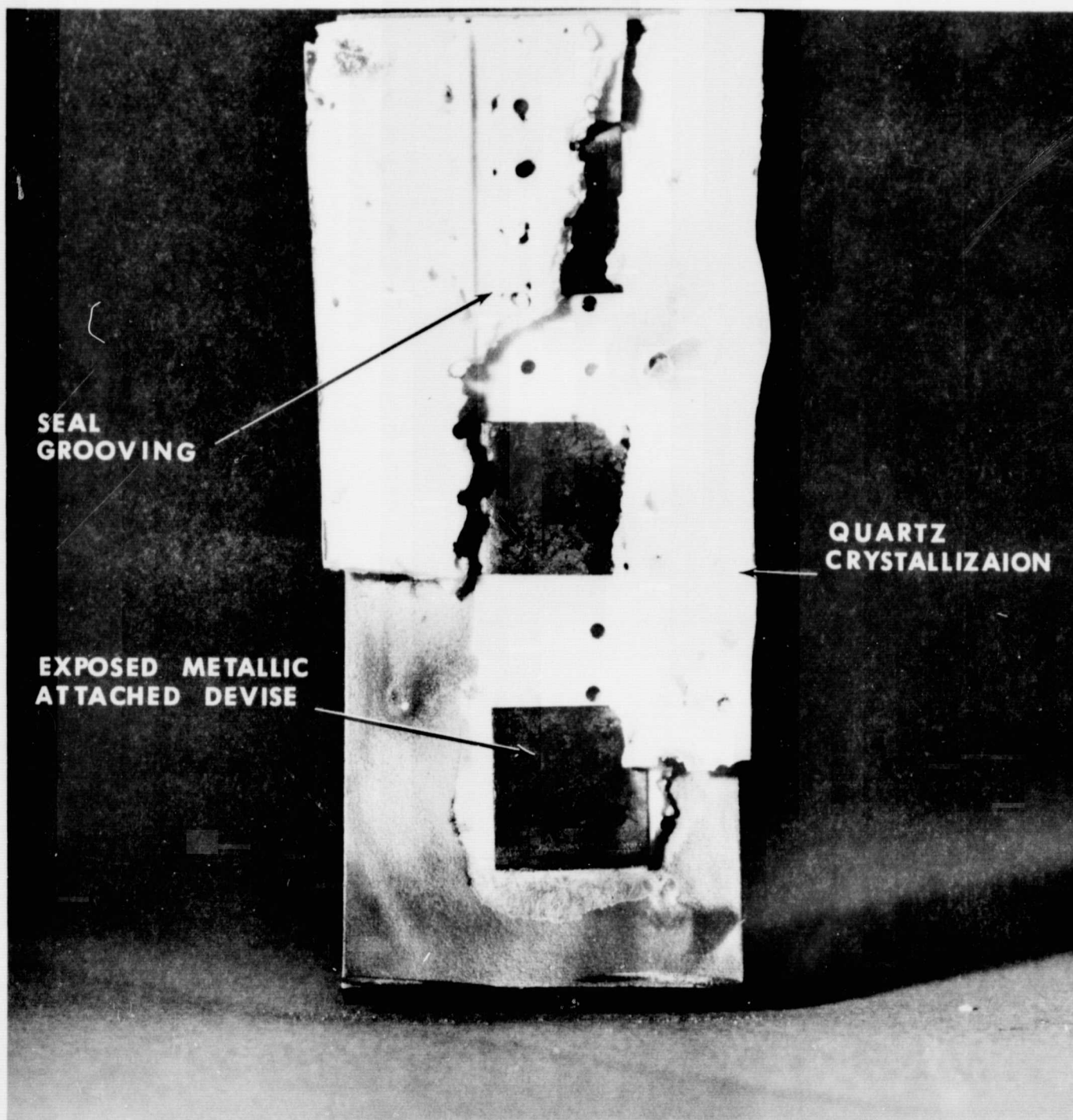
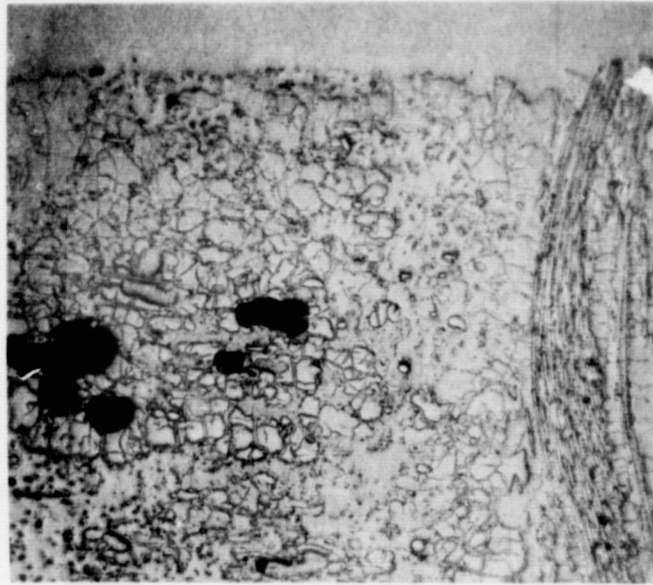


FIGURE 25

TEST #22, QUARTZ WOVEN FIBER SYSTEM VS. B-1900 TEST BLADE. TEST CONDITIONS: 305 m/s (1000 FT/SEC) SURFACE SPEED, 2.54×10^{-4} m/s (.010 INCH/SEC) INTERACTION RATE, AND 1589K (2400°F) TEMPERATURE. NOTE - SEAL DIS-INTEGRATED DURING INTERACTION ALSO SOME CRYSTALLIZATION OCCURRED ON LINE WITH TORCH IMPINGEMENT. NO BLADE WEAR.

XPN-53095





A

50X



B

180X



C

180x

FIGURE 26

WOVEN QUARTZ - TEST NO. 20: (A) MICROSECTION UNDER AND INCLUDING RUBBED SURFACE; (B) SCANNING ELECTRON PHOTOMICROGRAPH OF RUBBED SURFACE SHOWING BROKEN FIBERS AND PARTICLE/FIBER BOND SITES (ARROWS); (C) SCANNING ELECTRON PHOTOMICROGRAPH OF UNRUBBED SURFACE.

K-16375



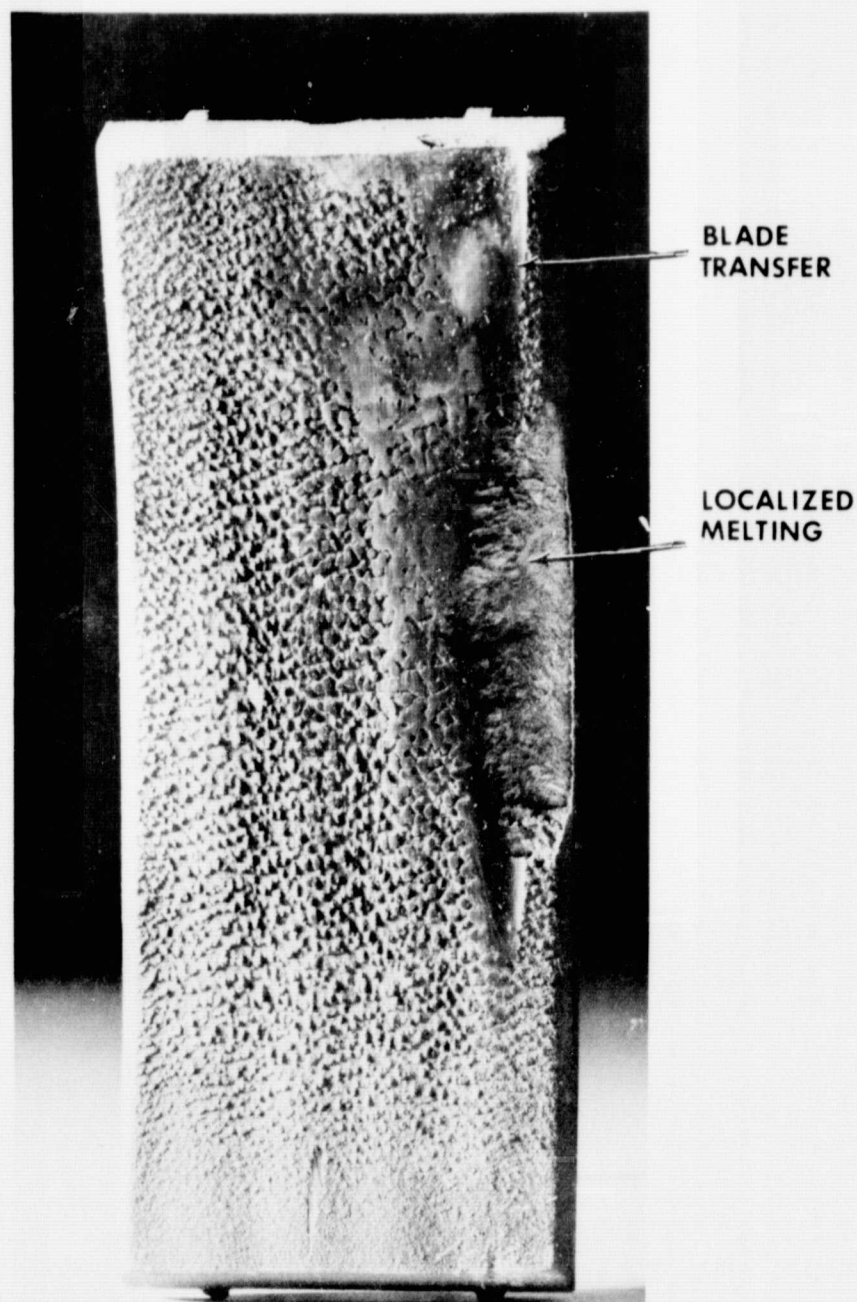


FIGURE 27

TEST #6, NiCoCrAlY WITH CeO₂ CERAMIC ADDITIVE SPRAY SYSTEM VS. B-1900 TEST BLADE. TEST CONDITIONS: 305 m/s (1000 FT/SEC) SURFACE SPEED, 2.54×10^5 m/s (.001 INCH/SEC) INTERACTION RATE, AND 1366K (2000 °F) TEMPERATURE. (LOCALIZED SEAL MELTING, HEAVY BLADE TRANSFER AND SEAL SMEARING WERE NOTED).

XPN-52104



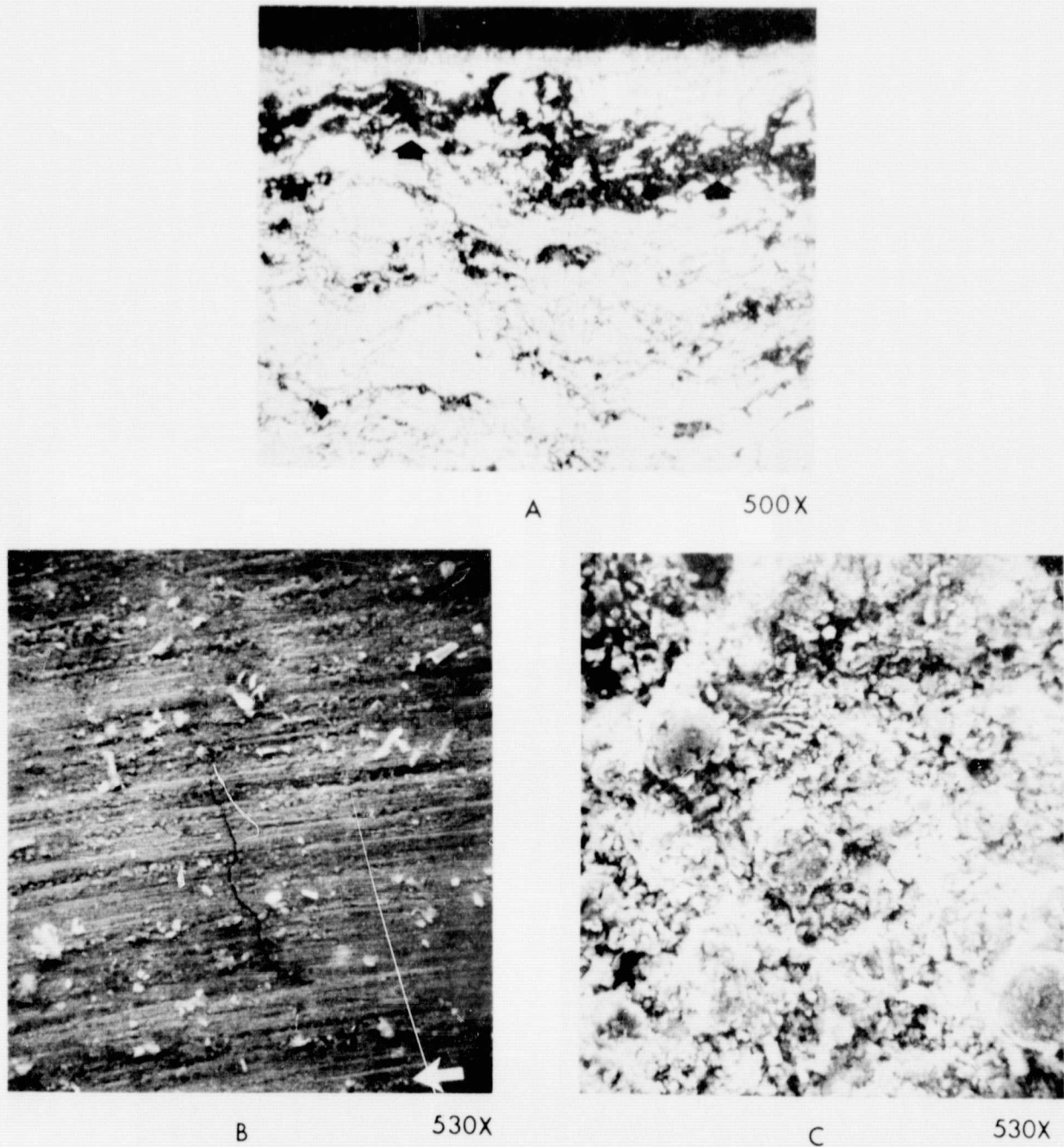


FIGURE 28

PLASMA SPRAYED $\text{CeO}_2/\text{NiCoCrAlY}$ COMPOSITE - TEST NO. 6:
(A) MICROSECTION UNDER AND INCLUDING RUBBED SURFACE
SHOWING OXIDIZED INTERFACIAL LAYER (ARROWS) BETWEEN
TRANSFERRED BLADE TIP MATERIAL AND COMPOSITE
COATING; (B) SCANNING ELECTRON PHOTOMICROGRAPH OF
RUB INDUCED SMEARED BLADE TIP DEPOSIT. ARROW
DENOTES RUB DIRECTION; (C) SCANNING ELECTRON PHOTO-
MICROGRAPH OF UNRUBBED SURFACE.

K-16374





FIGURE 29

TEST #2, CaO STABILIZED ZrO₂/CoCrAlY SEAL MATERIAL VS. B-1900 TEST BLADE. TEST CONDITIONS: 305 m/s (1000 FT/SEC) 2.54×10^{-5} m/s (.001 INCH/SEC) INTERACTION RATE, AND 1589K (2400°F) TEMPERATURE. NOTE - HEAVY SEAL SPALLING AND DELAMINATION OCCURRED DURING POST TEST COOL DOWN.

XPN-52103





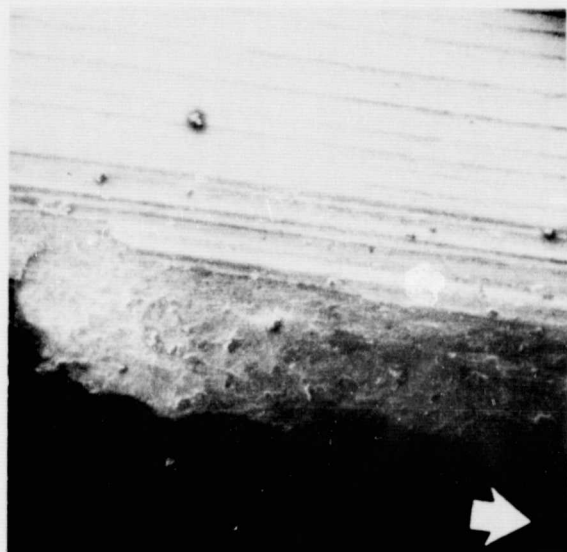
A

200X



B

420X



C

42X



D

440X

FIGURE 30



GRADED PLASMA SPRAYED CaO STABILIZED $\text{ZrO}_2/\text{CoCrAlY}$ - TEST NO. 3: (A) MICROSECTION UNDER AND INCLUDING RUBBED SURFACE SHOWING TRANSFERRED AND OXIDIZED BLADE TIP MATERIAL (ARROWS). (B) SCANNING ELECTRON PHOTOMICROGRAPH OF UNRUBBED SURFACE. (C) SCANNING ELECTRON PHOTOMICROGRAPH OF RUB-INDUCED SMEARED BLADE MATERIAL DEPOSIT. ARROW DENOTES RUB DIRECTION. (D) SCANNING ELECTRON PHOTOMICROGRAPH OF RUBBED SURFACE IN AREA OF MINOR BLADE MATERIAL DEPOSIT. ARROW DENOTES RUB DIRECTION.

K-16373

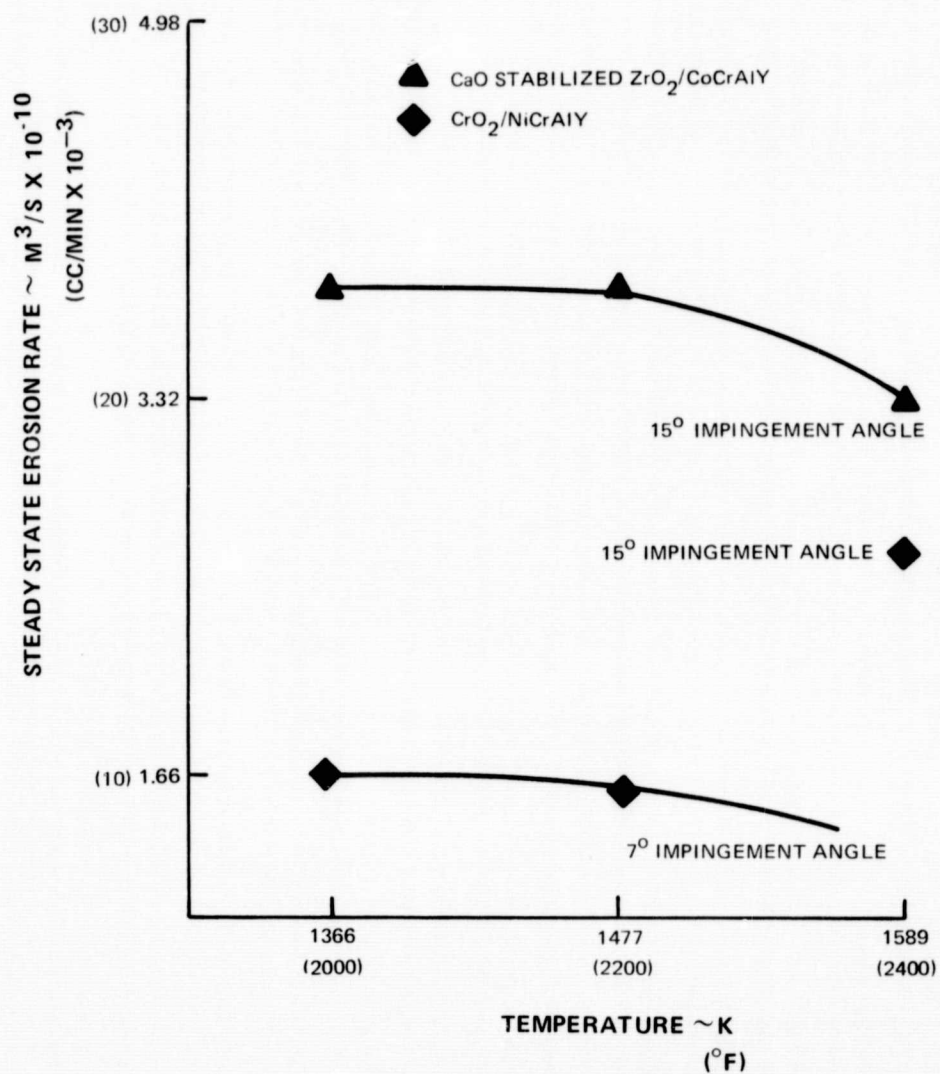


FIGURE 31

VOLUME LOSS PARTICULATE EROSION RATE VS TEMPERATURE
FOR BLADE TIP MATERIALS

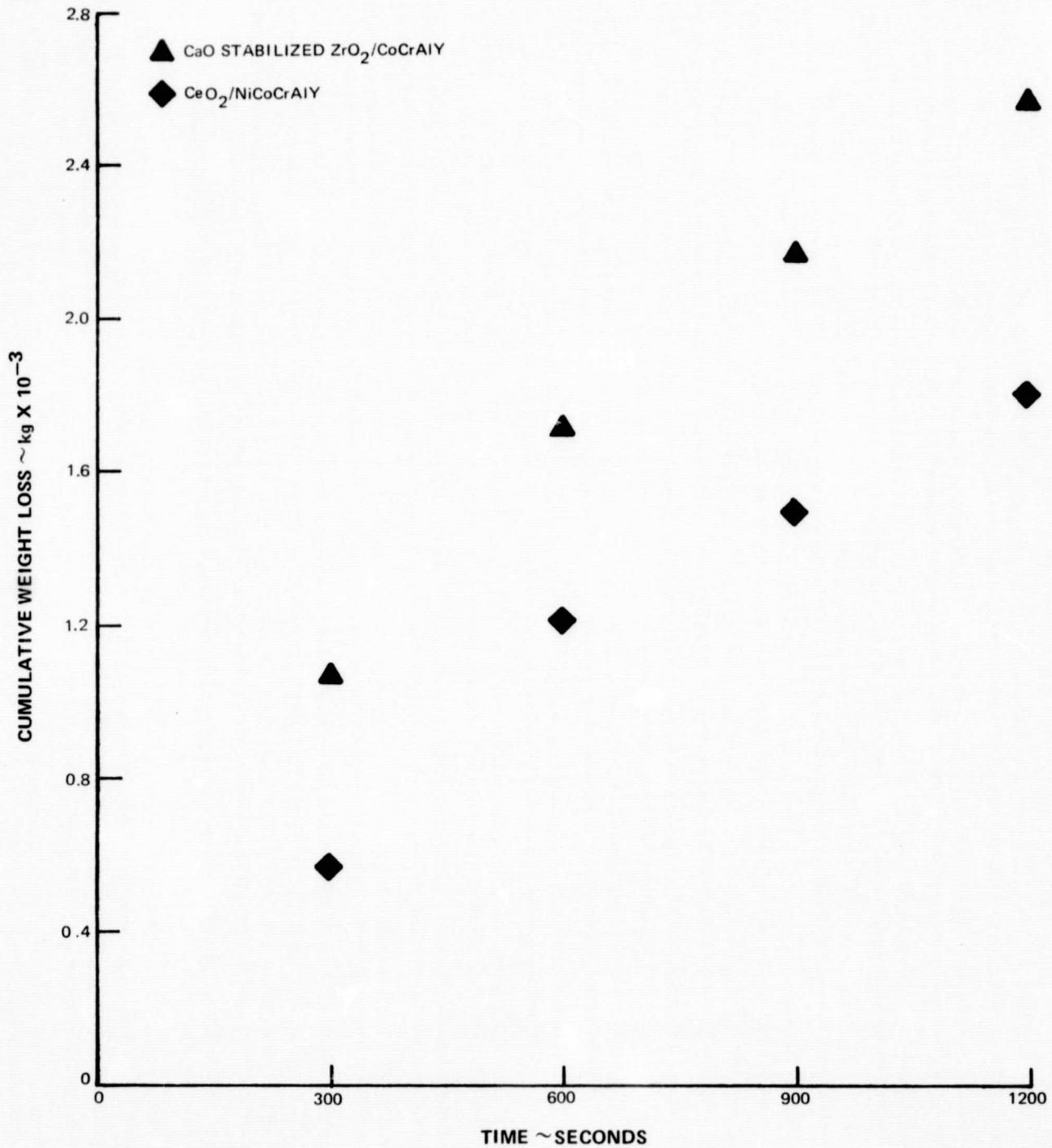


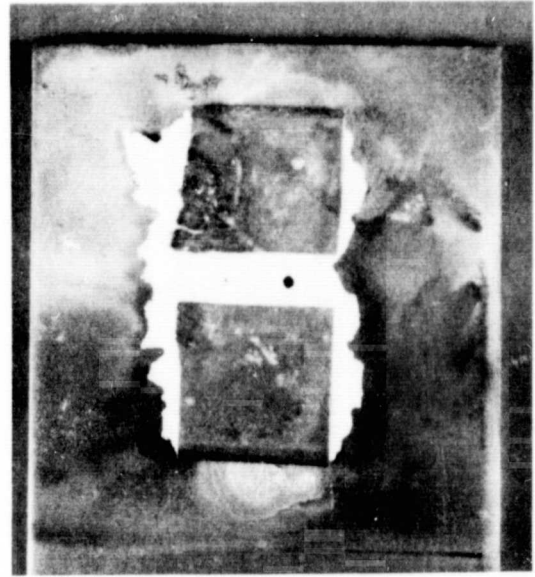
FIGURE 32

EROSION WEIGHT LOSS VS TIME COMPARISON

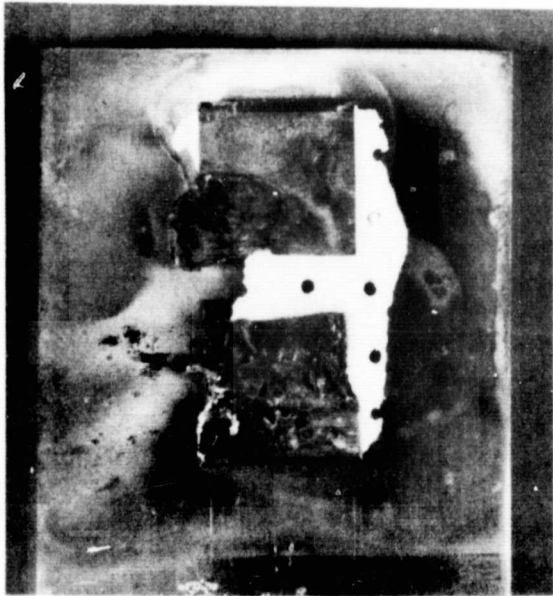
TEMPERATURE = 1583 K (2400°F)
IMPINGEMENT ANGLE = 15°



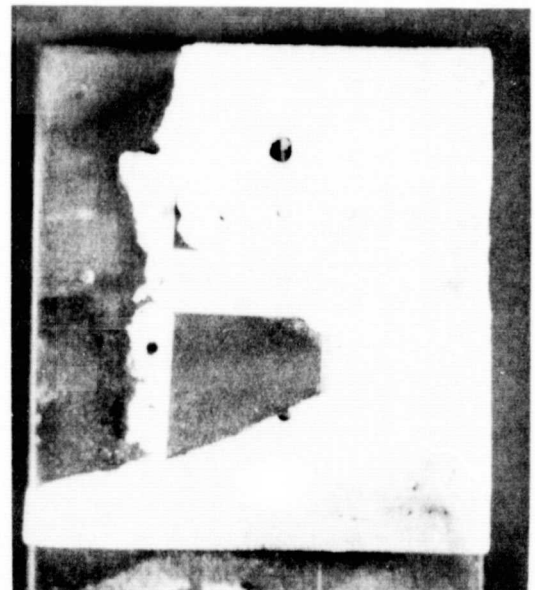
1366K
(2000 °F)



1477K
(2200 °F)



1589K
(2400 °F)



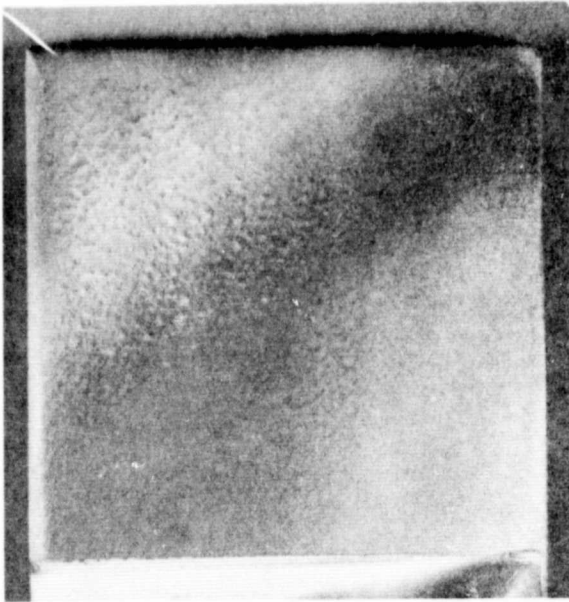
1589K
(2400 °F)
(WITHOUT PARTICULATE)



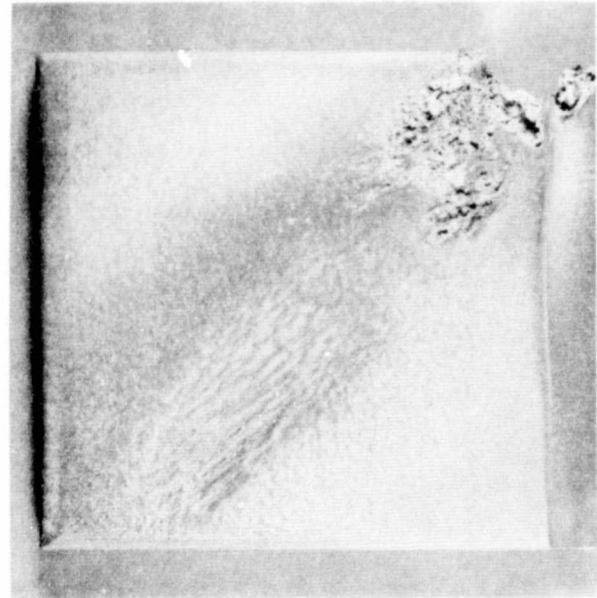
FIGURE 33

POST-PARTICULATE EROSION IMPINGEMENT SURFACE OF QUARTZ WOVEN FIBERS IMPREGNATED WITH SILICA SPECIMENS. TEST PARAMETERS: TEST TEMPERATURES INDICATED, 15° IMPINGEMENT ANGLE, 1200 SECOND TEST DURATION, .35 MACH GAS VELOCITY, 80 GRIT - Al₂O₃ ABRASIVE PARTICLES, AND 7.50 X 10⁻³ kg/s (6.0 LBS/HR) MASS FLOW RATE. ARROW INDICATES PARTICLE FLOW DIRECTION. MAG 2X

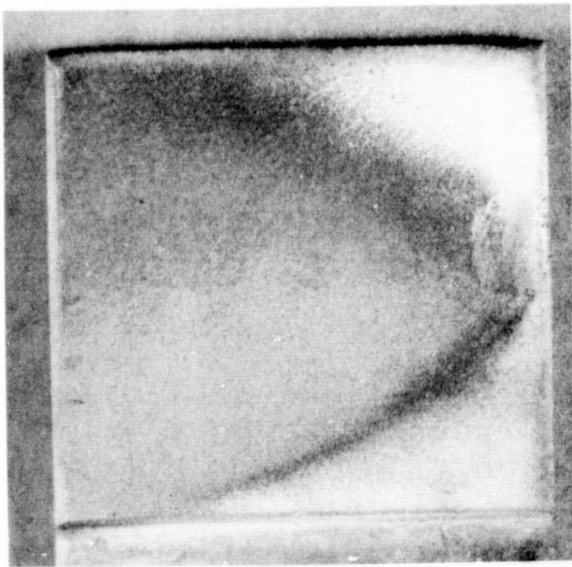
XPN-54833



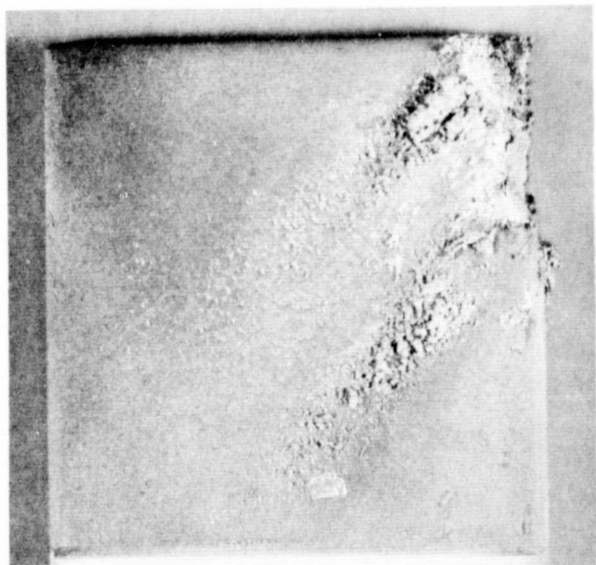
1366K
(2000 °F)



1477K
(2200 °F)



1589K
(2400 °F)



1589K
(2400 °F)

(WITHOUT PARTICULATE)

FIGURE 34

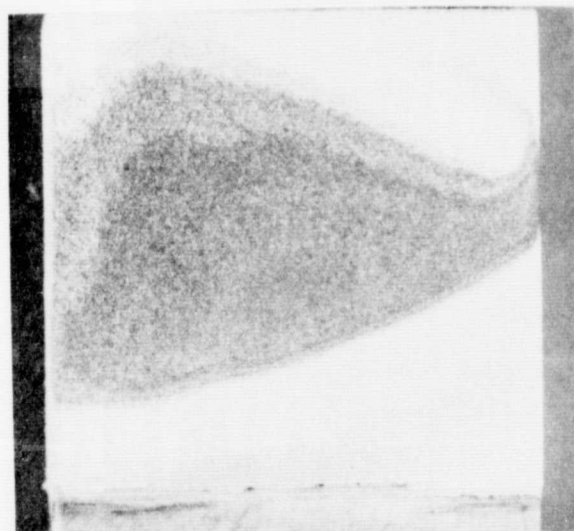


POST-PARTICULATE EROSION IMPINGEMENT SURFACE OF PLASMA SPRAYED $\text{CeO}_2/\text{NiCoCrAlY}$ SPECIMENS. TEST PARAMETERS: TEST TEMPERATURES INDICATED, 1589K (2400 °F) WITH ABRASIVE CONDUCTED AT 15° REMAINING AT 7° IMPINGEMENT ANGLE, 1200 SECOND TEST DURATION, .35 MACH GAS VELOCITY, 80 GRIT - Al_2O_3 ABRASIVE PARTICLES, AND $7.50 \times 10^{-3} \text{ kg/s}$ (6.0 LBS/HR) MASS FLOW RATE. ARROWS INDICATE PARTICLE FLOW DIRECTION. MAG 2X

XPN-54834



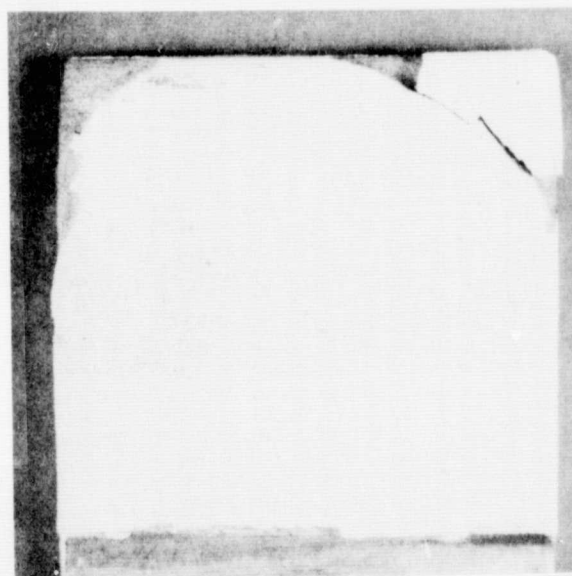
1366K
(2000 °F)



1477K
(2200 °F)



1589K
(2400 °F)



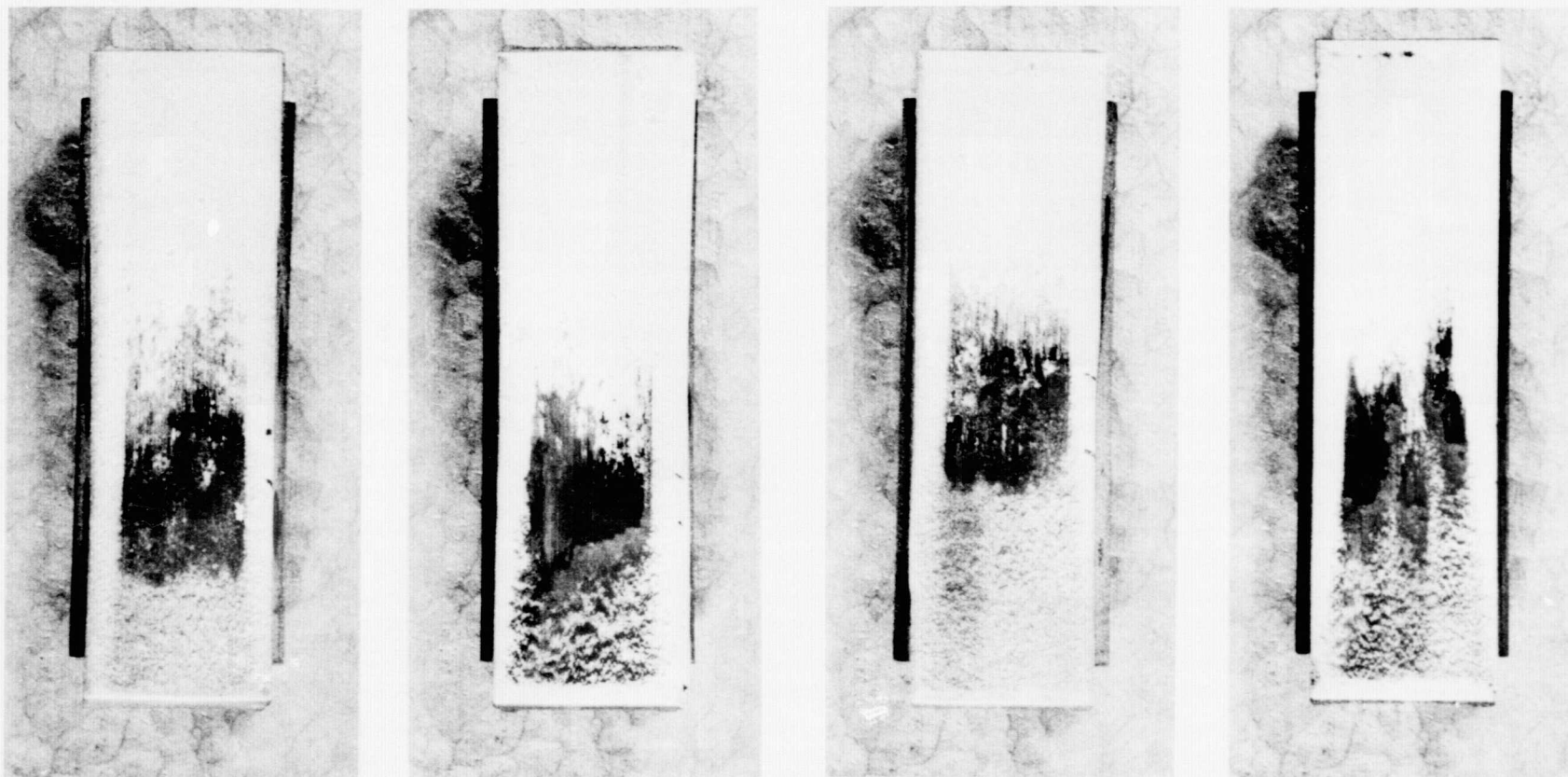
1589K
(2400 °F)
(WITHOUT PARTICULATE)

FIGURE 35



POST PARTICULATE EROSION IMPINGEMENT SURFACE OF CaO STABILIZED ZrO₂ TOP COAT, ZrO₂/CoCrAlY INTERMEDIATE LAYER SPECIMENS. TEST PARAMETERS: TEST TEMPERATURES INDICATED, 15° IMPINGEMENT ANGLE, 1200 SECOND TEST DURATION, .35 MACH GAS VELOCITY, 80 GRIT - Al₂O₃ ABRASIVE PARTICLES, AND 7.50×10^{-3} kg/s (6.0 LBS/HR) MASS FLOW RATE. ARROW INDICATED PARTICLE FLOW DIRECTION. MAG 2X

XPN-54836



A

B

C

D



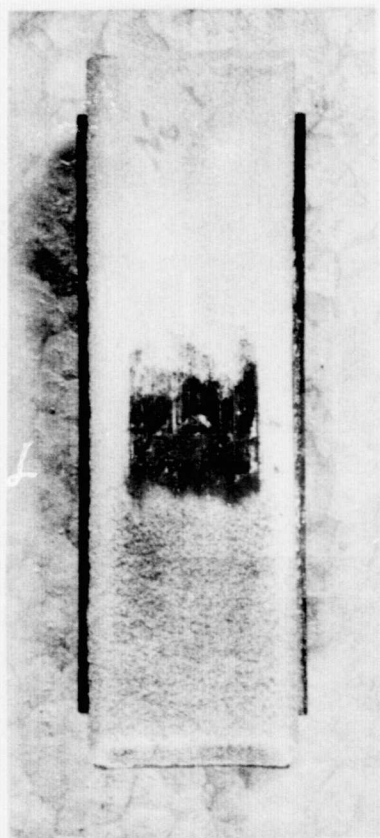
FIGURE 36

Y_2O_3 STABILIZED $ZrO_2/CoCrAlY$
GRADED LAYER CERAMIC RUB SPECIMENS

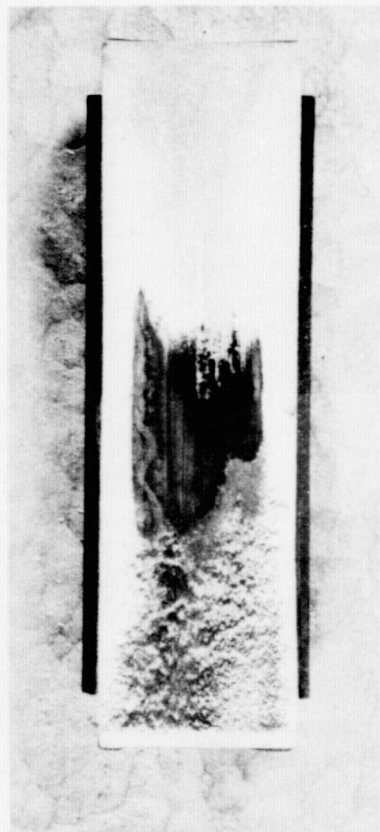
C, D - CERIUM OXIDE ADDITIVE INCLUDED WITHIN THESE
SPECIMENS

B, D - TESTED AT 1589 (2400 °F) TEMPERATURE

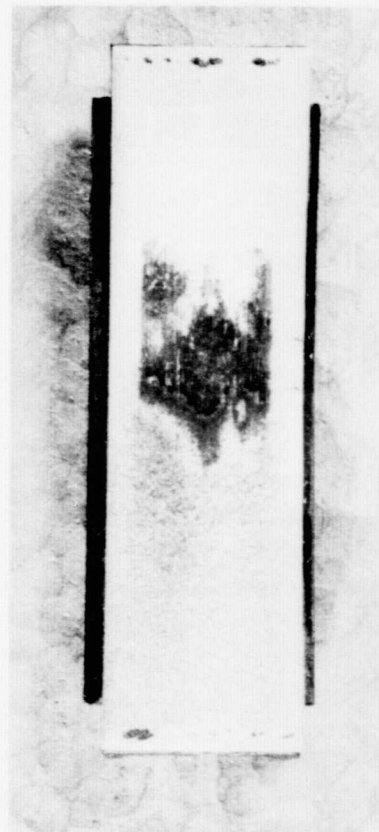
A, C - TESTED AT AMBIENT TEMPERATURE



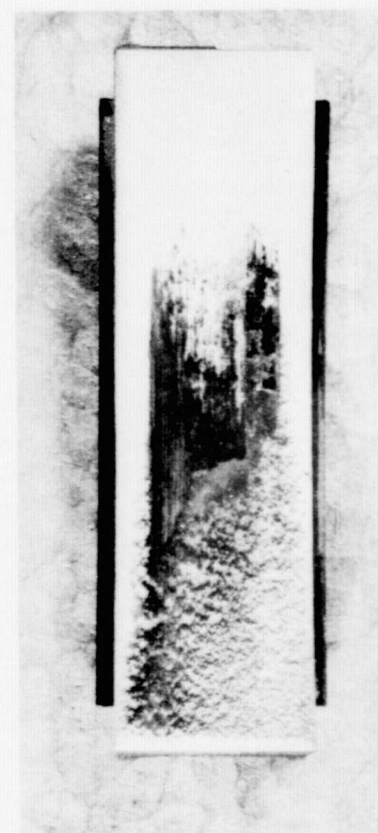
A



B



C



D



FIGURE 37

Y_2O_3 STABILIZED $ZrO_2/CoCrAlY$ CONTINUOUSLY GRADED
CERAMIC RUB SPECIMENS

C, D - CERIUM OXIDE ADDITIVE INCLUDED WITHIN THESE
SPECIMENS

B, D - TESTED AT 1589K (2400 °F) TEMPERATURE

A, C - TESTED AT AMBIENT TEMPERATURE

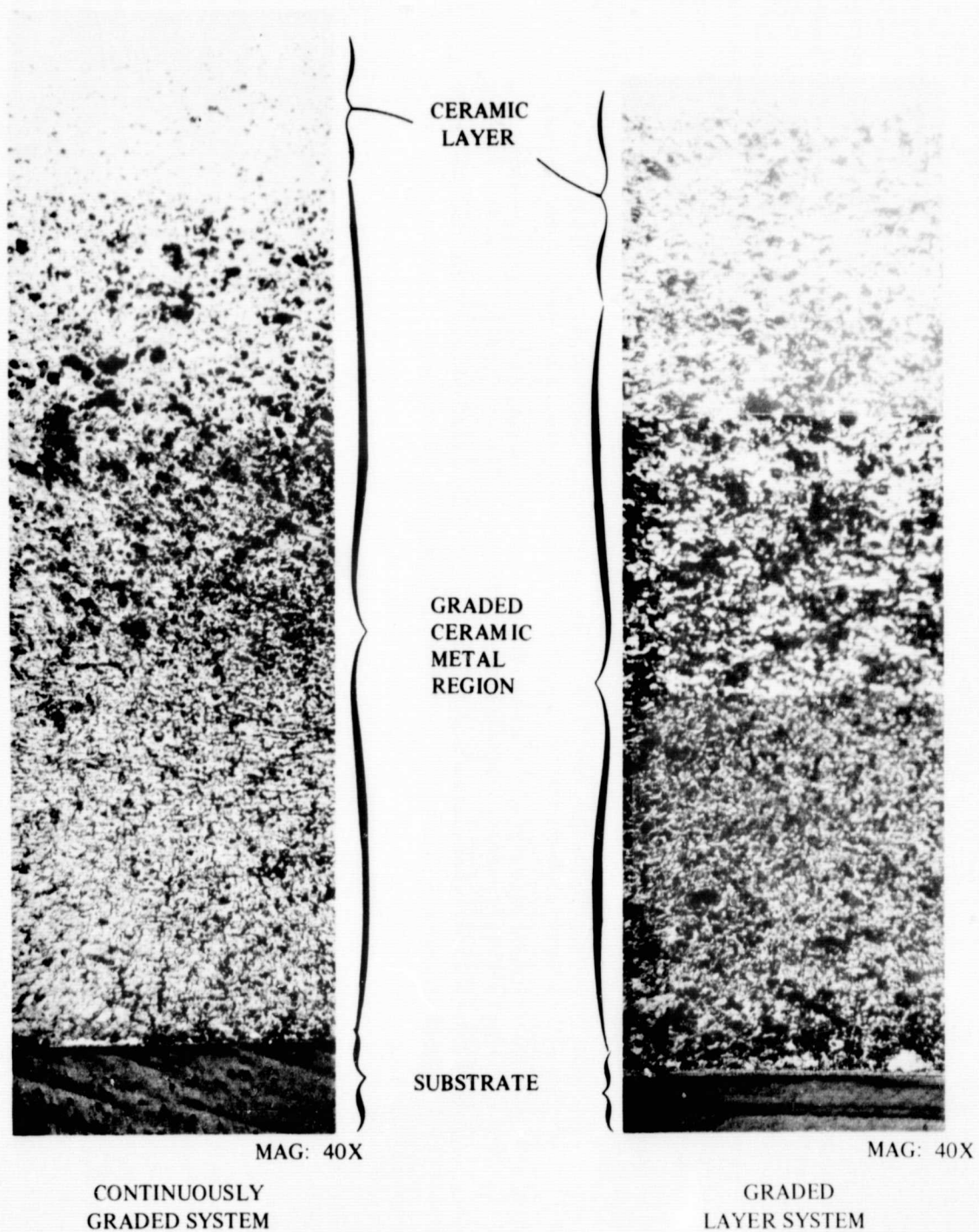


FIGURE 38

TYPICAL RADIAL CROSS SECTION THROUGH SPRAYED GRADED
 $Y_2O_3-ZrO_2/CoCrAlY$ SEAL SYSTEMS

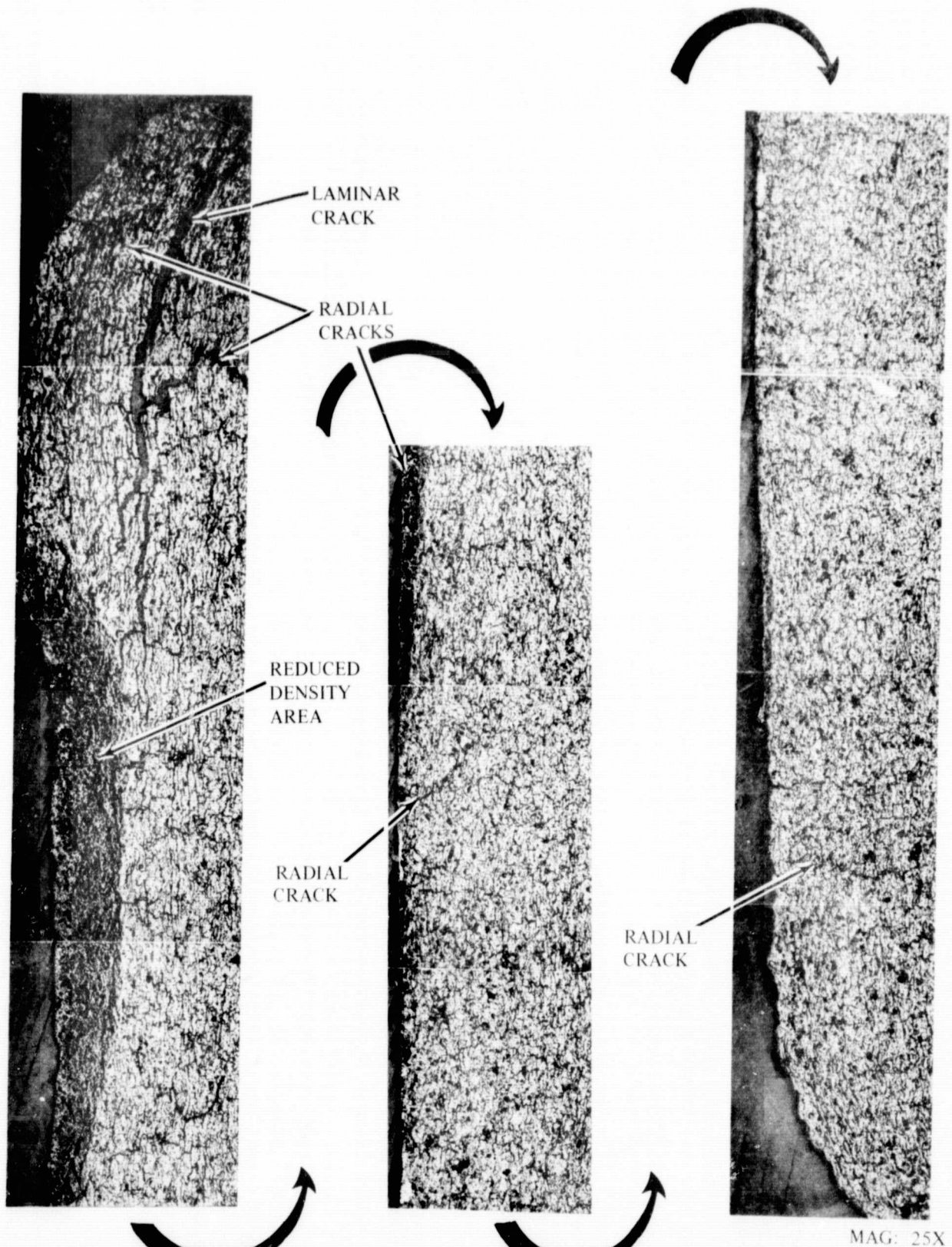
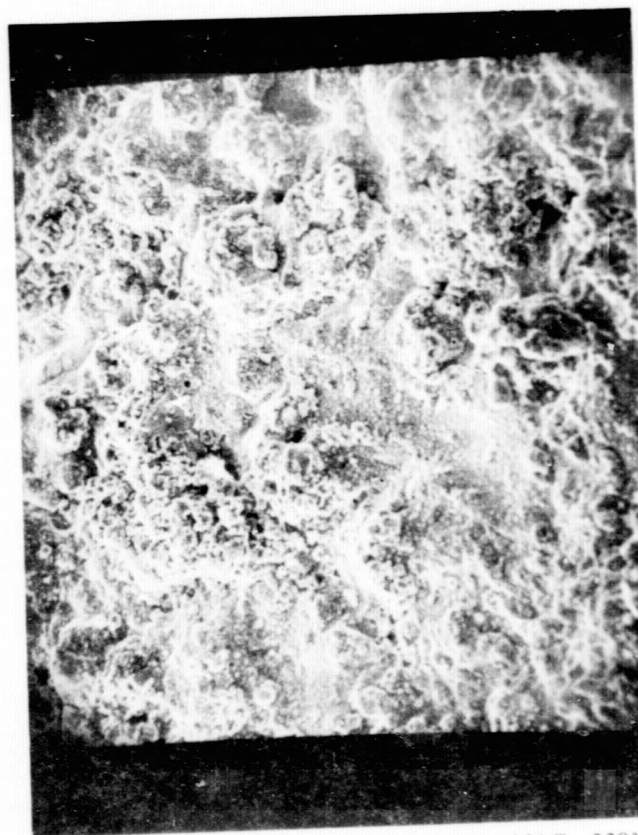


FIGURE 39
SECTION THROUGH RUBBED AREA OF CONTINUOUSLY
GRADED $\text{Y}_2\text{O}_3\text{-ZrO}_2/\text{CoCrAlY}$ SEAL



MAG: 220X

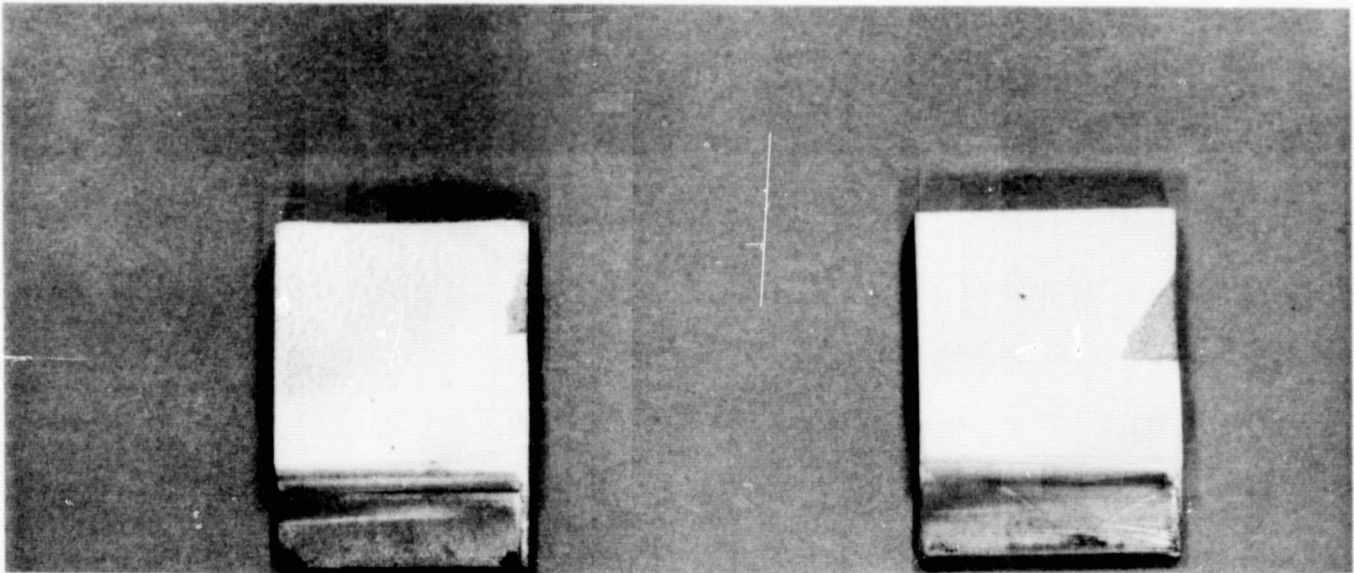
SURFACE IN GROOVE
(NOTE SMEARED, FUSED APPEARANCE)



MAG: 220X

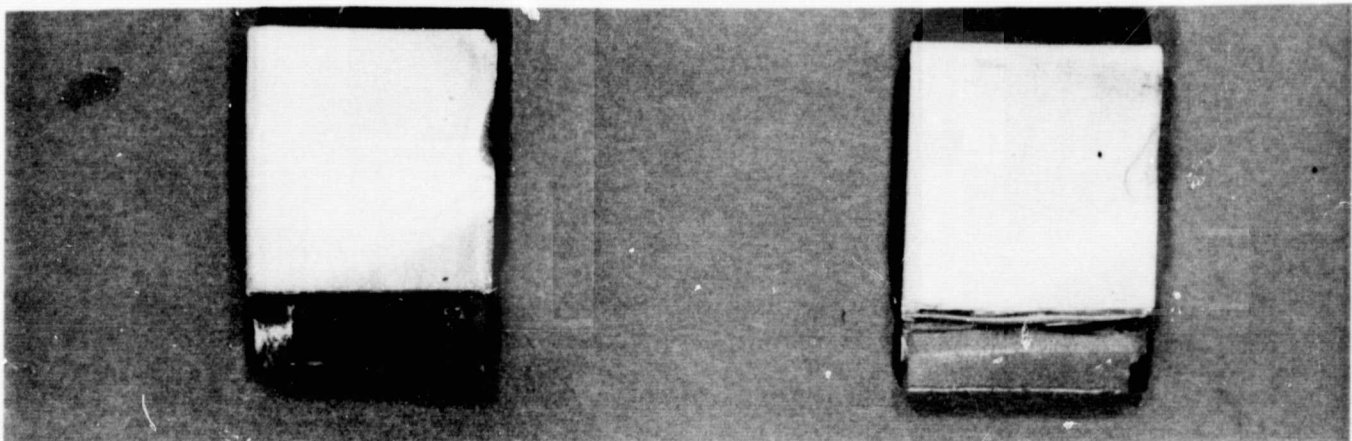
UNRUBBED SURFACE

FIGURE 40
RUBBED AND UNRUBBED SURFACES OF SPRAYED CONTINUOUSLY GRADED
 $\text{Y}_2\text{O}_3\text{-ZrO}_2/\text{CoCrAlY}$ SEAL TESTED AT 2400F



Y₂O₃ STABILIZED ZrO₂ TOP COAT,
ZrO₂/CoCrAlY GRADED INTERMEDIATE
LAYERS.

Y₂O₃ STABILIZED ZrO₂ WITH
CeO₂ ADDITIVE TOP COAT,
ZrO₂/CoCrAlY GRADED
INTERMEDIATE LAYERS.



Y₂O₃ STABILIZED ZrO₂ TOP COAT,
ZrO₂/CoCrAlY CONTINUOUSLY
GRADED INTERMEDIATE REGION.

Y₂O₃ STABILIZED ZrO₂ WITH
CeO₂ ADDITIVE TOP COAT,
ZrO₂ WITH CeO₂/CoCrAlY
CONTINUOUSLY GRADED INTER-
MEDIATE REGIONS.

FIGURE 41



POST PARTICULATE IMPINGEMENT SURFACE OF CERAMIC SPECIMENS. TEST PARAMETERS: 1589K (2400°F) SPECIMEN TEMPERATURE, 15° IMPINGEMENT ANGLE, 1200 SECOND TEST DURATION, .35 MACH GAS VELOCITY. 80 GRIT-Al₂O₃ ABRASIVE PARTICLES, AND 7.50 X 10⁻³ kg/s (6.0 LBS/HR) MASS FLOW RATE.

CN-50847

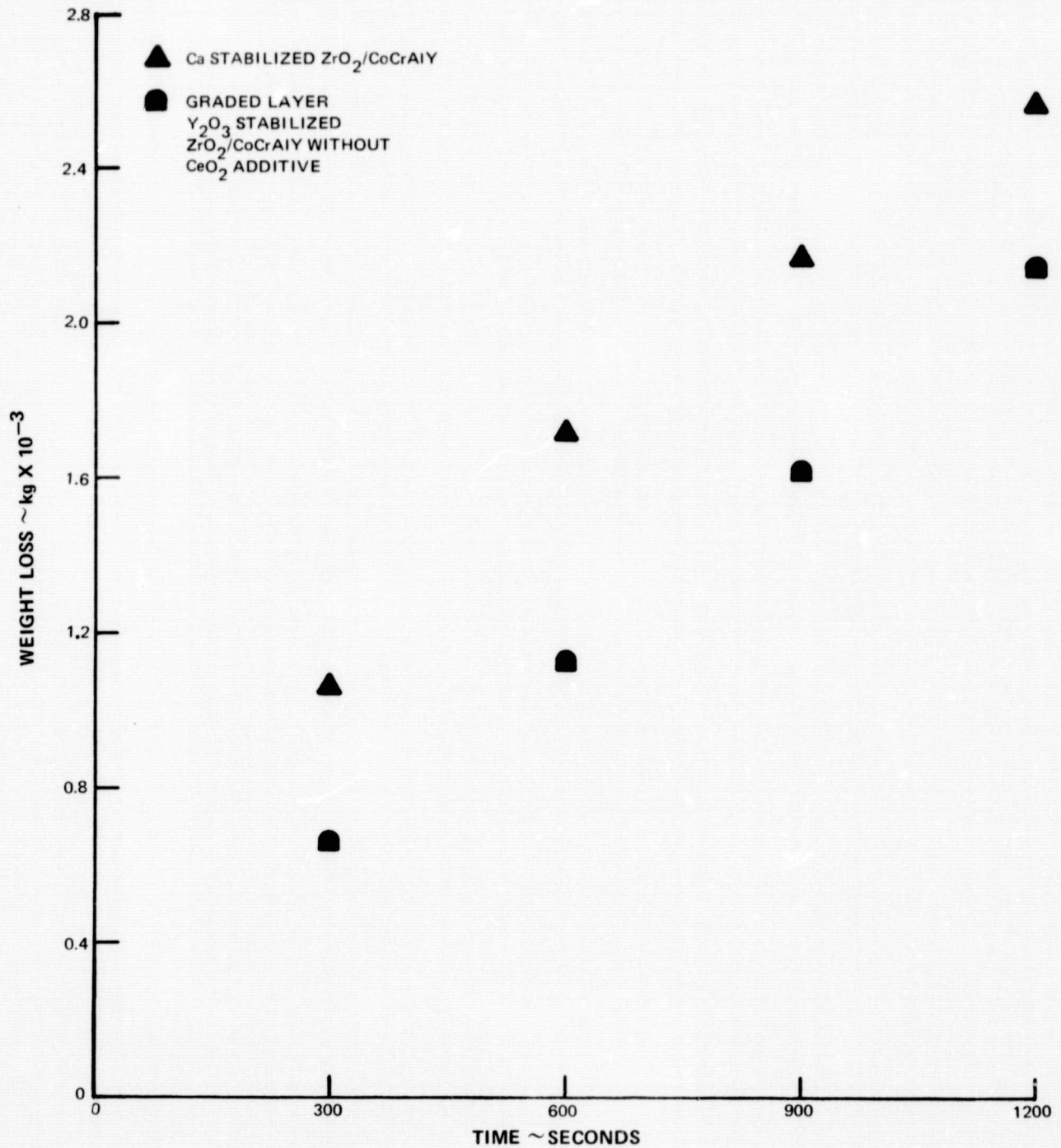


FIGURE 42

EROSION WEIGHT LOSS VS TIME COMPARISON

TEMPERATURE = 1589 K (2400°F)

IMPINGEMENT ANGLE = 15°

REFERENCES

- (1) Final Report, "Development of Abradable Gas Path Seals," NASA CR-134689 (PWA-5081), L. T. Shiembob, Contract NAS3-18023.
- (2) Final Report, "Advanced Ceramic Seal Program (Phase I)," (PWA 6635), P. W. Schilke, Contract NO0140-73-C-0320.
- (3) Report, "Advanced Ceramic Turbine Seal System Fourth Quarterly and Phase II Summary Report," (PWA 5242) M. J. Wallace, 3/31/75, Contract NO0140-74-C-0586.

APPENDIX A

Test Equipment and Procedures

A. Dynamic Abradability Rig

1. Rig Description

Rub tests to evaluate rub tolerance and abradability of candidate gas path seal systems were performed in the dynamic abradability rig shown in Figure A. This rig consists of a rotor drive system and a seal specimen feed system.

The rotor drive system is comprised of an air turbine capable of driving disks up to 0.203m (8.0 inch) diameter at speeds up to 50,000 rpm. Interchangeable disks for either knife edge or blade tip configurations are bolted to one end of a horizontal spindle shaft. The other end of the spindle shaft is connected to the drive turbine through a torque meter (used for knife edge tests) or a short coupler shaft.

The seal specimen feed system is comprised of a dead-weight loaded carriage assembly to which the seal specimen is fastened by suitable fixtures. This carriage assembly can feed the specimen radially into the rotor at controlled rates from 2.54×10^{-6} m/s (.0001 inch/sec) to 5.08×10^{-4} m/s (.020 inch/sec). Normal reaction force between the rotor and seal specimen is measured by a load cell installed in the carriage feed control system. An axial motion mechanism has also been incorporated to simulate typical traverse rates experienced in most engine environments. Two different specimen heating systems were employed, one for knife edge tests and another for blade tip tests. Two oxy-acetylene heaters and an electric air heater were used for knife edge rub tests as shown in Figure B. One of the oxy-acetylene heaters and the electric air heater were directed at the seal specimen surface. The other oxy-acetylene heater was directed at the back of the seal specimen. The oxy-acetylene heater directed at the seal surface was turned off immediately before the rub interaction to prevent knife edge heat damage. The second oxy-acetylene heater and electric air heater were effective in maintaining seal specimen temperature after the front heater was extinguished.

For blade tip rub tests, two oxy-acetylene heaters were used on the surface of the seal specimen as shown in Figure C, one on each side of the rotor. Seal specimen temperature and rotor speed were brought up to test conditions gradually and stabilized prior to rub interaction. Both heaters were operated continuously during the interaction.

Rotor speed, seal specimen temperature at the center of the rub area, carriage travel, normal load and torque (for knife edge tests only) are recorded continuously during rub interaction. Speed change of the rotor during rub interaction with the air turbine nozzle pressure held constant was used as an indication of torque due to rubbing during blade tip tests. Speed is sensed by a magnetic pulse counting system built into the drive turbine. Seal specimen temperature is measured with an optical pyrometer system. A linear voltage transformer system is used to measure carriage assembly travel. Knife edge torque is measured with a Vibrac torque meter which uses a calibrated shaft, two slotted disks and a light beam sensor which measures the

twist in the calibrated shaft by the amount of light transmitted through the window opened by relative rotation of the slotted disks. These parameters were all recorded simultaneously on a multi-channel high-speed lightbeam strip chart.

Periodic calibration of test stand instrumentation led to the disassembly and inspection of the torquemeter upon completion of knife edge testing. Torquemeter shaft and disks were found to be damaged which affected the accuracy of recorded torque measurements. A discussion with the torquemeter vendor indicated that the absolute magnitude of the torque values were, consequently, off calibration. Since the absolute torque values have been in question because of unknown effects of vibrational twisting due to non-continuous rubbing and limited response characteristics, our main concern was the effect on the relative difference between two test points. We have been assured by the vendor that the permanent twist applied to the torquemeter shaft was not detrimental to the relative torque numbers and, therefore, the torque comparison values presented in Figures 8-10 and 13 are valid. However, these torque values should be viewed in conjunction with both wear measurements and pertinent observations in order to make any judgment on comparable abrasability results.

Seal and rotor wear was measured after test and a volume ratio was calculated as a basis for relative abrasability comparison. The volume ratio was defined as the amount of rotor wear or adhesion volume divided by the seal wear volume. Small values for the volume ratio are desirable; ideally zero.

2. Test Components

Seal specimens were designed to simulate an engine seal structure as closely as possible. The abrasable and structural substrate materials and the radial thicknesses were identical to typical engine parts. The method of bonding the abrasable material to the substrate was the same as would be expected to be used in an engine application. Knife edge seal material specimens were bonded to segments of curved rings approximately 0.127 m (5.0 inch) diameter by 2.54×10^{-2} m (1.0 inch) wide by 7.62×10^{-2} m (3.0 inch) long as shown in Figure D. Blade tip seal material specimens were fabricated to cast Mar-M-409 segments approximately 0.254 m (10.0 inch) diameter by 1.91×10^{-2} m (0.75 inch) wide by 7.62×10^{-2} m (3.0 inch) long as shown in Figure E.

A Waspaloy rotor with an integral parallel sided, square tipped knife edge, shown in Figure F, was used for the knife edge tests. The knife edge profile closely resembles the configuration used on shrouded low pressure turbine blades. Dimensions of the knife edge are: diameter - 0.127 m (5.0 inch), height - 5.08×10^{-4} m (0.020 inch). Reoperation of the disk after testing was necessary to restore the flat knife edge tip.

A 0.203 m (8.0 inch) blade tip diameter disk with replaceable blades shown in Figure G was used for the blade tip rub tests. The blade tip specimens were made of cast B-1900, a typical high temperature turbine blade nickel alloy material. The circumferential thickness of the blade specimen of 3.175×10^{-3} m (0.125 inch) was selected to approximate the average circumferential contact length of a typical engine blade tip. The width of the

blade specimen was $1.27 \times 10^{-2}\text{m}$ (0.5 inch) and the radial length above the rim of the disk was approximately $7.62 \times 10^{-3}\text{m}$ (0.3 inch). Three (3) holes were drilled through the blade to reduce windage effects on the specimen heaters.

B. Erosion Test Rig

1. Rig Description

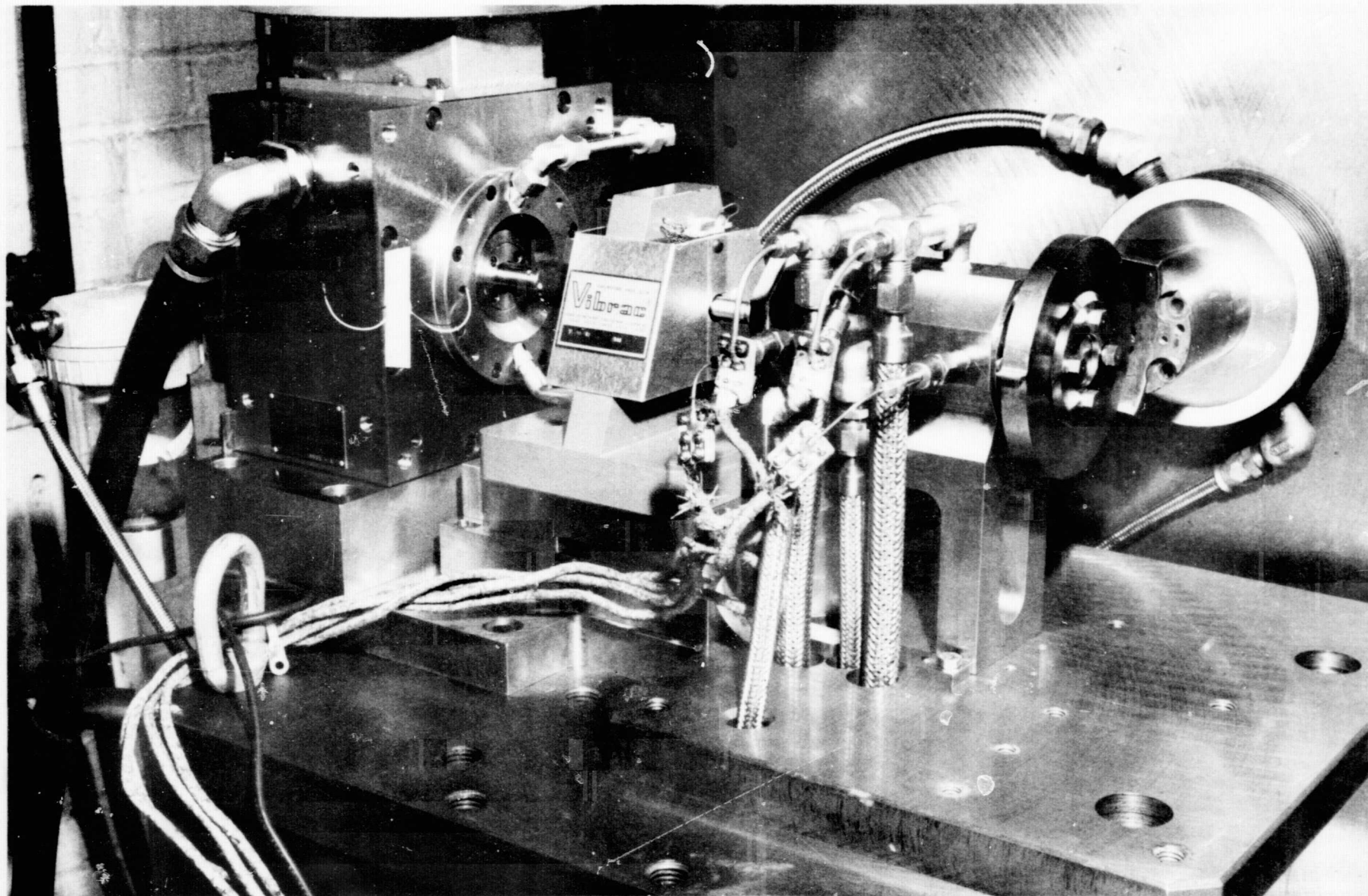
The erosion test rig used in this program is shown in Figure H. This rig was designed to test abradable seal materials under simulated engine temperature and chemical conditions. This rig burns JP-5 fuel in air and can produce a $1.905 \times 10^{-2}\text{m}$ (0.75 inch) diameter jet of hot gas with a nozzle discharge velocity up to Mach 1.0 and specimen surface temperatures in excess of 1589K (2400°F) at impingement angles as low as 7 degrees. The rig is equipped for introduction of particulate matter into the combustor to produce an abrasive hot gas stream. Size 80 grit Al_2O_3 particles were injected into the gas stream at a mass flow rate of approximately $7.50 \times 10^{-3}\text{kg/s}$ (6.0 lbs/hr) for the tests described in this report. A gas velocity of Mach 0.35 and impingement angles of 7 and 15 degrees were also used.

2. Test Component

Erosion test specimens were $3.81 \times 10^{-2}\text{m}$ (1.5 inch) square samples of the abradable material bonded to one end of a $3.81 \times 10^{-2}\text{m}$ (1.5 inch) by $5.08 \times 10^{-2}\text{m}$ (2 inch) flat metal backing plate as shown in Figure I. Abradable seal material thickness, bonding method and substrate material was the same as would be anticipated in a typical engine application. The specimen was held at a predetermined angle and distance away from the hot gas discharge nozzle by a fixture which gripped the exposed end of the metal substrate as shown in Figure J.

3. Erosion Rate Determination

The test specimen weight was measured prior to and at 300 second intervals during the test. The total test duration was 1200 seconds. The average slope of the weight loss-time curve was calculated and converted to an equivalent volume rate of change using estimated densities of the abradable surface materials.



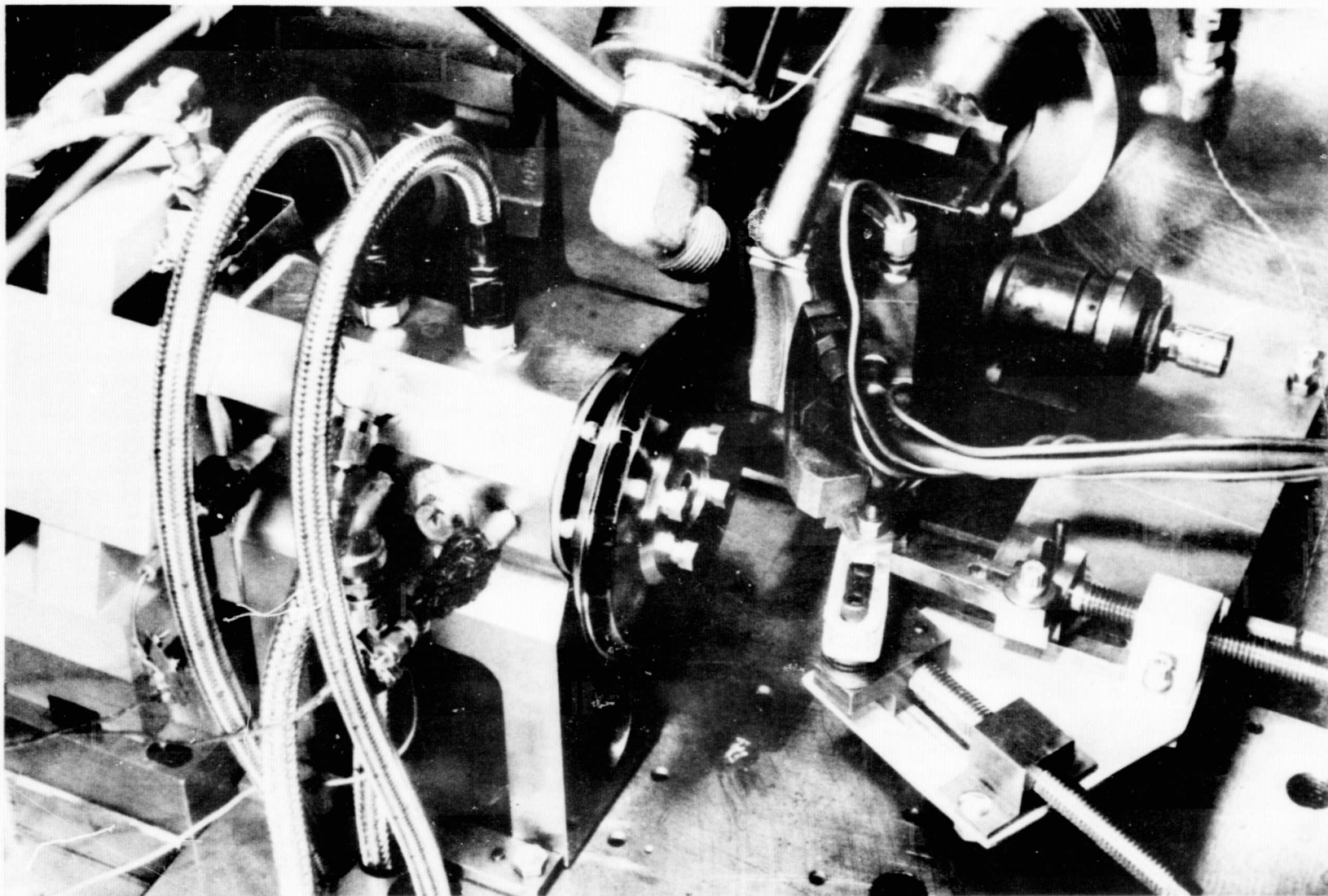
-79-



FIGURE A

DYNAMIC ABRADABILITY RIG
FRONT VIEW SHOWING TURBINE, TORQUE UNIT, TURBINE
SPINDLE.

X-37457



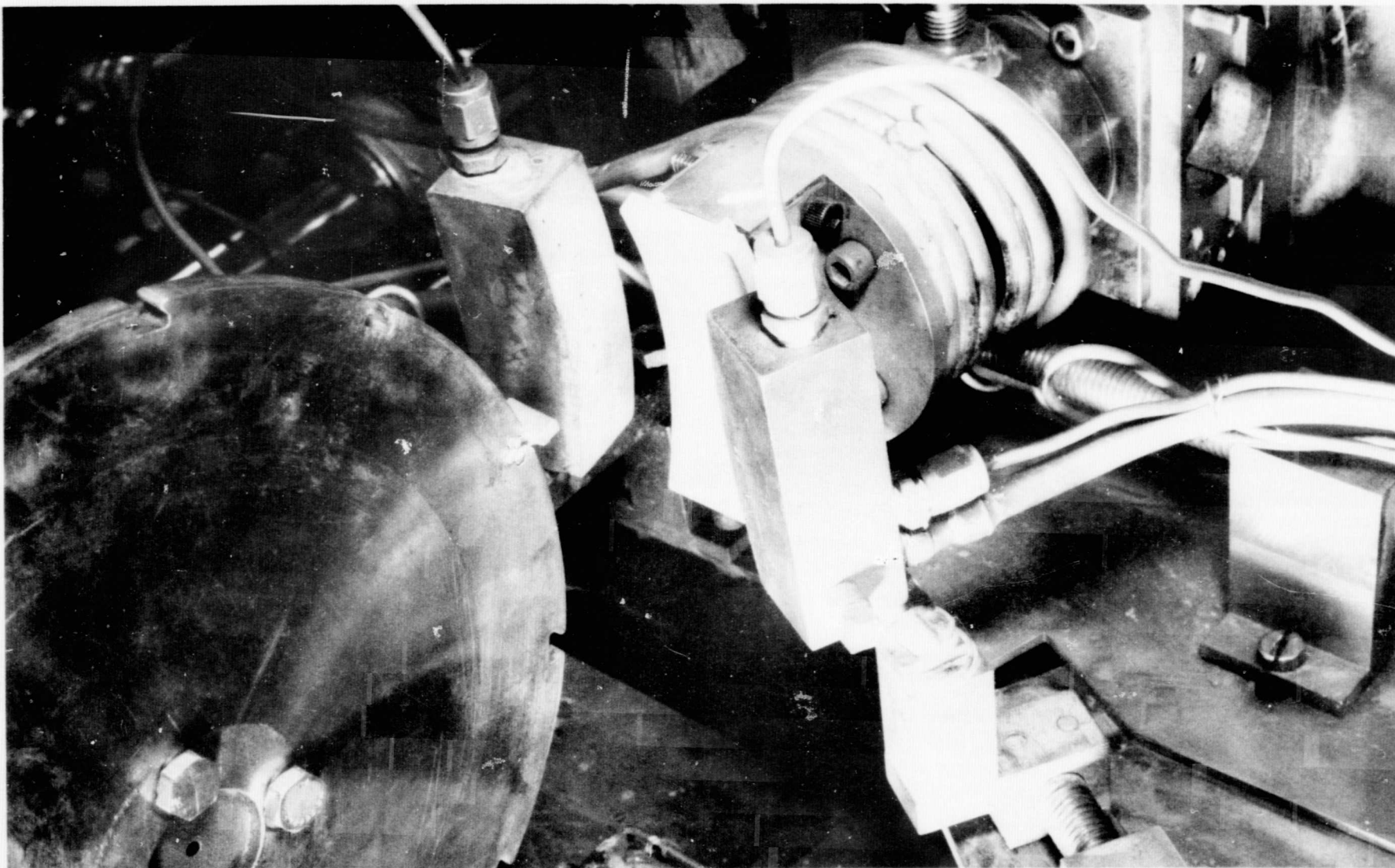
-80-



FIGURE B

DYNAMIC ABRADABILITY RIG - HEATING AND TEMPERATURE
MONITORING SYSTEM FOR KNIFE EDGE TESTING AT 1366K
(2000 °F) SEAL SURFACE TEMPERATURE TEST CONDITION.

XPN-52478



-81-



FIGURE C

DYNAMIC ABRADABILITY RIG - DOUBLE OXY-ACETYLENE
BURNER SYSTEM UTILIZED FOR OBTAINING 1589K (2400 °F)
SEAL SURFACE TEMPERATURE.

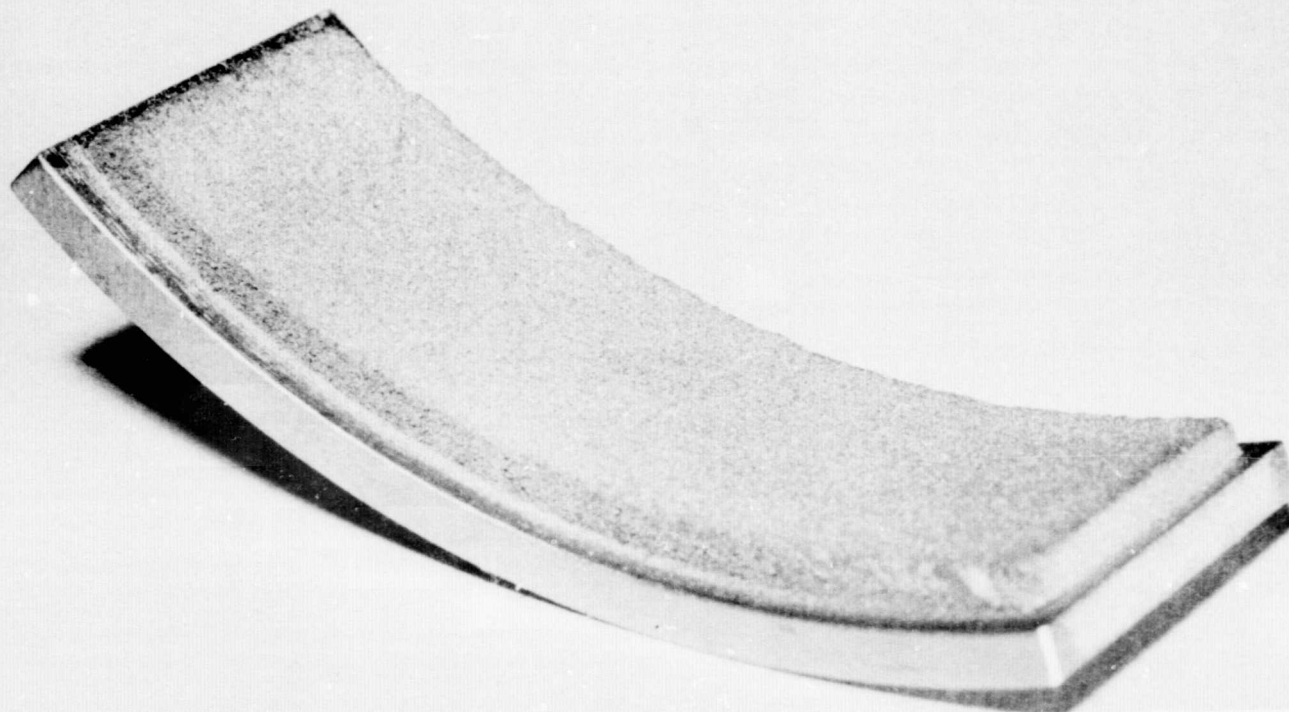


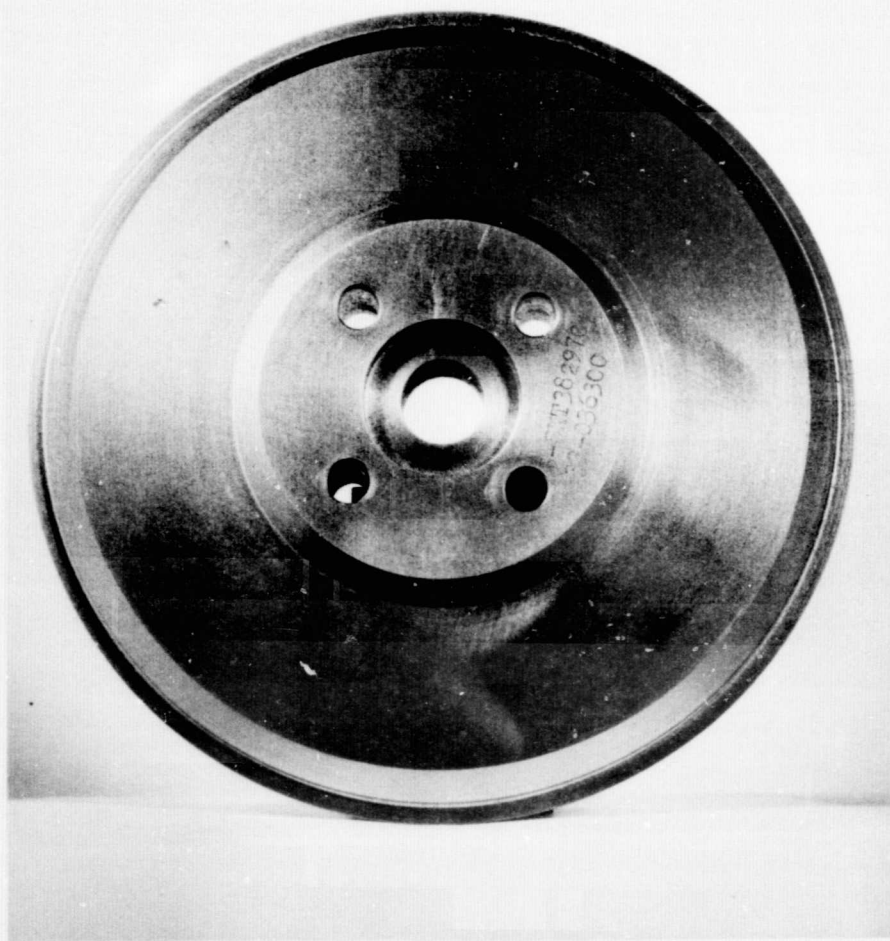
FIGURE D
TYPICAL CONFIGURATION OF KNIFE EDGE SEAL SPECIMEN
K-17136



FIGURE E

TYPICAL CONFIGURATION OF CERAMIC SPRAYED RUB
SPECIMEN DEPOSITED ON CURVED METAL SUBSTRATE.
CN-50848





84

XPN-41045A



FIGURE F

TYPICAL WASPALOY KNIFE EDGE ROTOR USED FOR RUB TESTING.

XPN-41045A

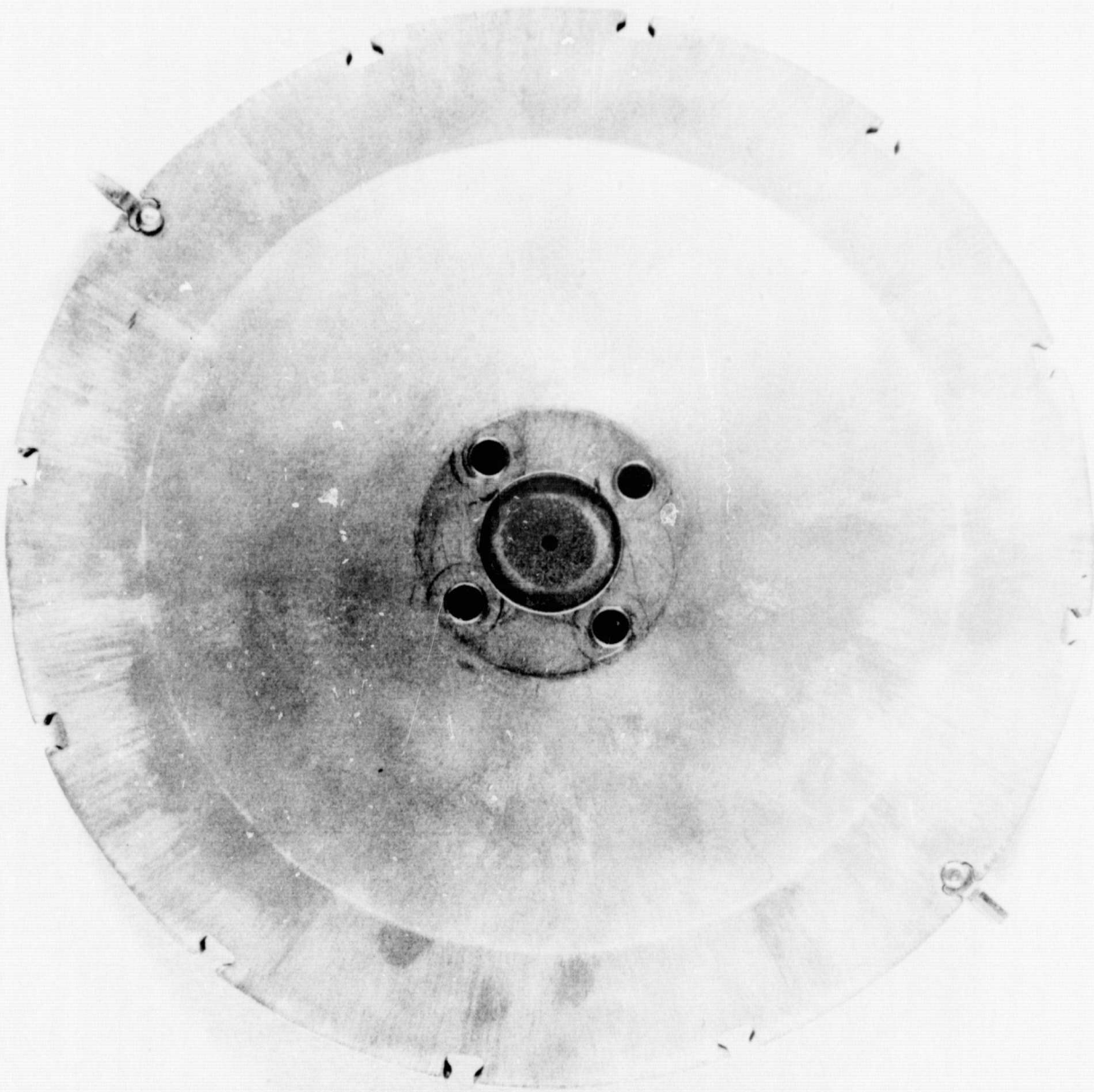


FIGURE G

BLADED DISK USED FOR RUB TEST EVALUATION.
CN-50850



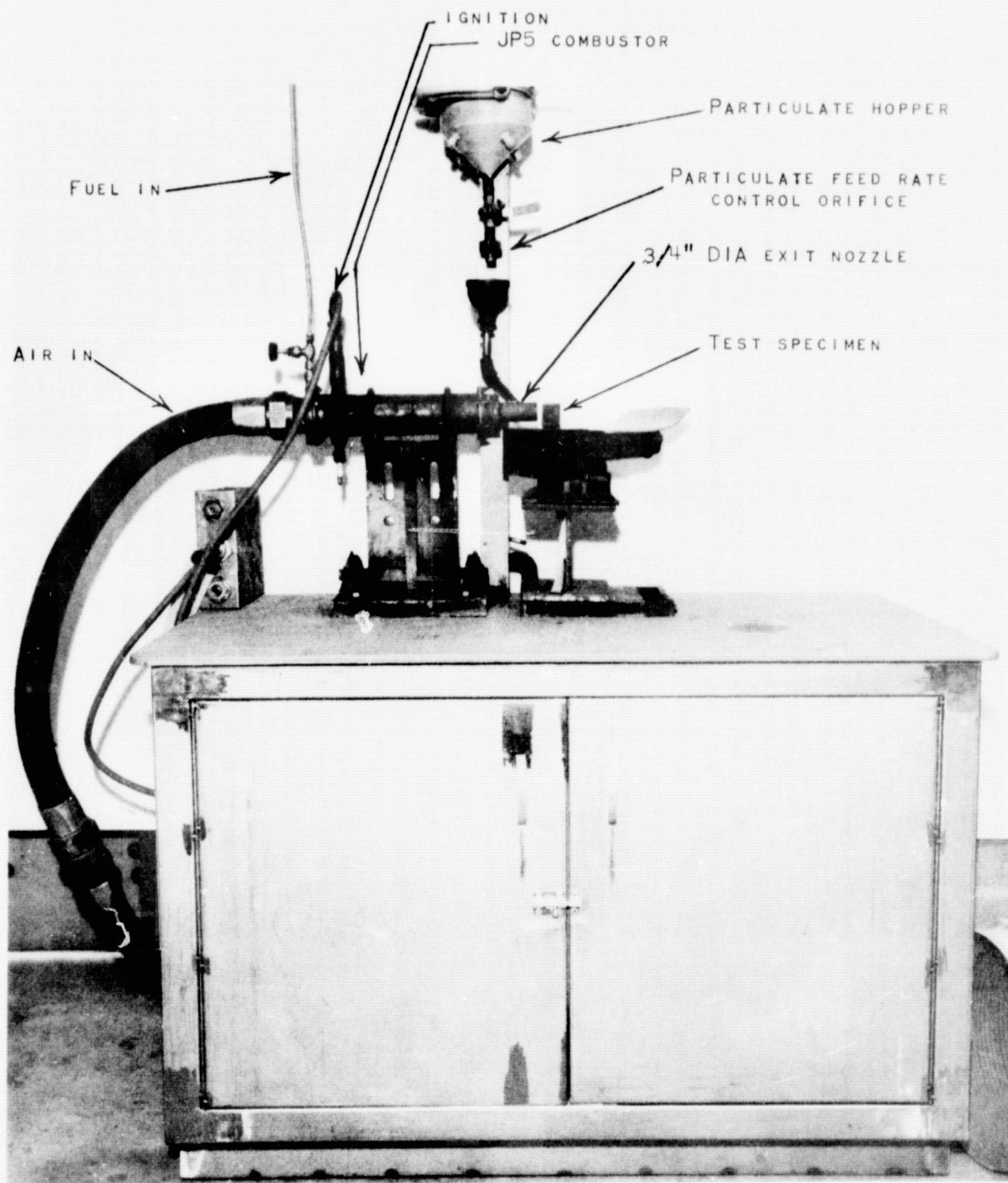
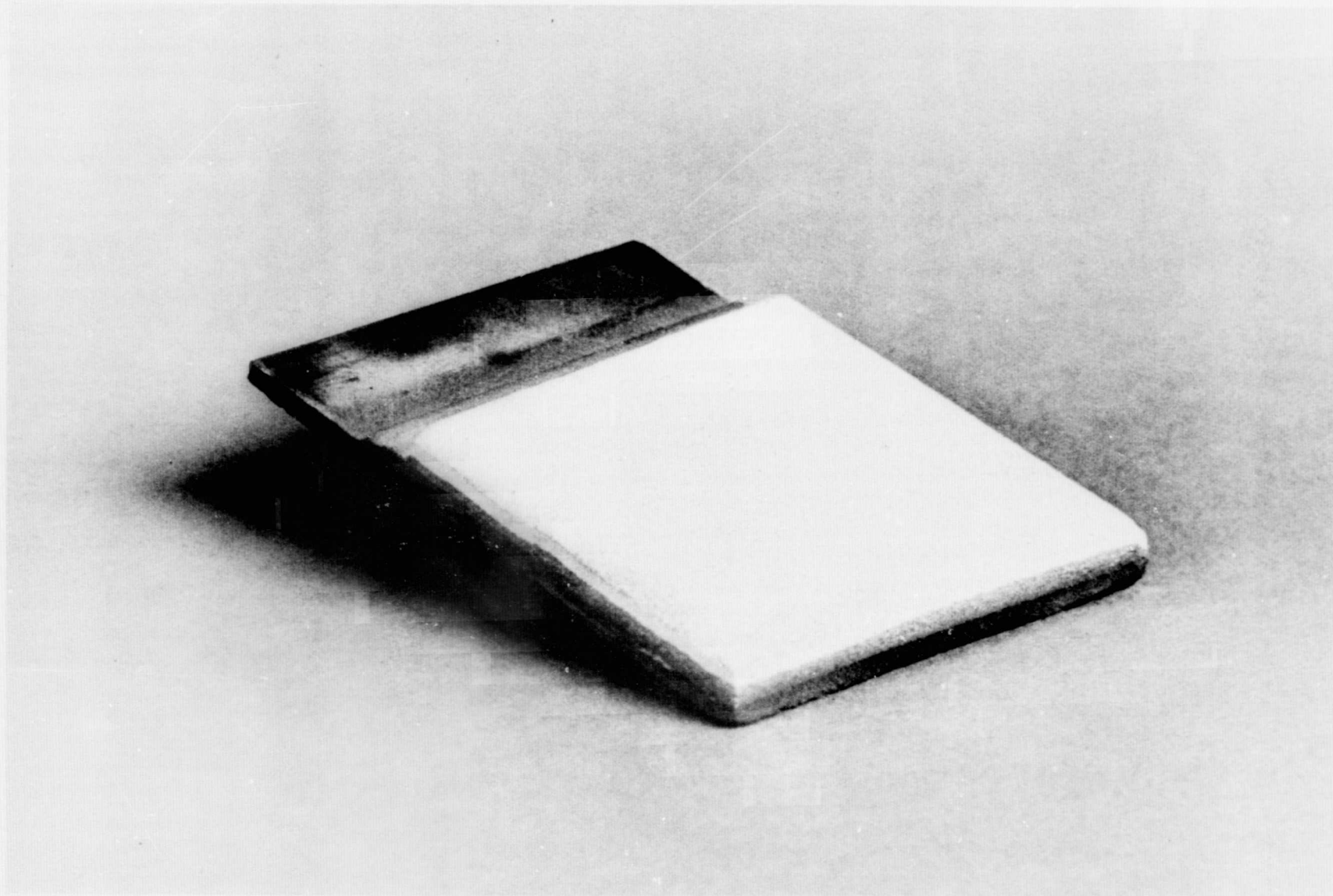


FIGURE H

HOT PARTICULATE EROSION RIG (SHOWN WITHOUT ELECTRIC
AIR HEATER).

K-6549





-87-



FIGURE 1

TYPICAL CONFIGURATION OF CERAMIC SPRAYED EROSION
SPECIMEN DEPOSITED ON FLAT METAL SUBSTRATE.

CN-50849

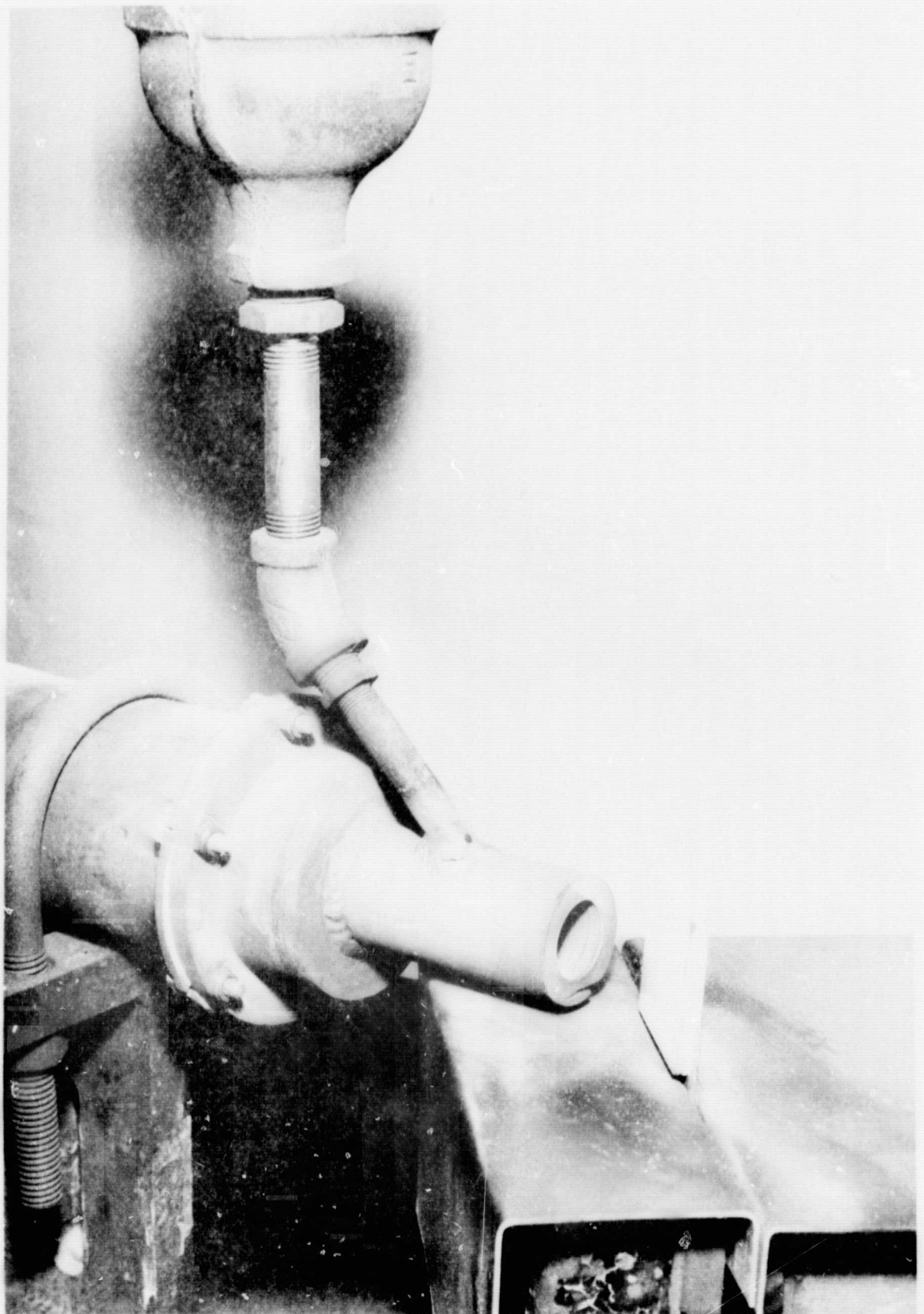


FIGURE J

CLOSEUP OF HOT PARTICULATE EROSION RIG SET UP
Z-46163



APPENDIX B
RUB TEST DATA SUMMARY
TABLE XVI

Test Conditions						Seal Specimen			Knife Edge			Post Test Information					
Test No.	Knife Edge Material	Inter-action Rate m/s $\times 10^{-5}$	Surface Speed m/s	Setup Temperature K	Penetration Depth Setup $m \times 10^{-4}$	Transfer/ Glazing	Seal Wear $m \times 10^{-4}$	Rub Pattern	Heat Discoloration (# Location Total Length)	Rad KE Wear $m \times 10^{-5}$	Pickup $m \times 10^{-6}$	Actual Temperature K	Load kg	Torque N-m	RPM Drop	VWR	Remarks
<u>NiCrAlY 13% Dense Fibermetal</u>																	
11	Waspaloy	2.54	305	Amb	7.62	Light glazing	7.11	(1) Cont.	3 Locations 100°	No KE Wear	3 Locations 3.3 max.	Amb	1.36	.036	980	+.028	Intermittent glowing
16	Waspaloy	2.54	305	1144	7.62	Medium glazing	8.38	Cont.	4 Locations 60°	0.50	None	1060	.22	.028	400	.022	Intermittent glowing
12	Waspaloy	2.54	305	1366	7.62	Medium glazing	5.08	Cont.	8 Locations 180°	0.50	None	1116	.68	.055	1000	.022	Continuous glowing
26*	Waspaloy	2.54	305	1366	7.62	Light glazing	5.59	Cont.	2 Locations 45°	No KE Wear	3 Locations 2.5 max.	1046	.68	.440	1400	+.009	Intermittent glowing
13	Waspaloy	2.54	183	1366	7.62	Light glazing	4.06	Cont.	3 Locations 60°	No KE Wear	3 Locations 25.4 max.	1088	.68	.012	400	+.653	Intermittent glowing
24	Waspaloy	.254	305	Amb	7.62	Heavy glazing	7.87	Cont.	10 Locations 135°	1.01	None	Amb	.68	.031	400	.074	Intermittent glowing
18	Waspaloy	.254	305	1366	7.62	Medium glazing	8.13	Cont.	2 Locations 200°	0.25	None	1046	0.0	N/A	100	.041	Intermittent glowing
25	Waspaloy	25.4	305	Amb	7.62	Heavy glazing	5.59	Cont.	Heavy 360°	32.7	None	Amb	4.08	.391	4100	4.81	Continuous glowing
17	Waspaloy	25.4	305	1366	7.62	Light glazing	8.38	Cont.	1 Location 20°	No KE Wear	1 Location 17.8 max.	1032	.45	.046	300	+.013	Continuous glowing
28**	Waspaloy	2.54	305	Amb	7.62	Heavy glazing	8.12	Cont.	1 Location 180°	1.78	1 Location -30° 12.7 max.	Amb	.45	(Sweep) .621	1560	.005	Intermittent glow Continuous glow (sweep)
<u>Pack Aluminide Coated Hastelloy-X Honeycomb</u>																	
7	Waspaloy	2.54	305	Amb	7.62	None	6.60	Cont.	1 Location 10°	No KE Wear	1 Location 66.0 max.	Amb	.45	0.0	200	+.021	Intermittent glowing
15	Waspaloy	2.54	305	1144	7.62	Light glazing	8.63	Cont.	1 Location 10°	No KE Wear	1 Location 40.6 max.	1088	.22	.034	150	+.007	No visible glowing

APPENDIX B
RUB TEST DATA SUMMARY
TABLE XVI (Cont'd.)

Test Conditions					Seal Specimen			Knife Edge			Post Test Information						Remarks
Test No.	Knife Edge Material	Inter-action Rate m/s $\times 10^{-5}$	Surface Speed m/s	Setup Temperature K	Pene-tration Depth Setup $m \times 10^{-4}$	Transfer/ Glazing	Seal Wear $m \times 10^{-4}$	Rub Pattern	Heat Discoloration (# Location Total Length	Rad KE Wear $m \times 10^{-5}$	Pickup $m \times 10^{-6}$	Actual Temperature K	Load kg	Torque N·m	RPM Drop	WWR	
8	Waspaloy	2.54	305	1366	7.62	None	5.59	End rubs only	1 Location 5°	No KE Wear	1 Location 25.4 max.	1088	0.0	0.0	200	+028	No visible glowing
9	Waspaloy	2.54	183	1366	7.62	Light glazing	4.57	End rubs only	1 Location 5°	No KE Wear	1 Location 66.0 max.	1227	.68	0.0	100	+058	No visible glowing
23	Waspaloy	.254	305	Amb	7.62	None	6.35	Cont.	1 Location 10°	None	2 Locations 51.0 max.	Amb	.22	.012	270	+015	Light sparking
14	Waspaloy	.254	305	1366	7.62	Light glazing	4.57	Cont.	1 Location 10°	No KE	1 Location 20.3 max.	1144	.22	.023	100	+008	Intermittent glowing
10	Waspaloy	25.4	305	1366	7.62	Light glazing	4.32	Cont.	4 Locations 20°	No KE Wear	4 Locations 30.5 max.	1127	1.13	.012	100	+046	Intermittent glowing
27**	Waspaloy	2.54	305	Amb	7.62	Minimal cell smearing	7.11	Cont.	3 Locations 10°	No KE Wear	2 Locations 116.8 max.	Amb	.45	(Sweep) .014	520	+004	Intermittent glow Continuous glow (sweep)

APPENDIX B
RUB TEST DATA SUMMARY
TABLE XVI (Cont'd.)

Test Conditions						Seal Specimen			Blade			Post Test Information					
Test No.	Blade Material	Inter-action Rate $\frac{m}{s} \times 10^{-5}$	Surface Speed $\frac{m}{s}$	Setup Temperature K	Pene-tration Depth Setup $m \times 10^{-4}$	Transfer/ Glazing	Seal Wear $m \times 10^{-4}$	Rub Pattern	Heat Discoloration	Blade Wear $m \times 10^{-4}$	Pickup (inch)	Actual Temperature K	Load kg	Torque N·m	RPM Drop	WR	Remarks
<u>Quartz Woven Fiber System</u>																	
19	B-1900	2.54	305	Amb	7.62	None	4.57	Cont.	None	None	None	Amb	.91	---	300	0	Specimen chipped during interaction(3)
20	B-1900	2.54	305	1366	7.62	None	7.62	Cont.	None	None	None	1310	1.36	---	0	0	Clean groove, some light chipping of seal material
21	B-1900	2.54	305	1589	7.62	N/A	N/A	N/A	None	None	None	1505	.41	---	0	N/A	Seal disintegrated at rubbing interface midway during interaction
22	B-1900	25.4	305	1589	7.62	N/A	N/A	N/A	None	None	None	1505	.45	---	100	N/A	Seal disintegrated at rubbing interface midway during interaction
<u>Sprayed NiCoCrAlY with CeO₂ Additive System</u>																	
1	B-1900	2.54	305	Amb	7.62	Heavy blade transfer & seal smearing	No visible wear	Cont.	---	N/A	None	Amb	N/A	---	420	Indeterminate	Blade failed midway during interaction
5	B-1900	2.54	305	1589	7.62	Heavy blade transfer	No visible wear	Cont.	Heavy	6.60	None	1616	1.36	---	700	Indeterminate	Localized melting through to backing adjacent to rubbing surface
6	B-1900	2.54	305	1366	7.62	Heavy blade transfer & seal smearing	No visible wear (4)	Cont.	Heavy	6.35	None	1393	.91	---	100	Indeterminate	Localized melting and debonding near front torch impingement
<u>Sprayed CaO Stabilized ZrO₂/CoCrAlY System</u>																	
3	B-1900	2.54	305	1366	7.62	Heavy blade transfer	No visible wear	Cont.	Heavy	8.64	None	1393	1.36	---	400	Indeterminate	No spalling or debonding of ceramic top coat
2	B-1900	2.54	305	1589	7.62	Heavy blade transfer	No visible wear	Cont.	Heavy	9.40	None	1699	1.36	---	500	Indeterminate	Heavy delamination and spallation of zirconia(5)
4	B-1900	2.54	183	1589	7.62	Heavy blade transfer	No visible wear	Cont.	Heavy	5.84	None	1616	1.81	---	1100	Indeterminate	Heavy delamination and spallation of zirconia(5)

APPENDIX B
RUB TEST DATA SUMMARY
TABLE XVI (Cont'd.)

ORIGINAL PAGE IS
OF POOR QUALITY

Test Conditions					Seal Specimen			Blade			Post Test Information						
Test No.	Blade Material	Inter-action Rate m/s $\times 10^{-5}$	Surface Speed m/s	Setup Temperature K	Penetration Depth Setup $m \times 10^{-4}$	Transfer/ Glazing	Seal Wear $m \times 10^{-4}$	Rub Pattern	Heat Discoloration	Blade Wear $m \times 10^{-4}$	Pickup (inch)	Actual Temperature K	Load kg	Torque N·m	RPM Drop	WVR	Remarks
Sprayed, Graded Layer Y_2O_3 Stabilized $ZrO_2/CoCrAlY$ without CeO_2																	
31	B-1900	2.54	305	Amb	7.62	Heavy blade transfer	.76	Cont.	Heavy	8.89	None	Amb	1.5	---	200	15	Heavy blade transfer some light seal grooving
32	B-1900	2.54	305	1589	7.62	Heavy blade transfer	0.0	Cont.	Heavy	7.62	None	1589	.5	---	300	Indeterminate	Heavy blade wear, no seal spalling
Sprayed, Graded Layer Y_2O_3 Stabilized $ZrO_2/CoCrAlY$ with CeO_2																	
33	B-1900	2.54	305	Amb	7.62	Heavy blade transfer	0.0	Cont.	Heavy	7.87	None	Amb	1.5	---	300	Indeterminate	Metal transfer/ceramic spalling in rubbed area
34	B-1900	2.54	305	1589	7.62	Heavy blade transfer	.51	Cont.	Heavy	8.63	None	1616	1.5	---	300	70	Localized edge groove, heavy blade transfer
Sprayed, Continuously Graded Y_2O_3 Stabilized $ZrO_2/CoCrAlY$ without CeO_2																	
29	B-1900	2.54	305	Amb	7.62	Heavy blade transfer	0.0	Cont.	Heavy	6.60	None	Amb	1.0	---	300	Indeterminate	Metal transfer/ceramic spalling in rubbed area
30	B-1900	2.54	305	1589	7.62	Heavy blade transfer	2.03	Cont.	Heavy	6.60	None	1560	2.0	---	400	2.5	Localized seal grooving, no seal spalling or delamination
Sprayed, Continuously Graded Y_2O_3 Stabilized $ZrO_2/CoCrAlY$ with CeO_2																	
35	B-1900	2.54	305	Amb	7.62	Heavy blade transfer	0.0	Cont.	Heavy	8.38	None	Amb	.5	---	560	Indeterminate	Some seal spalling at center of rub
36	B-1900	2.54	305	1589	7.62	Heavy blade transfer	.25	Cont.	Heavy	8.38	None	1616	.5	---	460	95	Very light seal grooving, no seal spalling

(1) Continuous rub extending for most of 60° arc of seal segment

(2) + Denotes knife edge pickup occurrence

(3) Initial interaction area (end of specimen) broke off during interaction

(4) A light 17.8×10^{-5} m localized groove occurred when seal specimen shifted during testing.

(5) Spalling occurred during post test cool down

*Repeat of test No. 12 with "smooth" knife edge

**Sweep test (sweep after penetration) at 2.54×10^{-4} m/s for 5.08×10^{-3} m

APPENDIX B
RUB TEST DATA SUMMARY
TABLE XVI-A

Test Conditions					Seal Specimen			Knife Edge				Post Test Information						
Test No.	Knife Edge Material	Inter-action Rate (inch/sec)	Surface Speed (ft/sec)	Setup Temperature (°F)	Pene-tration Depth Setup (inch)	Transfer/ Glazing	Seal Wear (inch)	Rub Pattern	Discoloration (# Location (Total Length))	Rad KE Wear (inch)	Pickup (inch)	Actual Temperature (°F)	Load (lbs)	Torque (in-lbs)	RPM Drop	WVR	Remarks	
<u>NiCrAlY 33% Dense Fibermetal</u>																		
11	Waspaloy	.002	1000	Amb	.030	Light glazing	.028	Cont. (1)	3 Locations 100°	No KE Wear	3 Locations .0013 max.	Amb	3.0	0.32	980	+.028 (2)	Intermittent glowing	
16	Waspaloy	.001	1000	1600	.030	Medium glazing	.033	Cont.	4 Locations 60°	.0002	None	1150	0.5	0.25	400	.022	Intermittent glowing	
12	Waspaloy	.001	1000	2000	.030	Medium glazing	.020	Cont.	8 Locations 180°	.0002	None	1550	1.5	0.48	1000	.022	Continuous glowing	
26*	Waspaloy	.001	1000	2000	.030	Light glazing	.022	Cont.	2 Locations 45°	No KE Wear	3 Locations .0001 max.	1125	1.5	3.83	1400	+.009	Intermittent glowing	
13	Waspaloy	.001	600	2000	.030	Light glazing	.016	Cont.	3 Locations 60°	No KE Wear	3 Locations .0010 max.	1500	1.5	0.11	400	+.053	Intermittent glowing	
24	Waspaloy	.0001	1000	Amb	.030	Heavy glazing	.031	Cont.	10 Locations 135°	.0004	None	Amb	1.5	.27	400	.074	Intermittent glowing	
18	Waspaloy	.0001	1000	2000	.030	Medium glazing	.032	Cont.	2 Locations 200°	.0001	None	1125	0.0	N/A	100	.041	Intermittent glowing	
25	Waspaloy	.010	1000	Amb	.030	Heavy glazing	.022	Cont.	Heavy 360°	.0129	None	Amb	9.0	3.40	4100	4.81	Continuous glowing	
17	Waspaloy	.010	1000	2000	.030	Light glazing	.033	Cont.	1 Location 20°	No KE Wear	1 Location .0007 max.	1100	1.0	0.40	300	+.013	Continuous glowing	
28**	Waspaloy	.001	1000	Amb	.030	Heavy glazing	.032	Cont.	1 Location 180°	.0007	1 Location .0005 max.	Amb	1.0	(Sweep) 5.40	1560	.005	Intermittent glow Continuous glow (sweep)	
<u>Pack Aluminide Coated Hastelloy-X Honeycomb</u>																		
7	Waspaloy	.001	1000	Amb	.030	None	.026	Cont.	1 Location 10°	No KE Wear	1 Location .0026 max.	Amb	1.0	0.0	200	+.021	Intermittent glowing	
15	Waspaloy	.001	1000	1600	.030	Light glazing	.034	Cont.	1 Location 10°	No KE Wear	1 Location .0016 max.	1500	0.5	0.30	150	+.007	No visible glowing	
8	Waspaloy	.001	1000	2000	.030	None	.022	End rubs only	1 Location 5°	No KE Wear	1 Location .0010 max.	1500	0.0	0.0	200	+.028	No visible glowing	

APPENDIX B
RUB TEST DATA SUMMARY
TABLE XVI-A (Cont'd.)

Test Conditions						Seal Specimen			Knife Edge			Post Test Information					
Test No.	Knife Edge Material	Inter-action Rate (inch/sec)	Surface Speed (ft/sec)	Setup Temperature (°F)	Pena-tration Depth Setup (inch)	Transfer/ Glazing	Seal Wear (inch)	Rub Pattern	Heat Discoloration (# Location Total Length)	Rad KE Wear (inch)	Pickup	Actual Temperature (°F)	Load (lbs)	Torque (in-lbs)	RPM Drop	WR	Remarks
9	Waspaloy	.001	600	2000	.030	Light glazing	.018	End rubs only	1 Location 5°	No KE Wear	1 Location .0026 max.	1750	1.5	0.0	100	+.058	No visible glowing
23	Waspaloy	.0001	1000	Amb	.030	None	.025	Cont.	1 Location 10°	None	2 Locations .0020 max.	Amb	0.5	.11	270	+.015	Light sparking
14	Waspaloy	.0001	1000	2000	.030	Light glazing	.018	Cont.	1 Location 10°	No KE Wear	1 Location .0008 max.	1600	0.5	0.20	100	+.008	Intermittent glowing
10	Waspaloy	.010	1000	2000	.030	Light glazing	.017	Cont.	4 Locations 20°	No KE Wear	4 Locations .0012 max.	1570	2.5	0.11	100	+.046	Intermittent glowing
27**	Waspaloy	.001	1000	Amb	.030	Minimal cell smearing	.028	Cont.	3 Locations 10°	No KE Wear	2 Locations .0046 max.	Amb	1.0	(Sweep) .13	520	+.004	Intermittent glow Continuous glow (sweep)

APPENDIX B
RUB TEST DATA SUMMARY
TABLE XVI-A (Cont'd.)

Test Conditions						Seal Specimen		Blade			Post Test Information						
Test No.	Blade Material	Inter-action Rate (inch/sec)	Surface Speed (ft/sec)	Setup Temperature (°F)	Pene-tration Depth Setup (inch)	Transfer/ Glazing	Seal Wear (inch)	Rub Pattern	Heat Discoloration	Blade Wear (inch)	Pickup (inch)	Actual Temperature (°F)	Load (lbs)	Torque (in-lbs)	RPM Drop	WR	Remarks
<u>Quartz Woven Fiber System</u>																	
19	B-1900	.001	1000	Amb	.030	None	.018	Cont.	None	None	None	Amb	2.0	---	300	0	Specimen chipped during interaction(3)
20	B-1900	.001	1000	2000	.030	None	.030	Cont.	None	None	None	1900	3.0	---	0	0	Clean groove, some light chipping of seal material
21	B-1900	.001	1000	2400	.030	N/A	N/A	N/A	None	None	None	2250	0.9	---	0	N/A	Seal disintegrated at rubbing interface mid-way during interaction
22	B-1900	.010	1000	2400	.030	N/A	N/A	N/A	None	None	None	2250	1.0	---	100	N/A	Seal disintegrated at rubbing interface mid-way during interaction
<u>Sprayed NiCoCrAlY with CeO₂ Additive System</u>																	
1	B-1900	.001	1000	Amb	.030	Heavy blade transfer & seal smearing	No visible wear	Cont.	---	N/A	None	Amb	N/A	---	420	Indeter- minate	Blade failed midway during interaction
5	B-1900	.001	1000	2400	.030	Heavy blade transfer	No visible wear	Cont.	Heavy	.026	None	2450	3.0	---	700	Indeter- minate	Localized melting through to backing, adjacent to rubbing surface
6	B-1900	.001	1000	2000	.030	Heavy blade transfer & seal smearing	No visible wear (*)	Cont.	Heavy	.025	None	2050	2.0	---	100	Indeter- minate	Localized melting and debonding near front torch impingement
<u>Sprayed CaO Stabilized ZrO₂/CoCrAlY System</u>																	
3	B-1900	.001	1000	2000	.030	Heavy blade transfer	No visible wear	Cont.	Heavy	.034	None	2050	3.0	---	400	Indeter- minate	No spalling or debonding of ceramic top coat
2	B-1900	.001	1000	2400	.030	Heavy blade transfer	No visible wear	Cont.	Heavy	.037	None	2600	3.0	---	500	Indeter- minate	Heavy delamination and spallation of zirconia (5)
4	B-1900	.001	600	2400	.030	Heavy blade transfer	No visible wear	Cont.	Heavy	.023	None	2450	4.0	---	1100	Indeter- minate	Heavy delamination and spallation of zirconia (5)

APPENDIX B
RUB TEST DATA SUMMARY
TABLE XVI-A (Cont'd.)

Test Conditions						Seal Specimen			Blade			Post Test Information					
Test No.	Blade Material	Inter-action Rate (inch/sec)	Surface Speed (ft/sec)	Setup Temperature (°F)	Penetration Depth Setup (inch)	Transfer/ Glazing	Seal Wear (inch)	Rub Pattern	Heat Discoloration	Blade Wear (inch)	Pickup (inch)	Actual Temperature (°F)	Load (lbs)	Torque (in-lbs)	RPM Drop	WWR	Remarks
Sprayed, Graded Layer Y ₂ O ₃ Stabilized ZrO ₂ /CoCrAlY without CeO ₂																	
31	B-1900	.001	1000	Amb	.030	Heavy blade transfer	.003	Cont.	Heavy	.035	None	Amb	1.5	---	200	15	Heavy blade transfer, some light seal grooving
32	B-1900	.001	1000	2400	.030	Heavy blade transfer	.000	Cont.	Heavy	.030	None	2400	.5	---	300	Indeterminate	Heavy blade wear, no seal spalling
Sprayed, Graded Layer Y ₂ O ₃ Stabilized ZrO ₂ /CoCrAlY with CeO ₂																	
33	B-1900	.001	1000	Amb	.030	Heavy blade transfer	.000	Cont.	Heavy	.031	None	Amb	1.5	---	300	Indeterminate	Metal transfer/ceramic spalling in rubbed area
34	B-1900	.001	1000	2400	.030	Heavy blade transfer	.002	Cont.	Heavy	.034	None	2450	1.5	---	300	70	Localized edge groove, heavy blade transfer
Sprayed, Continuously Graded Y ₂ O ₃ Stabilized ZrO ₂ /CoCrAlY without CeO ₂																	
29	B-1900	.001	1000	Amb	.030	Heavy blade transfer	.000	Cont.	Heavy	.026	None	Amb	1.0	---	300	Indeterminate	Metal transfer/ceramic spalling in rubbed area
30	B-1900	.001	1000	2400	.030	Heavy blade transfer	.008	Cont.	Heavy	.026	None	2350	2.0	---	400	2.5	Localized seal grooving, no seal spalling or delamination
Sprayed, Continuously Graded Y ₂ O ₃ Stabilized ZrO ₂ /CoCrAlY with CeO ₂																	
35	B-1900	.001	1000	Amb	.030	Heavy blade transfer	.000	Cont.	Heavy	.033	None	Amb	.5	---	560	Indeterminate	Some seal spalling at center of rub
36	B-1900	.001	1000	2400	.030	Heavy blade transfer	.001	Cont.	Heavy	.033	None	2450	.5	---	460	95	Very light seal grooving, no seal spalling

- (1) Continuous rub extending for most of 60° arc of seal segment
 (2) + denotes knife edge pickup occurrence
 (3) Initial interaction area (end of specimen) broke off during interaction

- (4) A light (.007 inch) localized groove occurred when seal specimen shifted during testing
 (5) Spalling occurred during post test cool down

*Repeat of test No. 12 with "Smooth" knife edge
 **Sweep test (sweep after penetration) at .010 inch/sec for .200 inch